The Potential for Alternative Materials in Pavement Construction

A thesis

submitted in partial fulfilment

of the requirements for the degree

of

Masters of Science in Materials and Processing

at

The University of Waikato

by

Darcy Rogers

THE UNIVERSITY OF
WAIKATO
Te Whare Wānanga o Waikato

2018

Abstract

The current materials used in pavement construction were developed in the 1930s but materials development has not kept pace with increasing traffic demands since this time. This report considers the potential for alternative materials that could offer greater performance in a pavement and meet current transport demands. In order to determine if there were opportunities for alternative materials, the performance of the current materials and associated design methodologies were reviewed. This review found that the current materials have extremely variable performance, with life spans ranging from 1 year to over 20 years and often fail due to insufficient strength in the current materials. Considering this, two key failure scenarios responsible for the majority of failures where identified: Scenario 1 – underlying material fails due to poor load spreading of the upper layers and Scenario 2 – where the upper layers fail through lack of strength or flexibility. By applying standard materials selection processes to consider materials that work under both of these scenarios it was found that wood, waste plastics and steel were options that could be considered as alternative pavement materials. It was found that three potential material configurations could be considered under each of these scenarios: homogenous materials, alternative asphalt matrices to bitumen and sandwich panels. The alternative materials outperformed the current pavement materials in terms of strength. Comparisons with the stiffness of the conventional pavement materials showed that the alternative materials were not as favourable in design methods that only consider the load spreading ability of the material (high stiffness). Field trials confirmed that materials with lower stiffness but much higher strength could offer greater performance than the current pavement materials and should be considered as alternative options to the current pavement materials.

Table of Contents

Table of Figures

1. Introduction

Historically the construction of road infrastructure is intimately linked to the military, economic and administrative needs of a civilisation. Advances in pavement materials were driven by not only these needs but also the level of transportation technology available. This resulted in the earliest engineered roadways appearing around 3000BC, the same time that mankind organised themselves into urban societies where regular trade routes were established between neighbouring towns. These early roadways arose from walking tracks that could no longer withstand the increased animal, sled and wagon traffic resulting from the newly formed trade routes. To protect the soft natural formation of these paths, both new materials and construction techniques were developed, capable of resisting the deformation and wear brought about from the increased traffic and loads. Initial developments varied by region due to availability of particular materials and consisted of wooden planks, stone, cement and even Bitumen. These materials normally only improved the surface of the road (wearing coarse, Figure 1) (Lay, 1992).

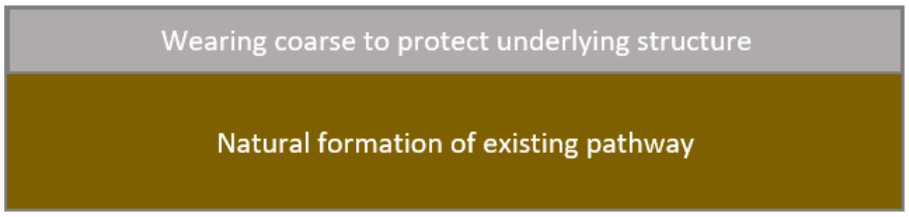

Figure 1 - Structure of first engineered pavements.

These first engineered roadways were prone to both abrasion and environmental damage where high levels of moisture caused the wearing coarse to rot (in the case of wooden planks) or sink into the muddy underlying natural formation. These issues were not overcome until the Romans consolidated the many technologies to produce strong and durable roadways lasting up to 100 years (PavementInteractive.org, 2008a).

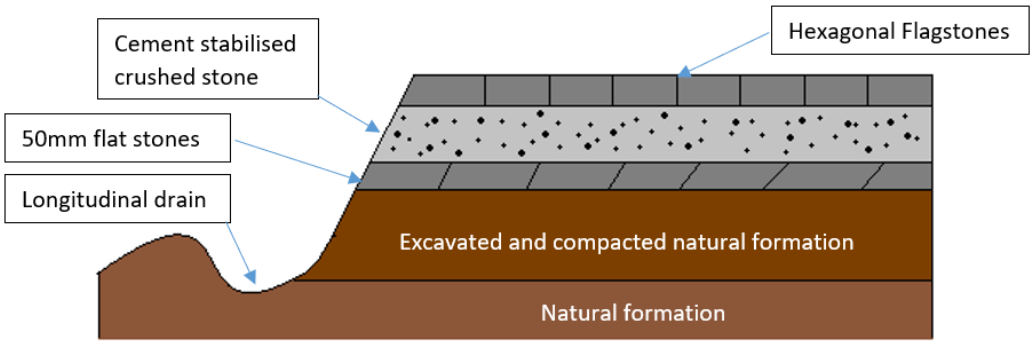

Figure 2 - Structure of Roman pavements.

These multi-layered structures (Figure 2) consisted of deposits of variously sized crushed stone (or brick), a cementitious layer and a wearing course of hexagonal flagstones. The key feature of these pavements was the longitudinal drains which limited the adverse effects of excessive moisture on pavement life. These pavements are believed to have lasted up to 100 years and are estimated to have cost the equivalent of $2 million by today's standards (PavementInteractive.org, 2008a).

After the demise of the Roman Empire, this level of pavement technology was not to be bettered until the Industrial Revolution where a wearing course of smaller, unbound crushed stone (typically referred to as Unbound Granular Materials, UGM or simply basecourse) was found to give similar performance to the large flagstones used in Roman designs. The increased traffic speeds associated with the invention of the combustion engine and the subsequent widespread use of pneumatic tyres rapidly abraded the unbound surface aggregate, requiring frequent maintenance to ensure the integrity of the pavement remained intact. To alleviate these increased demands on the pavement, the crushed rock of the wearing coarse was bound together using binders such as coal tar, bitumen and cement. The addition of these binders produced hard wearing surfaces that were able to withstand the increased stress of motorised vehicles. Variations of the composition of binder and aggregate allowed the strength, stiffness, skid resistance, durability and cost effectiveness of the surface to be tailored to the circumstances (Lay, 1992).

This method of pavement construction still persists to this day where modern pavements combine this binder technology with multi-layered structures similar to the original Roman design. In the modern pavement the stiffness of

each layer is progressively reduced with pavement depth to protect the underlying formation (Figure 3).

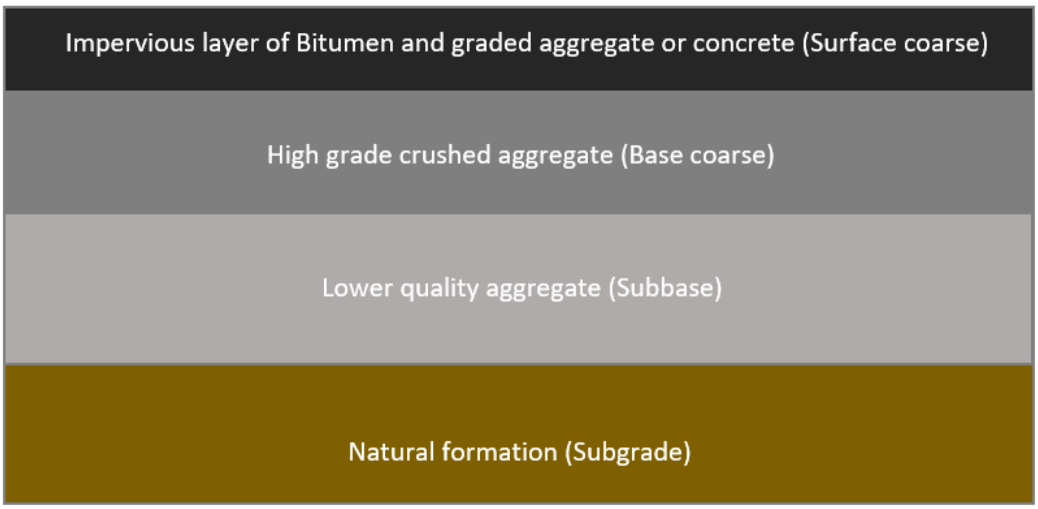

Figure 3 - Typical structure of a modern pavement.

The upper most layer is called the surface course (or surfacing) and is typically asphalt, concrete or a thin layer of bitumen (~2mm) with aggregate bonded to its surface, referred to as chip seal (Figure 4). If this layer is deep lift asphalt (depth >100mm) or concrete it will be the main load bearing layer due to its relatively high stiffness, whereas this function is performed by the basecourse in lower cost pavements which use chip seal or thin asphalt layers (<50mm) as the surface layer. The critical function of both of these surfaces layers is to provide water proofing to the underlying pavement as the stiffness of the lower, unbound layers is severely reduced by the presence of excessive moisture.

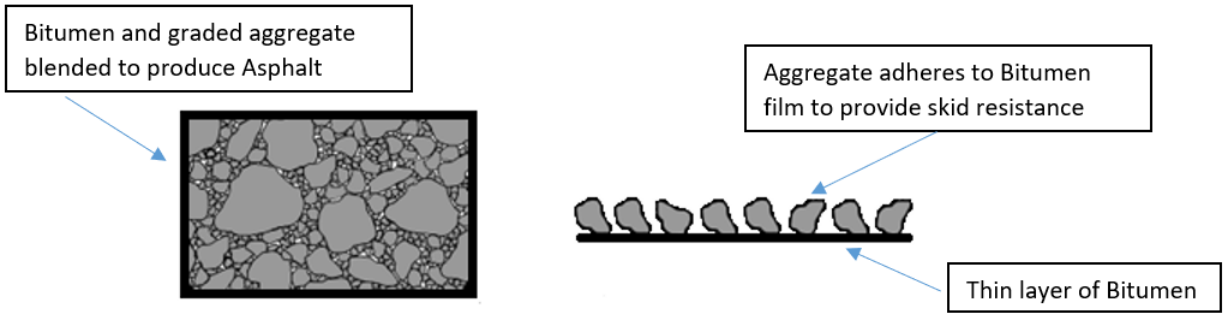

Figure 4 - Composition of typical surfacing layers, Asphalt (left) and Chip seal (right).

This design (or variations thereof) makes up the bulk of modern engineered pavements and is used in all but the highest stress situations. In these highly stressed pavements such as ports and airfields, concrete is used rather than

asphalt due to its superior stiffness, despite its much higher cost and longer construction time (Lay, 1992).

Modern pavement materials appear to be not too dissimilar from their historical counterparts however research in this area has led to advances in the understanding of the behaviour of these materials and therefore current materials far outperform the first iterations of these materials. This can be seen in Figure 5 below where the depth of the supporting layers of the pavement have been significantly reduced due to advances in both design and understanding of material properties (FHWA, 2017).

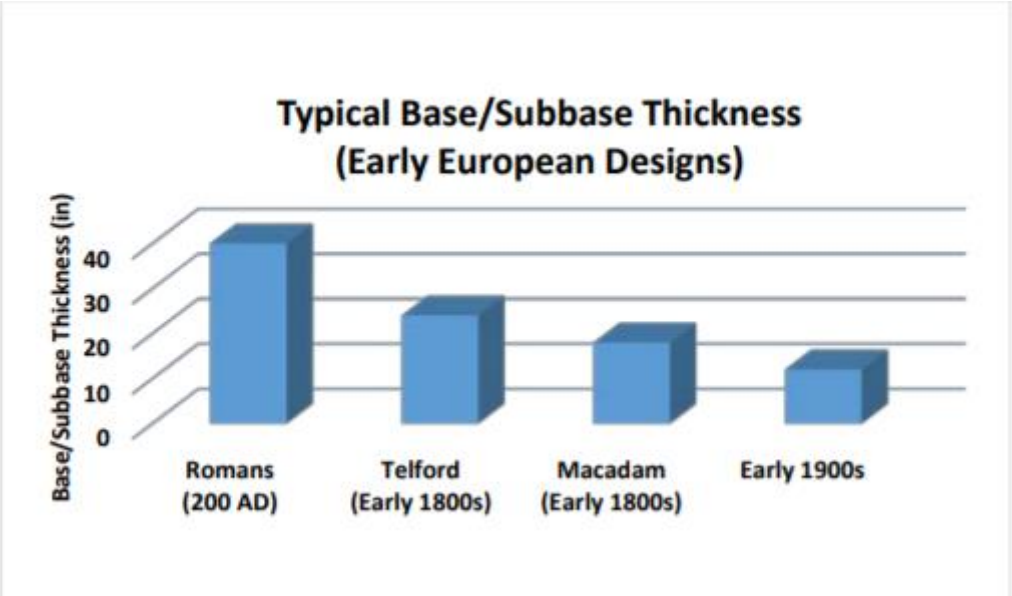

Figure 5 - Evolution of supporting layer depth (FHWA, 2017).

Despite this, a review of current pavement construction in New Zealand reveals that most new construction begins to fail within 10 years of being constructed (Jooste, 2017). This is especially concerning when pavements are typically designed to last 25 years (Jameson, 2008). As the industry has played it relatively safe in terms of materials, the current materials (established over 80 years ago as cars became common place) are being challenged by increasing traffic demands and maintenance budgets that are less than the cost to maintain the network condition to an acceptable level (AIA, 2017; Greaves, 2017).

Table 1 lists the most common pavement defects that require some form of maintenance treatment on New Zealand roads (NZTA, 2015).

Table 1: Common pavement defects that require maintenance intervention on NZ roads.

Failure	***Description***	***Mode of failure***	***Critical Property***
Rutting 	Deformation of the pavement in the wheel paths increasing roughness and the likelihood of water accumulating in this area during rain fall (increased risk of aquaplaning).	Repeated compressive stress applied at the surface is greater than strength of the material resulting in deformation.	Strength
Shoving 	Deformation of the pavement resulting in shear failure of the pavement which forms bumps in the pavement surface. Typically accompanied by rutting.	Applied compressive stress at the surface is greater than the confining pressure that stops the material from failing due to shear. Results in shear forces that push material to the surface forming a surface bump.	Strength
Cracking 	Cracks form at the surface of the pavement allowing water to travel to the lower pavement layers reducing their respective strengths. This increases the likelihood of deformation/rutting in the pavement.	Permanent deformation in the pavement or very high deflections (due to lack of support from the underlying layers) cause the pavement to yield resulting in cracking of the pavement.	Strength / Fatigue Strength
Potholes 	Holes form in the surface of the road increasing the roughness of the pavement.	Typically form due to cracking followed by ingress of water under the cracked surface causing holes to form under stress dues to traffic and hydraulic action.	Strength / Fatigue Strength
Ravelling / Scabbing	Loss of particles from the surface of the	Typically found in bitumen based	Durability, Impact

	pavement, increasing the roughness of the pavement.	surfacings where sufficient oxidation of the bitumen has taken place. This reducesits flexibility and increasing the likelihood of fracture due to impact loadings.	Strength / Fracture Toughness
Low Texture 	Reduction in surface macro-texture which can reduce the surface friction.	Reduction in texture is typically caused by either abrasion at the surface or movement (yielding) of the bitumen fraction to the surface of the pavement (commonly referred to as flushing). This yielding of the bitumen (flushing) is commonly caused by venting of water trapped within the lower layers of the pavement. Bitumen is low in strength and will therefore yield and flow under the vapour pressure of water entrapped in the pavement, resulting in bitumen being pushed to the surface.	Abrasion Resistance / strength
Low Friction	Reduction in surface friction increasing the stopping distance of vehicles travelling upon it.	Reduction in surface friction is typically caused by either abrasion/polishing of the aggregate at the surface or movement (yielding) of bitumen to the surface which covers the surface aggregate.	Abrasion Resistance / strength
Shoving	Deformation of the pavement resulting in shear failure of the	Applied compressive stress at the surface is greater than the	Strength

	pavement which forms bumps in the pavement surface. Typically accompanied by rutting.	confining pressure holding it together causing the material to deform and accumulate at the surface.	

Table 1 shows that the majority of defects that result in maintenance can be attributed to the failure of materials (mostly due to lack of strength). The vast majority of roads in the world are constructed using aggregate and bituminous materials with over 90% of paved roads in Europe and America being constructed using asphalt (EAPA.org, 2015; NAPA, 1999) with the rest using concrete or a combination of aggregate and bituminous surfacing, such as chip seal. Of New Zealand's 66,000km of sealed roads, around 10% of the sealed roads are asphalt with the other 90% being constructed of chip seal. New Zealand also has a large portion of unsealed road (totalling ~26,000km) constructed of unbound aggregate (Gundersen, 2008).

The materials used in construction of the pavement have a profound effect on the amount of ongoing maintenance required. Considering the fact that the majority of pavement failures are attributed to strength failures it would suggest that to reduce the cost associated with pavement maintenance, high strength materials would be desirable. In the case of bituminous products such as asphalt and chip seal, bitumen is the matrix which adds strength to these materials. As it is the residue from the crude oil refining process it behaves as a very high viscosity oil exhibiting viscoelastic properties (Read & Whiteoak, 2003). Research has shown that the performance of bituminous materials is linked to its ability to resist strain when it is operation outside of its elastic limit (D'Angelo, 2009).

This would suggest that the strength of bitumen is too low to avoid many of the failures lists in Table 1 and therefore bitumen is failing due to plastic deformation. If the focus is only on improving the performance of bitumen when it is operating outside its elastic limits, any improvements to the bitumen

performance will only delay the inevitable failure rather than being designed to resist it altogether.

Concrete possesses much higher strength than bituminous materials and therefore is very stiff and will therefore do a good job of spreading traffic loading over the underlying layers. This high stiffness comes at the cost of lower flexibility which means that this material performs very well until it loses support, due to settlement of the underlying layers, and due to its lack of flexibility, it will crack (A.A.A Molenaar, 2004).

These materials have been common place since the 1930's however pavement construction requires large volumes of these materials. The key raw materials of bitumen, cement and aggregate used in pavement construction are finite resources therefore it is expected that supply of these materials will eventually come under pressure in the not too distant future. Bitumen is a waste material produced during the refining of crude oil. Oil production is expected to go into decline by 2030 (Sorrell, Speirs, Bentley, Brandt, & Miller, 2010) which will result in increased cost for bitumen and its manufactured products such as asphalt. Cement is the most logical alternative however its production is responsible for 7% of the worlds greenhouse gas emissions due to the volumes required and the high temperatures required during manufacture (C. Meyer, 2009), while aggregate is the second most consumed resource on earth (second only to water) where urbanisation is reducing the availability of viable quarry sites (Ecoserve & Network, 2004). Considering all of these factors it is not unreasonable to believe that alternative material will eventually be sought after to alleviate these issues.

A small amount of research has been undertaken into alternative pavement materials where there has been some use of binders derived from vegetable oil as an alternative to bitumen (Colas, 2017) and a concept developed for use of plastic to construct modular roads (KWS, 2017). Outside of this there has been very little research as the focus has been on variations of the existing materials through addition of polymers (such as epoxy, elastomers and plastics) to bitumen (Herrington & Alabaster, 2008; Lesueur, 2009) or use of waste concrete, glass and steel slag as alternative aggregate sources (Huang, Bird, &

Heidrich, 2007; Im, Zhou, Lee, & Scullion, 2014). For a step change in reducing the cost of sourcing materials and maintaining the current infrastructure at a reasonable cost, change is required in the way the industry evaluates suitable materials (rather than relying on historical knowledge). Materials selection processes are well established in other industries and the benefits of this can be seen in the prominence of composite materials used in a multitude of different industries (Ashby & Cebon, 2004). As the industry has only used a limited selection of materials, the design processes are targeted towards allowing only these materials to be used in the design process. For a materials selection process to be used to identify alternative materials, the key requirements for materials used in a pavement first need to be established, so that all materials can be considered under consistent requirements. Key requirements can be split into functional, economic and geometric requirements. Functional requirements can be established by reviewing current materials and design methods, economic requirements can be determined by reviewing current costs and performance, whereas geometric requirements can be realised by reviewing current and future traffic demands.

This report identifies the key requirements of a pavement so that this information can be used to identify potential alternative materials and establish whether these materials could be used in practice.

2. Functional Requirements

Pavements are the structures built upon natural formations (subgrades) and allow for the development of modern road networks. They consist of multi-layered structures used to provide a smooth riding surface and adequate surface friction for traffic, whilst protecting the underlying natural foundation (the subgrade) from distress caused by traffic (Adlinge & Gupta, 2013). This distress manifests itself as shear failure in the subgrade where the compressive stress applied at the surface of the subgrade is greater than the confining pressure holding it together (Figure 6). The ability of the upper layers in the pavement to disperse the applied traffic stress is critical to ensure that the bearing capacity of the layer below is not exceeded (or at least minimise the resultant distress), resulting in non-recoverable vertical strain.

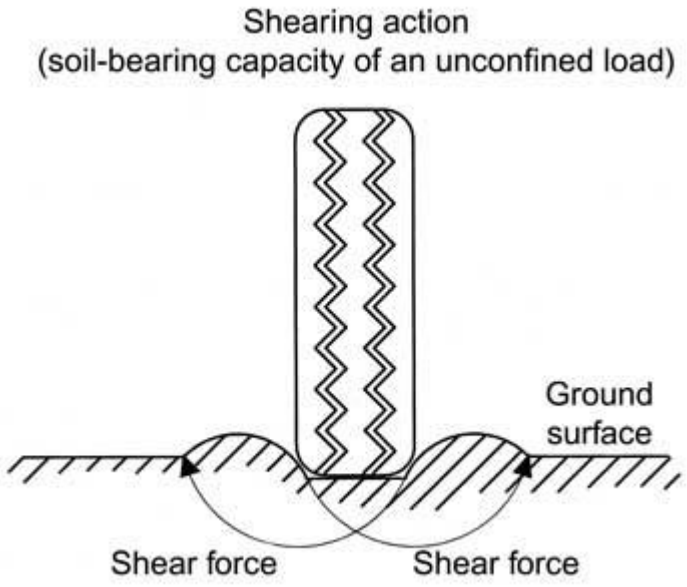

Figure 6 - Diagram of bearing (shear) failure in pavement (K. G. Meyer, 2002).

The layers within a pavement are depicted in Figure 7 and consist of materials which progressively increase in stiffness toward the surface of the pavement. These layers can be subdivided into;

Surface Course – Layer in contact with the traffic load. Its main purpose is to provide a smooth, waterproof, high friction surface that protects the underlying layers. If the surface course is constructed from asphalt, concrete or small elements (such as cobblestones) it will be the layer with the highest

load bearing capacity (resistance to shear failure) (PavementInteractive.org, 2008b). Chip seal is the other common type of surface course however it does not provide any structural strength to the pavement. Internationally, it is preferable to use this technique in conjunction with another type of surfacing that does provide some form of structural strength (such as asphalt). For economic reasons, around 65% of pavements in the 92,000km of New Zealand's road network have chip seal as the primary surfacing course, without a complimentary surfacing such as asphalt (Gundersen, 2008). Chip seal consists of a thin layer of bitumen (1mm-3mm) which adheres a layer of crushed stone to the surface of the underlying layer (typically basecourse) (Transit-New-Zealand, 2005). The chip seal surface does not offer any bearing capacity therefore the major load bearing layer in a pavement with a chip seal surface course will be the basecourse.

Basecourse – Layer immediately below the surface course which offers additional load bearing support and drainage as excess water entrapped in the lower pavement layers can significantly reduce the bearing capacity of the pavement. The basecourse layer is usually constructed of crushed stone aggregate with a maximum size (approximate width) of 20mm-40mm (NZTA, 2006). This aggregate can also be stabilised with a small amount of cement (1%-3%) to improve the bearing capacity of the layer (Lay, 2009). The basecourse is not always needed if the surface course can bear the traffic stresses on its own (i.e. concrete surfacing).

Subbase course – Layer that sits between the basecourse and the subgrade which consists of crushed stone around 60mm in size (and no greater than 100mm) (NZTA, 1986). This layer is primarily used as further support for the upper layers as well as offering drainage and as a means to reduce the movement of fine particles (such as clay) into the upper layers, which can reduce the bearing capacity of these layers (PavementInteractive.org, 2008b). If the pavement already possesses sufficient strength, this layer can sometimes be omitted completely in favour of only a basecourse layer.

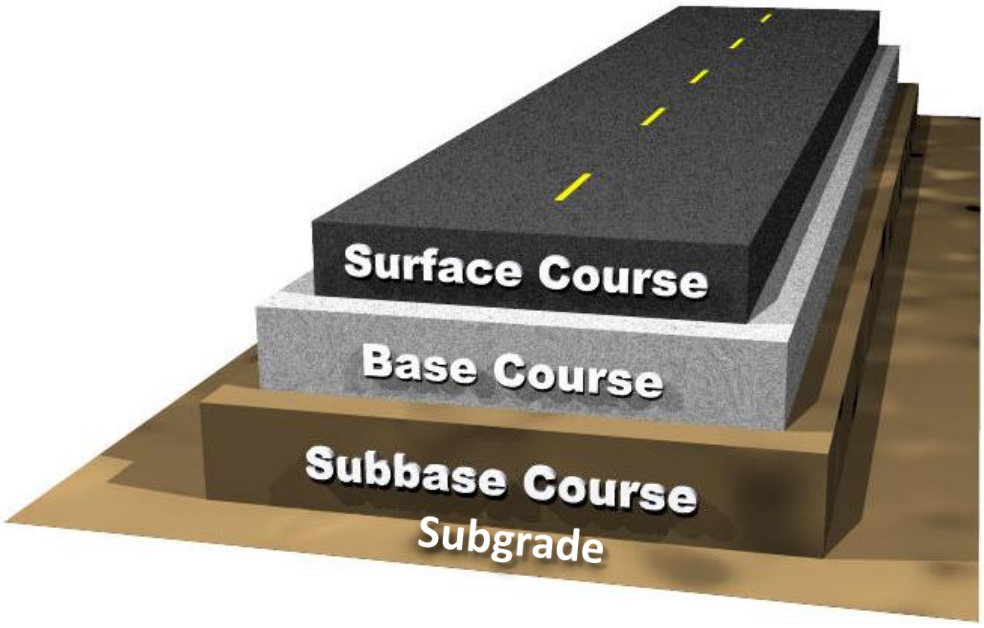

Figure 7 - Typical pavement structure (PavementInteractive.org, 2008b).

As long as failure presented at the surface does not cause, or eventually contribute to an increase in roughness, it cannot be considered as a failure of the pavement.

2.1. Design Methods

The design methods which are used to ensure the pavement does not require premature reconstruction (discussed in the previous section) can vary significantly both internationally and domestically. These design methods typically range from empirical methods, which rely on using correlations with historical performance, to more mechanistic approaches, which consider the mechanical properties of the materials used to construct the pavement (A.A.A Molenaar, 2004). In both methods the goal is to limit the amount of vertical displacement occurring in the subgrade which is the major consideration used to predict the life of a pavement (Austroads, 2008).

2.1.1. Soil Mechanics

The purpose of any pavement is to protect the soft underlying structure, referred to as the subgrade. For the subgrade to be protected, any applied stress at the surface must be sufficiently distributed to ensure that the stress applied to the subgrade is less than its cohesive strength (internal friction that stops soil particles from moving around). Modern pavement design methodologies typically assume the upper layers will have sufficient strength

to avoid failure if the underlying subgrade does not deform due to excessive stress (A.A.A Molenaar, 2004). This has led to the design of pavements focusing on maximising the stiffness of the upper layers to ensure the stress applied to the subgrade is minimised.

Soils are defined as an accumulation of mineral particles formed by the weathering of rock. The size of the mineral particles can range from less than 1µm to over 100mm (Knappett, 2012). Basecourse aggregate used in roading is essentially a type of soil where the distribution of mineral particles has been manufactured to meet certain requirements. This means that many of the principles in soil mechanics can also be applied to basecourse materials.

Soil mechanics offers an insight into the critical properties required to determine the stresses that the underlying unbound granular layers can cope with. Of particular interest for soil mechanics (relating to traffic loadings) is the bearing capacity of a soil. This is essentially the strength of the soil. Upon application of a critical normal stress, a wedge of soil is pushed downwards with the soil next to the wedge pushed sideways and upwards. In this case, particles will begin to rearrange by rolling and sliding past one another (BoeingConsulting.com, 1999). This results in shear failure within the pavement as depicted in Figure 8, below.

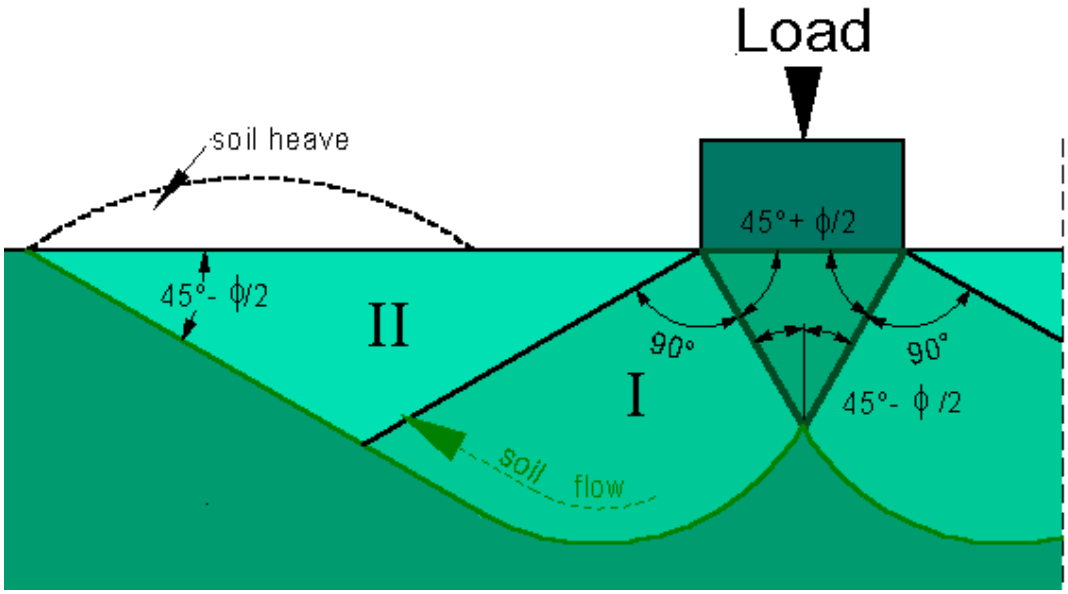

Figure 8 - Mechanism of shear failure in soils (BoeingConsulting.com, 1999).

The stresses involved in this mechanism are also shown schematically in Figure 9.

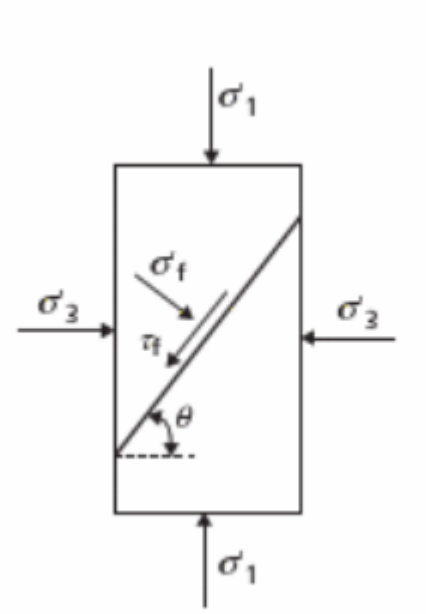

Figure 9 - Stresses present in a soil element (Knappett, 2012).

Application of a normal stress (σ1) will act to rearrange the soil particles. Due to soil particles being compacted against one another, a confining stress (σ3) will naturally be present which assists with interlocking of particles and increasing friction. Shear failure (τf) will eventually occur once a critical combination of normal and confining stress is reached (Figure 9). Typical values for shear strengths of soils are listed below in Table 2.

Table 2: The range of typical values for shear strengths of soils (G Arnold & Gaddum, 1995).

TERM	SHEAR STRENGTH (kPa)	FIELD TEST
Very Soft	0 - 24 kPa	Squeezes between fingers when fist closed.
Soft	24 - 48 kPa	Easily moulded by fingers.
Firm	48 - 96 kPa	Moulded by strong pressure of fingers.
Stiff	96 - 144 kPa	Dented by strong pressure of fingers.
Very Stiff	144 - 192 kPa	Dented only slightly by finger pressure.
Hard	> 192 kPa	Dented only slightly by pencil point.

In order to predict the potential for shear failure in a soil, Mohr-Coulomb theory is applied. This theory is used to determine failure criteria for materials undergoing complex stress scenarios. It is commonly used for materials that possess a much greater ultimate compressive strength than their ultimate tensile strength (Young & Budynas, 2002).

Use of Mohr-Coulomb theory typically requires both uniaxial compressive and uniaxial tensile tests to be undertaken. By plotting normal stress and confining stress at the point of shear failure in the soil, a Mohr circle can be produced (A.A.A Molenaar, 2004), as per Figure 10.

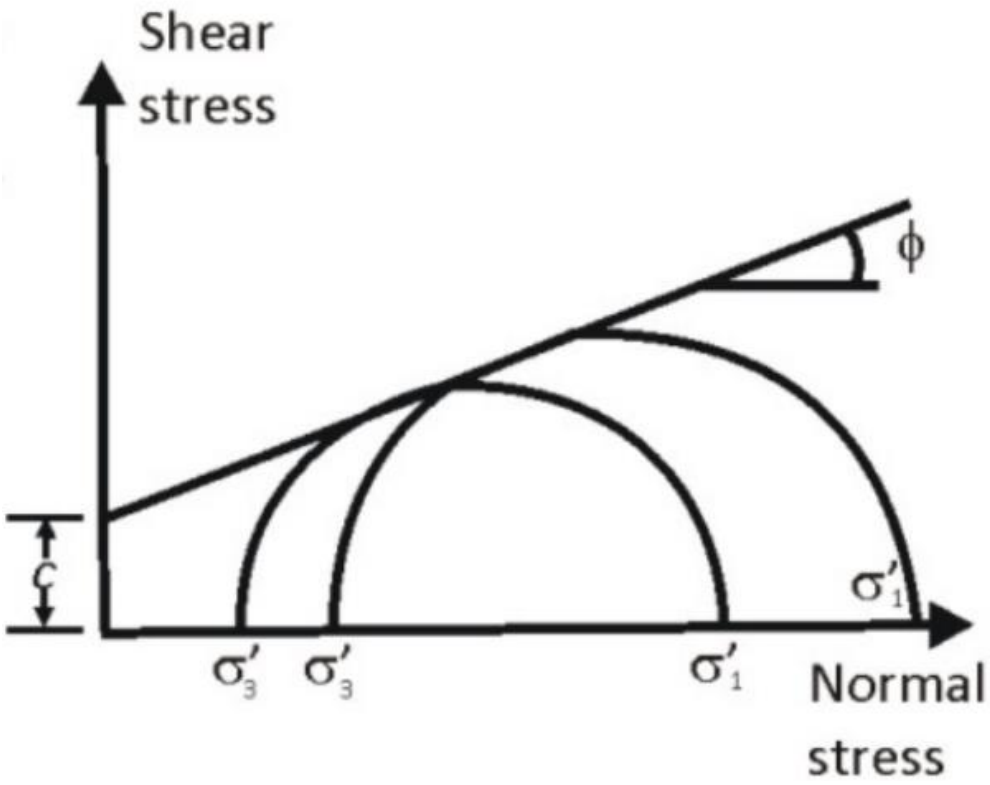

Figure 10 - Mohr-Coulomb failure criterion generated from triaxial tests performed by adding a confining pressure σ_3 and applying an axial stress σ_1 until shear failure. (Sitharam, 2015).

By repeating this test at multiple confining pressures, a failure envelope can be generated and therefore the cohesion (y-intercept/minimum stress that will cause shear failure) and the friction angle (slope/effect of confining pressure on failure stress due to internal friction of the particles) can be calculated (Sitharam, 2015). This is defined as the Coulomb equation:

$$\tau_f = c + \sigma_1 tan\phi$$

Equation 1

Where:

c = cohesion (kPa)

ϕ = friction angle or angle of shearing resistance

σ_1 = normal stress applied to induce shear failure (kPa)

τ_f = shear strength at failure (kPa)

The Coulomb equation shows that soil shear strength will increase with higher cohesion and/or friction angles in a given soil.

Upon application of a vertical stress to a basecourse material (due to compaction and subsequent trafficking), lateral stresses are formed in the material due to the interlock of particles. These stresses have been found to be the most important factor in limiting the degree of permanent deformation that occurs in a granular material (aggregate layers) during service (Selig, 1987). The addition of a lateral (confining) stress to the granular material increases friction between aggregate particles, lessening the degree of shear stress in the material. The exact residual stress of a granular material in service is difficult to determine due to: the nature of the material, the volume of the material involved and variations in geology and moisture content. Researchers have approximated that this could be as high as 130kPa however some agreement between laboratory results and in field performance has been found at 30kPa which is considered to be a fairly conservative value (G. K. Arnold, 2004).

Typical values for friction angle and cohesion have been characterised through testing of a number basecourse materials sourced from Australia, New Zealand and Northern Ireland. Triaxial shear tests, under repeated loading, were used to develop a relationship with in field performance of the materials using CAPTIF (Canterbury Accelerated Pavement Testing Indoor Facility). CAPTIF uses a revolving loaded wheel to replicate actual traffic conditions in a controlled environment (G. K. Arnold, 2004). It was found that there is a correlation with resistance to deformation (under traffic) and the properties determined from triaxial tests in the region where the material transitions from stable behaviour (stable increase in deformation) to a rapid increase in deformation (Werkmeister, Dawson, & Wellner, 2004). The cohesion and friction angles from these materials are listed in Table 3 below.

Table 3: Typical cohesion and friction angle results for basecourse (G. K. Arnold, 2004).

Material	Description	Repeat Load Triaxial Shear Test	
		c (kPa)	ϕ
NI Good	Premium quality crushed rock - graded aggregate with a maximum particle size of 40mm from Banbridge, Northern Ireland, UK.	5	39
NI Poor	Low quality crushed quarry waste rock - graded aggregate (red in colour) with a maximum particle size of 40mm from Banbridge, Northern Ireland, UK.	31	21
CAPTIF 1	Premium quality crushed rock – graded aggregate with a maximum particle size of 40mm from Christchurch, New Zealand.	19	28
CAPTIF 2	Same as CAPTIF 1 but contaminated with 10% by mass of silty clay fines.	0	25
CAPTIF 3	Australian class 2 premium crushed rock – graded aggregate with a maximum particle size of 20mm from Montrose, Victoria, Australia.	16	34
CAPTIF 4	Premium quality crushed rock – graded aggregate with a maximum particle size of 20mm from Christchurch, New Zealand.	15	22
CAPTIF Subgrade	Silty clay soil used as the subgrade for tests at CAPTIF from Christchurch, New Zealand.	10	14

The Mohr-Coulomb equation can be applied to determine the maximum vertical stress a granular material can withstand before shear failure would occur. The maximum normal stress that a granular material can withstand can be determined using the following procedure (Figure 11).

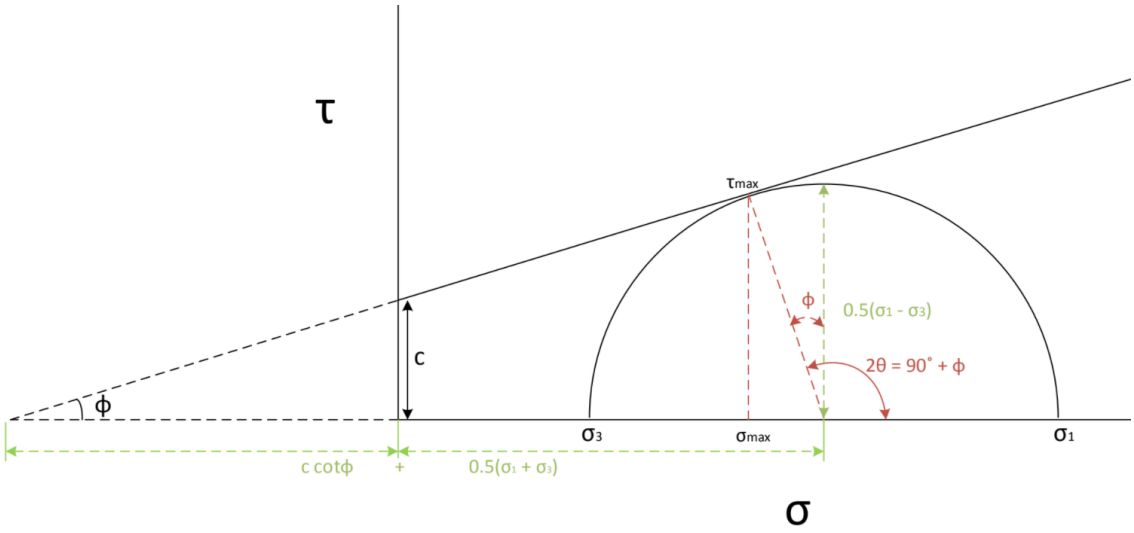

Figure 11 - Determination of Mohr-Coulomb failure parameters.

$$\theta = 45° + \frac{\phi}{2}$$

Equation 2

$$\sin\phi = \frac{\frac{1}{2}(\sigma_1 - \sigma_3)}{c\ \cot\phi + \frac{1}{2}(\sigma_1 + \sigma_3)}$$

Equation 3

Therefore:

$$(\sigma_1 - \sigma_3) = (\sigma_1 + \sigma_3)\sin\phi + 2c\ \cos\phi$$

Equation 4

And:

$$\sigma_1 = \sigma_3 \tan^2\left(45° + \frac{\phi}{2}\right) + 2c \tan 45° + \frac{\phi}{2}$$

Equation 5

Considering the friction angles and cohesion results in Table 3 and the commonly accepted confining pressure of 30kPa, application of this procedure can be used to determine the maximum normal stress that each of the basecourse materials from Table 3 can withstand (Table 4).

Table 4: Typical maximum normal stresses basecourse can withstand.

Material	Normal Stress to Induce Shear Failure	Contact Area Required to Spread an 20kN Single Wheel Load from a Truck
	σ_1(kPa)	m^2
NI Good	152.8	0.131
NI Poor	153.7	0.130
CAPTIF 1	146.3	0.137
CAPTIF 2	73.9	0.271
CAPTIF 3	166.3	0.120
CAPTIF 4	110.4	0.181
CAPTIF Subgrade	74.8	0.268

Table 4 shows that a typical basecourse material can withstand a normal stress due to traffic of around 150kPa with the weaker materials at around 70kPa. If a material is to be placed on top of these basecourses it would need to be able to spread the load of a typical truck tyre (20kN) over an area of 0.13m^2 to 0.27m^2.

2.1.2. Flexible Pavement

Pavements constructed of a bituminous upper layer (of either asphalt or chip seal) with unbound granular materials forming the lower layers, are referred to as flexible pavements (A.A.A Molenaar, 2004). The lower stiffness of the bituminous layer does not spread the traffic load as effectively as concrete however, due to the flexible nature of the bituminous layer, it can deflect with the underlying pavement. The strength of these types of pavements rely on the traffic load being spread across multiple layers to avoid deflection of the underlying pavement as Figure 12 (Texas-Department-of-Transport, 2001).

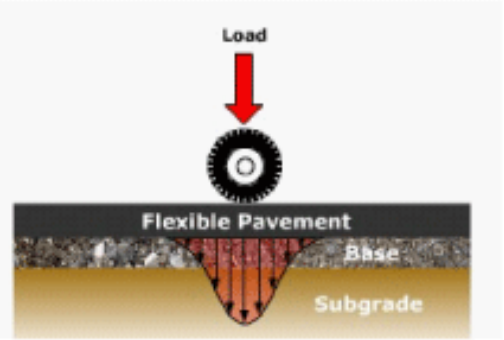

Figure 12 - Typical load distribution in a flexible pavement (Texas-Department-of-Transport, 2001).

Due to the nature of the materials used in flexible pavements, predicting the response to traffic (and therefore their performance) can be rather complex. Current accepted design methods use either empirical design with more advanced methods which consider the mechanical properties of the materials used referred to as mechanistic design (D. Timm, Birgisson, & Newcomb, 1998).

2.1.2.1. Empirical Methods

The majority of empirical methods are based on research carried out by the California Division of Highways in the 1930s. In this study a simple method was deduced to measure an empirical value for strength of the subgrade material (soil) by penetrating a steel plunger into the material and measuring the load required to achieve a displacement of 0.1" and 0.2". This value is compared to the values obtained by a standard material of crushed stone (as a percentage of the standard crushed stone value). The value obtained is termed the California Bearing Ratio (CBR) and is one of the major design inputs for empirical pavement design procedures (Read & Whiteoak, 2003).

In an empirical pavement design for a New Zealand pavement, the CBR value of the subgrade material is considered against the traffic volume expected during the pavements life expectancy, to determine the thickness of the pavement (Figure 13). This relationship was determined through the historic performance of known pavements in Australia and resembles similar work performed during the development of the CBR test in the 1930s. This research found that similar pavement thicknesses were required to reduce the plastic deformation occurring in subgrades with similar CBR values (Jameson, 2013; Porter, 1939).

Further research found that plastic deformation in the subgrade would occur faster with increased axle loading as well as increased traffic volume. As each vehicle will vary in axle loading (car, trucks etc.), each load repetition will vary in magnitude. In an empirical pavement design this variation is accounted for by converting the damage caused by a given vehicle into an equivalent number repetitions that would be required of a standard axle loading to cause that amount of damage to the pavement (Austroads, 2012; Jameson, 2013). This is referred to as equivalent standard axles (ESA) and is calculated using Equation 6.

$$ESA = \left(\frac{Actual\ axle\ load\ (eg.Truck)}{Reference\ axle\ load\ (eg.Car)}\right)^4$$

Equation 6

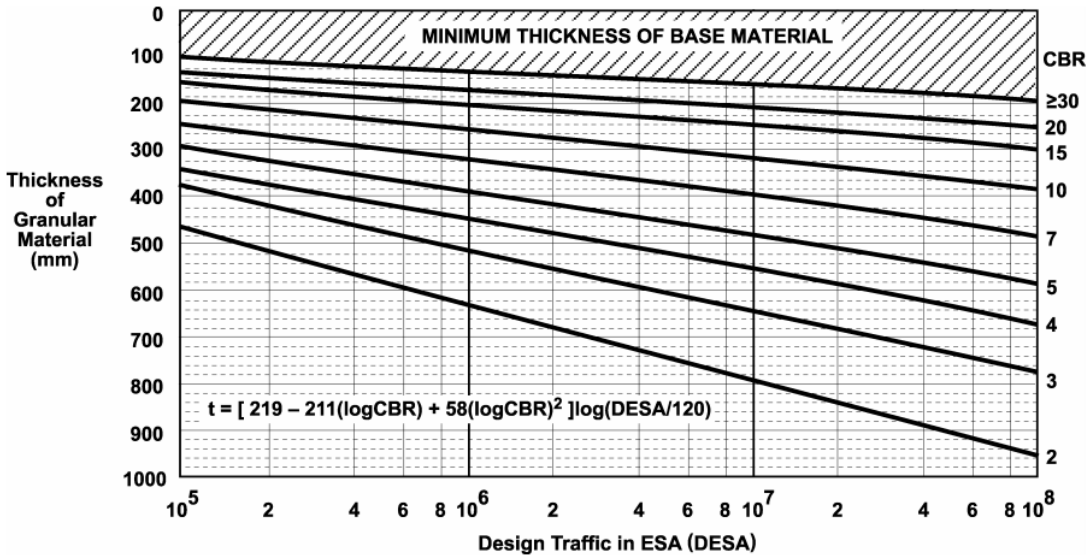

Figure 13 - Design chart for depth of granular material to be used in empirical design (Austroads, 2012).

Using the design chart in Figure 13, the total depth of the pavement can be determined to ensure that plastic deformation in the subgrade is kept to a minimum. The major drawback of this method is that it considers the only failure mode of the pavement to be due to plastic deformation of the subgrade resulting in unevenness at the surface of the pavement. In this case the mechanical properties of each of the layers in the pavement are not considered. As aggregate sources can vary dramatically from region to region pavements constructed with equivalent depths but of different aggregate source can produce significant differences in performance.

2.1.2.2. Mechanistic Method

In a mechanistic pavement design, the contribution of the mechanical properties of each component within the pavement is considered to predict the response of the entire pavement to an applied traffic stress (Jameson, 2013). This allows the onset of failure in the pavement to be predicted from the maximum allowable stresses and strains that the materials in the pavement can withstand. In reality, the complexity of undertaking a mechanistic pavement design is unworkable as it is extremely difficult to predict and accurately characterise the behaviour of the unbound granular materials (crushed stone aggregate) used within the pavement (Jameson, 2013).

In practice a compromise is made between the short comings of an empirical design and the complexity of a mechanistic design which is normally called mechanistic-empirical pavement design. This design method is used as the response of unbound materials (such as stone aggregates and soils) to an applied stress is complex and basic mechanical properties are not able to accurately predict the onset of plastic deformation in a pavement layer. The most commonly considered mechanical property used to characterise these materials is resilient modulus. Resilient modulus is essentially an estimation of the stiffness of an unbound material. Upon applying a stress to an unbound material, the strain induced is predominantly recoverable (elastic) with a portion of it being non-recoverable (plastic, due to reorientation and abrasion of the particles). The resilient modulus only considers the elastic (recoverable strain) portion of the response in the material which gives the pavement designer an indication of the materials stiffness (Figure 14) (Christopher, Schwartz, Boudreau, & Berg, 2006).

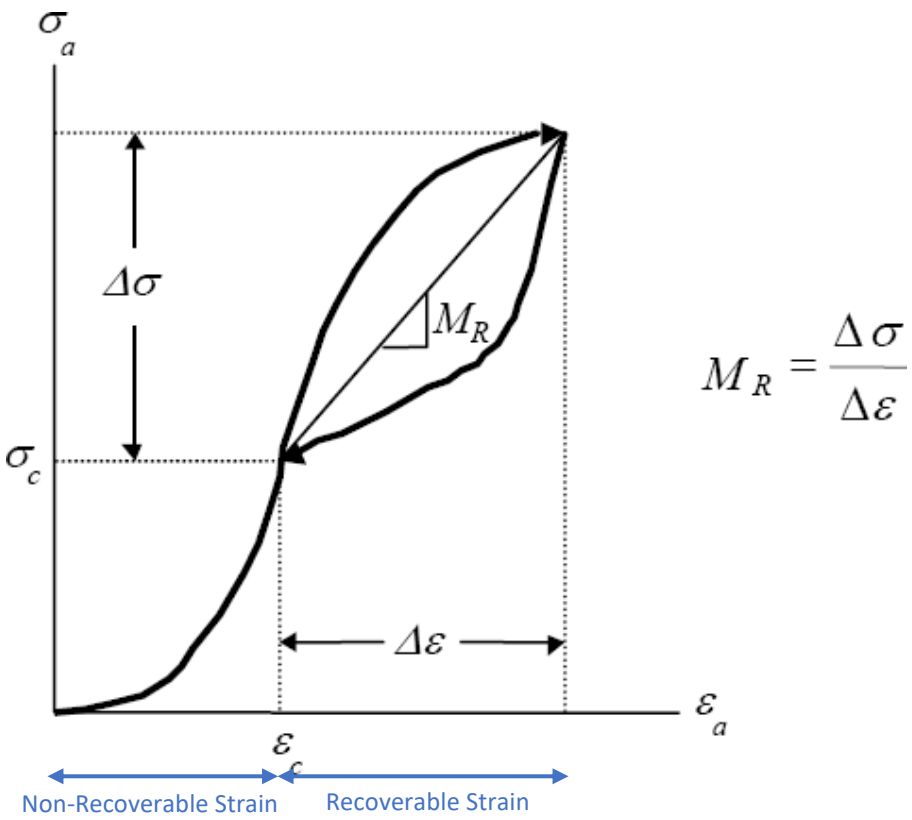

Figure 14 - Determination of resilient modulus (Christopher et al., 2006).

It should be noted that this behaviour is quite different to classic material behaviour where the initial deformation is elastic (recoverable) followed by plastic deformation (non-recoverable) once the materials maximum strength has been exceeded. As pavement materials are predominantly made up of compacted aggregate particles, a confining pressure (σ_c, Figure 4) needs to be applied to allow for reorientation of the particles, resulting in interlocked aggregate particles. This reorientation of particles results in a small amount of non-recoverable strain (ε_c, Figure 4) before an axial (σ_a, compressive) stress is applied to the material. By applying an axial stress to interlocked particles within the material, it will begin to behave elastically and resist any further permanent deformation until its maximum strength is exceeded (resulting in further plastic deformation) (Christopher et al., 2006). The measurement of resilient modulus will be very dependent on the ability of the aggregate to form an interlocked structure therefore, the success of a pavement design hinges on this particle interlock (achieved in the lab) being representative of what is achieved during construction.

Despite this uncertainty and the fact that resilient modulus is not a classical measurement of a materials resistance to elastic deformation, it does allow the

pavement designer to predict the transfer of stress through the pavement (due to traffic loading) using what is called elastic layer theory. Elastic layer theory is based on equations 7-9 that consider the vertical stress occurring at a depth and radial distance from a circular point load (Yoder & Witczak, 1975).

$$\sigma_z = p\ (1 - \frac{z^3}{(a^2+z^2)^{1.5}})$$

Equation 7

$$\sigma_r = (\frac{p}{2}\frac{(1+2\nu)-2(1+\nu)z}{(a^2+z^2)^{1.5}} + \frac{z^3}{(a^2+z^2)^{1.5}}$$

Equation 8

$$a = \sqrt{\frac{P}{\pi p}}$$

Equation 9

Where:

P = Single wheel load (kN)

p = Contact pressure (kPa)

a = Radius of the load contact area (m)

z = Vertical depth from point load (m)

r = Radial distance from point load (m)

v = Poisson's ratio

Equations 7-9 show that the vertical stress from a point load will reduce with depth and radial distance from the point load. These equations were developed for homogenous, isotropic and elastic materials which can lead to issues with consistency of performance when using UGM's as they contain inhomogeneity's (introduced during the construction process and due to the natural variation in the materials), are anisotropic (properties differ in vertical and horizontal directions) and as previously discussed, only exhibit partially elastic behaviour (Christopher et al., 2006; Seyhan, Tutumluer, & Yesilyurt, 2005). This means that equations 7 and 8 cannot accurately determine if all regions in the pavement can cope with the calculated stress, leading to

localised failures. Due to the complexity of modelling behaviour of UGM alternative methods of design using these materials can become quite complex, whereas the Boussinesq equations have been found to produce an acceptable correlation with actual performance with asphalt and UGM's used in flexible pavements (Gupta, Kumar, & Rastogi, 2014). This has allowed a relative value for the strain occurring at the top of the subgrade (due to a given traffic loading) which is then calibrated against the real-world performance of known pavements. This is called the strain criterion (Equation 10) and allows the pavement designer to estimate the required number of passes, of a given traffic load, to cause unacceptable deformation in the subgrade and therefore failure of the entire pavement. This forms the empirical part of mechanistic empirical pavement design (Austroads, 2012).

$$N = \left[\frac{9300}{\varepsilon}\right]^7$$

Equation 10

Where:

N = Subgrade strain criterion (number of passes to failure)

ε = Vertical compressive strain (in micro-strain) accumulating at top of subgrade

The mechanistic-empirical method also acknowledges that vertical displacement in the subgrade is not the only mechanism that causes distress in the pavement as the tensile strains (due to bending) occurring in bound layers (such as asphalt or cement stabilised basecourse/subbase) are considered (Figure 15). This allows the fatigue performance of these layers (at the calculated tensile strains) to be characterised allowing the flexural fatigue lives of these layers to be determined (Greg Arnold, Morkel, & van der Weshuizen, 2012; Austroads, 2012).

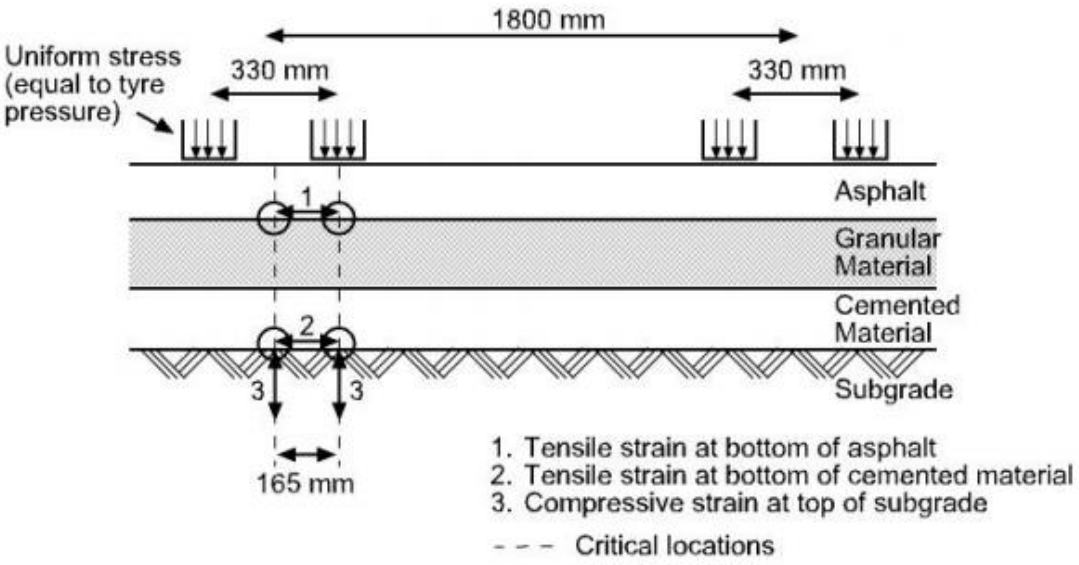

Figure 15 - Model of strains considered in mechanistic-empirical pavement design.

The major weakness in this design method is that it does not consider failure of unbound granular material (such as basecourse or sub-basecourse aggregate) as a possibility. In reality, the particles in an unbound granular material re-orientate as the material is dynamically and repeatedly loaded with each passing vehicle. This is termed the 'shakedown effect' where the re-orientation of these particles leads to further compaction of the material. Initially this will present itself as vertical displacement at the surface of the unbound layer. In a suitable granular material, further compaction due to 'shakedown' will lead to the interlocking of the aggregate particles which forms a stable layer where further compaction / deformation is very limited (Werkmeister et al., 2004). To determine the capacity for an unbound granular material to form this stable level of compaction, the repeat load tri-axial (RLT) tests are employed. This type of testing simulates in-service conditions by applying a series of increasing repeated loads to a confined sample of pre-compacted unbound granular material (Arnold 2004). The development of permanent strain in the material with increasing load cycles is used to determine whether the granular aggregate particles are able to re-orientate to form a stable incompressible material (Figure 19.a) (Werkmeister, Dawson et al. 2004). Granular materials that do not form this interlocked particle network will produce unstable behaviour (Figure 19.b). Intermediate stability (Figure 19.c) occurs when the

aggregate particles forming the interlocked structure degrade (due to abrasion) and become unstable.

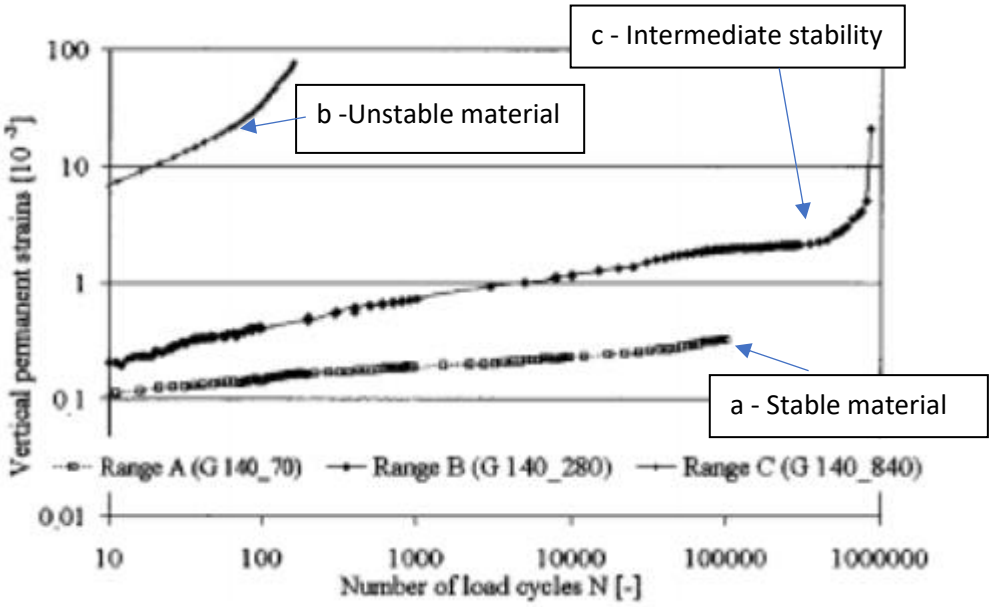

Figure 16 - Typical results from RLT test at a single repeated load (Werkmeister et al., 2004).

This type of testing is used by some pavement designers as a supplementary design criteria to allow for more confidence when designing the pavement against deformation (Greg Arnold, Werkmeister, & Alabaster, 2008).

Overall, the mechanistic-empirical pavement design methodology is a significant improvement over the purely empirical method, however the success of this method still relies on calibrating it against historical performance. This correlation with historical data appears to be due to the use of materials containing predominantly crushed stone aggregates. The complex behaviour of these materials under stress as well as their inhomogeneous nature makes accurately predicting their performance under traffic loadings extremely difficult.

2.1.3. Concrete Pavements

The design of concrete pavements (also known as rigid pavements) is very similar to the design of a granular pavement with an asphalt or chip seal surfacing. The major difference results from the response of the concrete surface to an applied traffic load. Figure 17 (below) shows the distribution of load when the tyre from a vehicle passes over a concrete (rigid) pavement and an asphalt (flexible) pavement (Texas-Department-of-Transport, 2001).

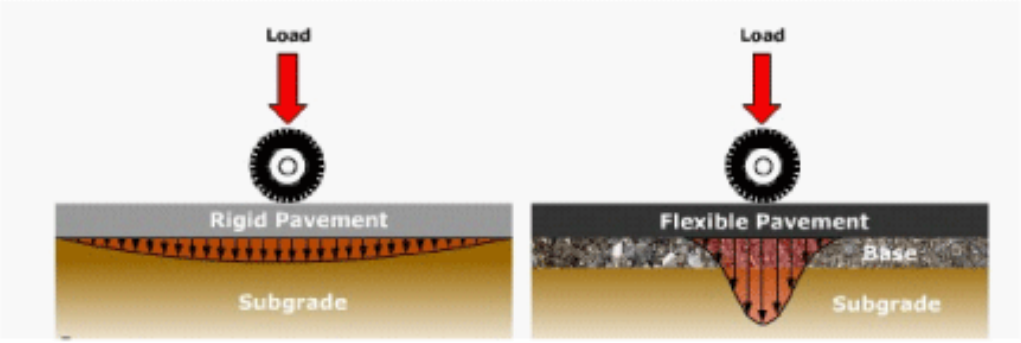

Figure 17 - Typical load distribution in concrete (rigid) and asphalt (flexible) pavements (Texas-Department-of-Transport, 2001).

It can be seen that a rigid pavement is much more effective at spreading the load applied by a wheel than a flexible pavement. This is due to the concrete possessing a significantly higher flexural modulus (~30GPa vs ~5GPa) than the asphalt (Haranki, 2009; Peploe, 2008). This means that any applied traffic stress will produce a lower amount of deformation in the pavement and in some cases will allow the concrete layer to be constructed straight over the subgrade, without the need for the supporting base and subbase course layers (Texas-Department-of-Transport, 2001).

As concrete pavements are much less flexible than their asphalt counterparts (failure strain (tensile) of ~0.01% compared to ~0.5%) the predominant failure mode is cracking. This consideration, coupled with concrete's superior ability to distribute traffic loads over the subgrade, results in a design procedure that focuses more on limiting the flexural stress in the concrete rather than vertical strain in the subgrade (Austroads, 2012).

Concrete pavements are typically cut into slabs after application to ensure thermal stresses do not cause (or contribute to) early failure. To determine the

depth of these concrete slabs, the design procedure typically requires knowledge of not only the traffic volume but also the maximum axle loadings that the pavement is expected to withstand. This is essential to ensure that the predicted fatigue life is within acceptable limits (30-40 years depending on traffic volumes) and the maximum flexural strength is not exceeded (resulting in cracking of the pavement) (Jameson, 2013). Knowledge of the strength of the subgrade is also required, however, the design method still uses the CBR value to determine this, therefore it still relies on empirically derived measurements to determine the overall pavement depth (Austroads, 2012).

To obtain more useful information on subgrade strength, the plate bearing test is employed (in some countries). This test uses a steel plate of known diameter (normally 750mm) to apply an incrementally increasing load to the subgrade. The settlement (deformation) of the subgrade is measured at each load increment until the subgrade begins to settle at a rapid rate. At this point the maximum strength of the subgrade has been exceeded and it will begin to fail (Figure 18). This is referred to as modulus of substructure reaction (k) which is determined using Equation 11 (A.A.A Molenaar, 2004; Southern-Testing, 2015).

$$k = P/w$$

Equation 11

Where;

k = Modulus of subgrade reaction (MPa/m)

P = Vertical stress at top of subgrade (MPa)

w = Vertical displacement at top of subgrade (m)

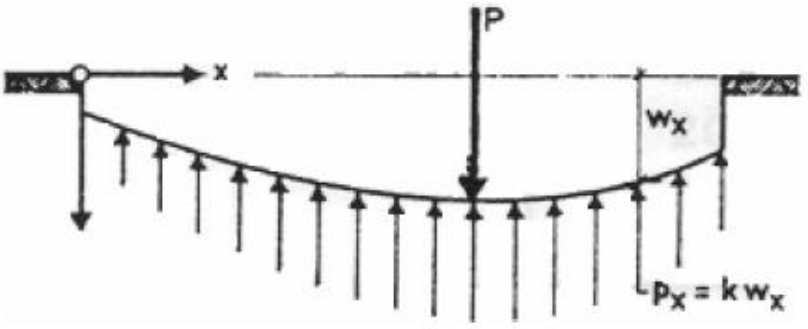

Figure 18 - Definition of modulus of subgrade reaction (A.A.A Molenaar, 2004).

The modulus of subgrade reaction (k) assumes that the subgrade behaves in an elastic manner and its reaction to an imposed stress (p) will be proportional to the deflection of the concrete (w) slab above it.

Table 5- Typical values of k for various types of subgrade (A.A.A Molenaar, 2004).

Subgrade	k_0 (N/mm^3)
Well graded gravel and gravel/sand-mixtures, hardly any fine material	0.08 – 0.13
Poor graded gravel, hardly any fine material	0.08 – 0.13
Gravel/sand/clay-mixtures	0.05 – 0.13
Well graded sand and sand with gravel, hardly any fine material	0.05 – 0.10
Poor graded sand, hardly any fine material	0.04 – 0.10
Sand/clay-mixtures	0.03 – 0.08
Very fine sand, sand with loam	0.03 – 0.05
Vast clay	0.01 – 0.03
Weak clay and peat	0.00 – 0.01

Table 5 shows how the values of modulus of subgrade reaction (k0 in this case) vary with subgrade type. Knowledge of this subgrade reaction determines the amount of support it offers to the concrete slab placed above it, which allows the pavement designer to ensure the depth of the concrete slab is sufficient to

avoid early failure of the concrete (Reynolds, Steedman, & Threlfall, 2007). The bearing capacity (maximum strength) of the subgrade is typically not considered as it has minimal effect on the performance of the concrete. This is due to the rigidity of the concrete offering sufficient distribution of the traffic stresses on to the surface of the subgrade, reducing the likelihood of its bearing capacity being exceeded. The uneven settlement of the subgrade is of concern as it can lead to unevenness of the concrete slabs. This unevenness can cause localised stresses at the edge of the slabs leading to cracking due to increased dynamic vehicle loadings (due to the increased roughness of the pavement) or due to the edges of adjacent slabs impacting one another (A.A.A Molenaar, 2004).

As concrete is a ceramic, it possesses high stiffness yet low fracture toughness. Design of a concrete pavement is concerned with ensuring that cracking does not occur in the slabs. Stresses that are considered to cause this are induced due to curing (shrinkage), thermal expansion and load. As the thermal expansion and curing properties will be very different when applying these calculations to alternative materials, the formulas relating to thermal and curing stresses are not transferable whereas the load formulae could offer some assistance in determining the performance of an alternative material under traffic loading. The most commonly accepted calculations for stresses in concrete were developed by Westergaard (H. Westergaard, 1926; H. M. Westergaard, 1948). For a circular load in the centre of a concrete slab, the tensile stress and deflection at the base of the slab are determined by:

$$\sigma = \frac{3P(1+\upsilon)}{2\pi h^2}\left\{ln\left(\frac{2l}{a}\right) + 0.5 - \gamma\right\}$$

Equation 12

$$w = \frac{P}{8kl^2}\left[1 + \frac{1}{2\pi}\left\{ln\left(\frac{a}{2l}\right) + \gamma - 1.25\right\}\left(\frac{a}{l}\right)^2\right]$$

Equation 13

$$a = \sqrt{\frac{P}{\pi p}}$$

Equation 14

$$l = \sqrt[4]{\frac{Eh^3}{12(1-\upsilon^2)k}}$$

Equation 15

Where:

σ = Flexural tensile stress (MPa)

w = Deflection (mm)

P = Single wheel load (N)

p = Contact pressure (MPa)

E = Young's modulus of elasticity of concrete(MPa)

v = Poisson's ratio of concrete

h = Thickness of concrete layer (mm)

k = Modulus of substructure reaction (MPa/mm)

a = Radius of circular loading area (mm)

l = Radius of relative stiffness of concrete layer (mm)

γ = Eulers constant (=0.5772156649)

From Equation 12 above, it can be seen that the properties that reduce the flexural tensile stress are:

- An increase in height of the concrete slab (h)
- Reduction in load applied at the surface (P)
- Increase in stiffness of underlying layer (modulus of subgrade reaction, k)
- Increase in contact area (a)

Factors that reduce deflection of a concrete slab, as outlined in Equation 13, are:

- An increase in height of the concrete slab (h)
- Reduction in load applied at the surface (P)
- Increase in stiffness of underlying layer (modulus of subgrade reaction, k)
- Increase in contact area (a)

Despite the much lower maintenance costs of concrete pavements, asphalt pavements are typically preferred in New Zealand due to their lower initial cost.

New Zealand's low traffic volume also makes concrete pavements hard to justify as nominal service lives would suggest that concrete pavements only last 10 years longer than asphalt pavements (20-30 years for asphalt, 30-40 years for concrete) (Austroads, 2012; Gribble, Patrick, & Land Transport, 2008).

3. Other Considerations

The previously discussed design methods have been developed for a specific set of materials. As only certain material properties are evaluated under these design methods, benefits that alternative pavement materials may bring will not be considered. The following sections consider the fundamental requirements of a pavement to identify other key material properties required of an alternative pavement material.

3.1.1. Beams on Elastic Foundations

As previously discussed, the loads imposed on a pavement are applied through the wheels of the vehicles travelling upon it. The forces applied to bound materials in a pavement (such as asphalt, concrete and cement stabilised basecourse) due to traffic are similar to loading of a loading a beam (Ruiz, Rasmussen, Chang, Dick, & Nelson, 2005; Yoder & Witczak, 1975). With every pass of a vehicle the pavement layers will deflect in a manner similar to those previously observed in Figure 7. The degree of this deflection will depend on the axle loading. In New Zealand the maximum allowable axle loading (without special permit) is 8200kg which equates to ~80.4kN or 20.1kN per wheel (NZTA, 2013).

Assuming the pavement is a beam supported at either end (as per Figure 19), conventional elastic beam theory (Equation 16) would allow for the calculation (by integration) of deflection (Equation 17) and therefore stresses and strains occurring along the beam for a given load (F) (Ashby & Cebon, 2004).

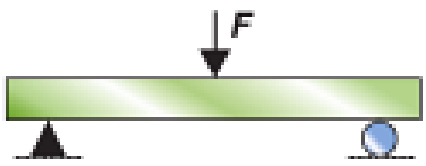

Figure 19 - Schematic of beam supported at either end (Ashby & Cebon, 2004).

$$EI\frac{dy^2}{dx^2} = M$$

Equation 16

Where:

E = Youngs Modulus

I = Moment of Inertia

y = Lateral deflection

x = distance along length of the beam

M = Bending moment

$$\delta = \frac{Fl^3}{48EI}$$

Equation 17

Where:

F = Applied load

δ = Deflection

l = length of the beam

This loading condition would occur if the underlying layer is very weak or deformation (due to repeated traffic loading) of the underlying layer is so significant that it is no longer able to support the beam through its mid-section. In most ideal cases the beam is supported across its entire length by the underlying formation. If a significant amount of plastic deformation occurs in the underlying pavement, the support of the surfacing material is reduced. This results in the surface deforming to the shape of the underlying pavement (as per Figure 20). The strain in a 40mm surface that has deformed to the shape of the underlying pavement can be calculated using the same formula used to calculate the length of the arc in a chord as follows.

$$S = R\theta$$

Equation 18

Where:

s = the length of the arc

R = radius of curvature

$$R = \frac{[rut\ depth]}{2} + \frac{[rut\ width]^2}{8 \times [rut\ depth]}$$

Equation 19

θ = angle

$$\theta = 2\ sin^{-1} \frac{[rut\ width]}{2R}$$

(Equation 20)

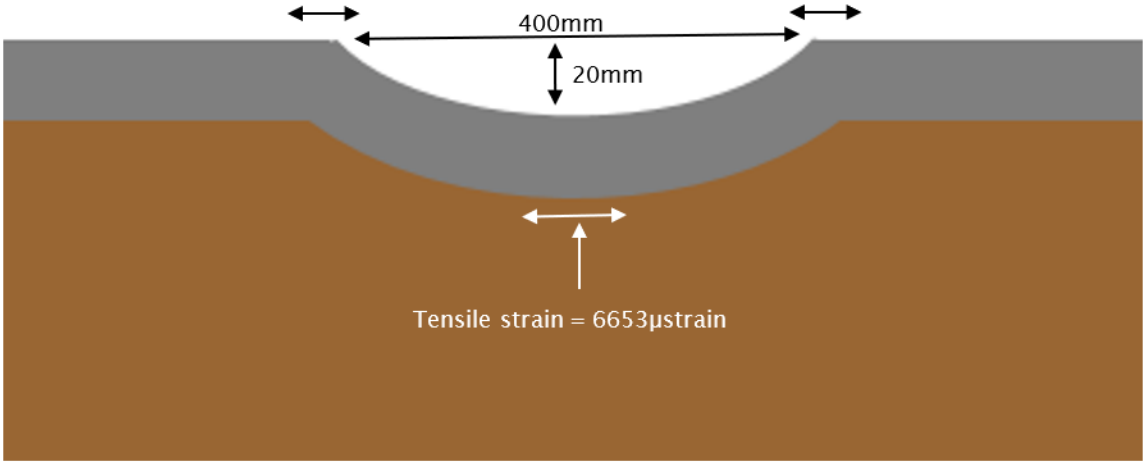

Figure 20 - Mechanism for deformation of asphalt surfacing due to weakness in the underlying pavement.

Application of this concept shown in Figure 20 allows the optimum flexural strength and strain of potential alternative materials to be considered and ensure that it is capable of being placed over a known subgrade strength without the risk or failure by cracking either by bridging pavement weakness or by being flexible enough to cope with the deformation.

3.1.2. Mechanical Properties

The typical values for certain mechanical properties of both asphalt and concrete are listed in Table 6 below.

Table 6: Typical mechanical properties for current pavement materials.

Mechanical Property	Compacted Basecourse	Asphalt	Concrete
Flexural Modulus (GPa)	0.15-1[1]	3-6[2]	20-35[3]
Compressive Strength (MPa)	0.7-1.5[4]	1-2[7]	20-40[8]
Tensile Strength (MPa)	0.1-1.7[13]	0.9-1.6[5]	2-5[6]
Elongation (%, tension)	N/A	0.4-0.6[9]	0.01[10]
Fracture Toughness (MPa $m^{1/2}$)	N/A	0.6-1.6[11]	0.8-1.1[12]
Poisson's Ratio	0.2[8]	0.35[8]	0.15[8]

1 = (Austroads, 2012)

2 = (Peploe, 2008)

3 = (Haranki, 2009)

4 = (Vorobieff, 2004)

5 = (Richardson & Lusher, 2008)

6 = (Olanike, 2014)

7 = (Berthelot, Crockford, & Lytton, 1999)

8 = (A.A.A Molenaar, 2004)

9 = (Prowell, 2010)

10 = (Swaddiwudhipong, Lu, & Wee, 2003)

11 = (Kim & El Hussein, 1997)

12 = (Abdel-Fattah & Hamoush, 1997)

13 = (Greg Arnold et al., 2012)

By comparing the properties outlined in Table 6 to the common pavement failure modes listed in Table 1, we are able to develop some insight into the mechanical properties that are required of a pavement material.

As asphalt does a poor job of distributing the stress imposed by traffic (when compared to concrete) it would be reasonable to suggest that an alternative material would require a flexural modulus similar to that of concrete (~20GPa) or at least greater than that of asphalt.

The compressive strength of asphalt is very dependent on the temperature and the presence of confining pressure. For comparisons sake, the compressive strength results of asphalt and concrete are of unconfined materials at 20°C. The compressive strength of both the asphalt and concrete are parameters that are seldom considered during the design process. This is interesting in the case of asphalt as it fails in compression (forming ruts in the road). Concrete does not have this issue therefore; compressive strength is considered to be sufficient. If we compared the values of compressive strength for both of these materials it becomes quite obvious that the compressive strength of asphalt (1-2MPa) is over tenfold lower than concrete (20-30MPa). This would suggest that the compressive strength of an alternative material would need to be closer to that of concrete to avoid the rutting that is observed in asphalt pavements.

Cracking of the surfacing layer is a failure mode common to both asphalt and concrete (A.A.A Molenaar, 2004; Patrick, Arampamoorthy, Kathirgamanathan, & Towler, 2013). This typically results from a loss of structural support of the surfacing layer therefore if an asphalt or concrete is to resist cracking it must possess sufficient flexural strength to bridge this loss in support. In this case tensile strengths have been compared as there is very little literature on the flexural strength of asphalt. The asphalt has a much lower tensile strength (0.9-1.6MPa) than concrete (2-5MPa) however this is not normally a concern as the much higher flexibility of the asphalt (0.4-0.6% strain elongation in tension) allows it to deform to match the underlying layer and regain its support. A further loss in support will result in cracking, however the flexibility of this material offers somewhat of a buffer zone before this failure occurs. The much higher tensile strength in concrete allows it to bridge any loss in support, however this will cause an increase in stress at the bottom the concrete layer increasing its low fracture toughness (0.8-1.1Mpa $m^{1/2}$) increases the likelihood of the critical fracture stress being exceeded which would result in cracking of the concrete, without any prior deformation (as seen in asphalt) due to its low flexibility (~0.01% elongation in tension). This would suggest that an alternative material needs high tensile (preferably flexural) strength and high fracture toughness (if brittle in nature) to ensure the pavement is strong enough to bridge any loss in support and avoid failure due to cracking.

The fatigue properties are also of interest for both materials however these results were not added to Table 6 of as it is difficult to find a comparative method for evaluating the fatigue properties of asphalt against concrete. This is due to the fact that the fatigue of concrete is determined under controlled stress conditions (single repeated, constant load) whereas asphalt is normally evaluated using controlled strain (single repeated, constant deformation). As the pavement is loaded by relatively constant maximum stress (caused by traffic), it would be reasonable to assume that the more appropriate method for evaluating the fatigue properties of an alternative pavement material would be to test it under controlled stress conditions similar to those used for testing concrete.

Comparing the mechanical properties of asphalt and concrete gives an understanding of the critical mechanical properties that an alternative material would require, however it does not offer any defined limits based on actual applied stresses and strains that occur in the pavement and inevitably leads us back down the path of evaluating materials by empirical means. The following section attempts to review the current loading conditions experienced in a pavement using more conventional principles of mechanical design.

3.1.3. Tyre Stresses

The stresses applied to the pavement by a tyre can have a dramatic effect on the life expectancy of the surface of the pavement (Read & Whiteoak, 2003). The typical directions that a stress can be exerted upon the pavement are displayed in Figure 21, below.

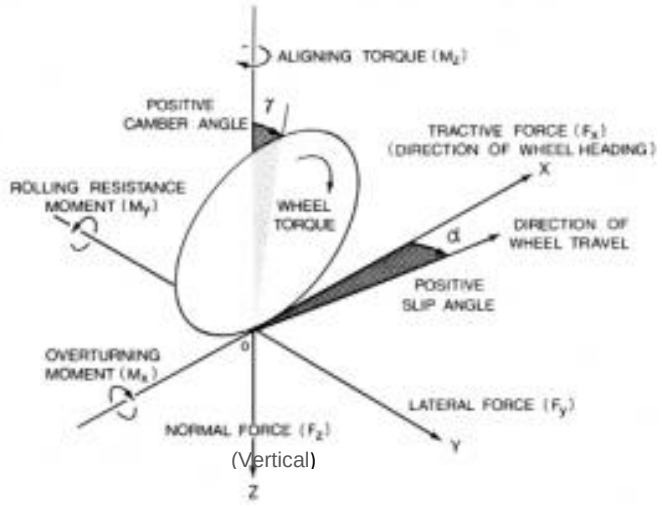

Figure 21 - Typical forces induced by a tyre upon a pavement surface (Tomasi, 2011).

If the stress in any of these directions is greater than the strength of the surfacing material it will lead to failure of the surface and potentially the entire pavement. This is common in pavements that have either thin overlays of asphalt or chip seal. These thin layers do not possess sufficient strength to resist the stresses imposed by a tyre and therefore results in cracking, abrasion or permanent deformation (rutting) of the surface (De Beer, Fisher, & Jooste, 1997).

The current assumption applied to pavement design techniques (discussed previously) is that vertical (normal) tyre stresses have a circular contact, are uniform across the contact area and are equal to (or lower than) the tyre's inflation pressure (De Beer & Fisher, 1997).

Research into this area has revealed that the contact area is non-circular and will increase with increasing axle load or a decrease in inflation pressure. This increase in contact area with axle load or reduction in inflation pressure would suggest that the contact stress would remain constant, however research suggests that the increase in contact area is less than the respective increase in

contact stress. This means that the contact stress increases with both increasing inflation pressure and axle load and is not equal to the inflation pressure, as previously suggested.

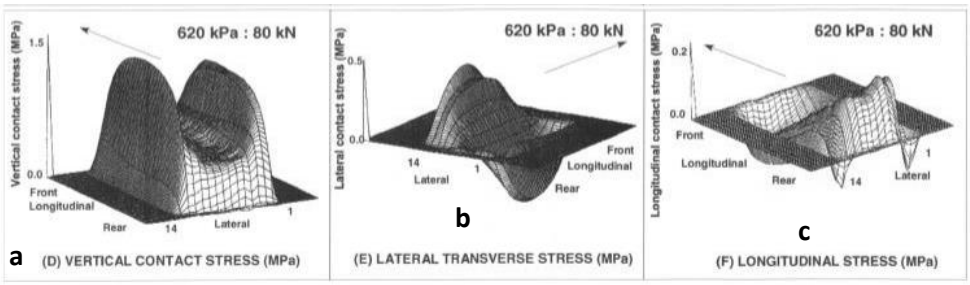

Figure 22 - Measured tyre contact stresses in the vertical (a), lateral (b) and longitudinal (c) directions (De Beer et al., 1997).

Figure 22 shows the typical distribution of stresses imposed by a tyre in the vertical, lateral and longitudinal directions. The vertical contact stresses (directed towards the pavement, a) reveal that the contact stresses are greatest at the centre (in both lateral and longitudinal directions) and at the edges of the tyre (lateral direction). This variation in contact stress is induced by the variation in tyre tread and the degree to which it is inflated. The vertical contact stress is the greatest in magnitude and will be responsible for the majority of plastic deformation occurring at the pavement surface (De Beer et al., 1997).

Lateral contact stresses (those acting normal to the direction of travel, b) are present at the same magnitude directed towards (both left, negative and right, positive) the centre line of the tyre. These lateral forces cancel each other out at the centre of the tyre therefore there is a net zero lateral force at this location on the tyre. It is believed that these lateral forces will cause a tensile stress to develop in the pavement at the edges of the tyre (De Beer et al., 1997; Read & Whiteoak, 2003).

Finally, the longitudinal contact stresses (c) are the smallest in magnitude. At the front of the tyre these longitudinal forces act in the opposite direction to the direction of travel, whereas in the rear of the tyre the longitudinal forces act in the same direction as the direction of travel. These forces are thought to be due to friction and rolling resistance of the tyre in contact with the road and

would contribute to abrasion of the surface (De Beer & Fisher, 1997; De Beer et al., 1997; Douglas, Werkmeister, & Gribble, 2009).

Table 7: Typical measured tyre contact stresses (Beer, 1996).

TEST NUMBER	TYPE OF STRESS	A STRESS (kPa)	B INFLATION PRESSURE (kPa)	MEASURED LOAD (kN)	RATIO A/B
1	Vertical maximum (side wall)	1 234	620	60	2
1	Vertical (centre of tyre)	798	620	60	1,15
32	Vertical maximum (side wall)	1 551	620	80	2,5
32	Vertical (centre of tyre)	788	620	80	1,27
2	Maximum transverse	444	620	60	0,72
3	Maximum longitudinal	93	620	60	0,15
6	Maximum longitudinal	102	620	60	0,17
9	Maximum longitudinal	83	620	60	0,13
18	Maximum longitudinal	178	620	60	0,29

Table 7 shows typical tyre contact stresses that have been recorded in each of the three coordinate directions (vertical, transverse/lateral and longitudinal). It should be noted that the vertical contact stress at the centre of the tyre is greater than the inflation pressure and twice the inflation pressure at the side walls of the tyre. This shows that the assumption that the contact stress of the tyre to be equal to the inflation pressure would grossly underestimate the compressive strength requirements of a pavement material (De Beer, Fisher, & Jooste, 2002).

The ratio of these relative stresses for an average truck tyre was determined to be approximately 10:1.5:1 (vertical:lateral:longitudinal) (De Beer et al., 2002). To cover all potential tyre and axle loading combinations an alternative material

would need to have sufficient compressive strength to resist the maximum vertical stress of ~1500kPa and a shear strength of at least 450kPa to resist both lateral and longitudinal contact stresses. Interestingly, the typical values for compressive strength of asphalt (1000-2000kPa, Table 6) reveals that it is very similar to the vertical stress that is applied by the tyre (~1500kPa). This would suggest that the vertical stress that a tyre could potentially impose upon an asphalt, would result in permanent deformation (rutting). This would explain why permanent deformation is not an issue in concrete as its compressive strength is significantly higher (20-40MPa) than the vertical stress imposed by a tyre.

The values discussed above relate to measurements for stationary and slow-moving vehicles. Another major consideration for pavement loadings is the stresses induced by cornering and braking of a vehicle. Current research would suggest that the tyre stresses induced by braking can increase the longitudinal contact stress by ~120kPa immediately after the brakes are applied. This value is dependent on the speed and mass of the vehicle as well as the coefficient of friction of the pavement surface (Yamashita, Matsutani, & Sugiyama, 2015). An increase in lateral contact stress will also occur when a vehicle attempts to manoeuvre a corner. This increase in contact stress is again dependent on the speed and mass of a vehicle as well as the inflation pressure. As a vehicle proceeds around a corner the weight of the vehicle shifts to the wheels nearest the outer radius of the curve. This results in an increase in vertical and lateral force over the tyres nearest the outer edge of the curve. Measured values for lateral force would be in the order of 25kN for a truck and 5kN for a car (Cenek et al., 2011). The increased vertical force on the tyre would increase the contact area therefore, the lateral contact stress would be dependent on the inflation pressure and mass of the vehicle. There is a lack of data for determining the contact area during cornering however if the worst case scenario is assumed (contact area during cornering is the same as the static value of 158mm x 200mm) lateral contact stress of a cornering truck would be approximately 790kPa (Cenek et al., 2011).

The amount of shear stress caused by a stationary wheel turning on the pavement surface (such a case arises when manoeuvring to park a vehicle) is also worth considering. This is normally termed 'screwing' of the tyres and can be responsible for the abrasion of some pavement surfaces. Literature would suggest that the turning torque under a static wheel is around 170N.m which equates to a maximum shear stress of ~56kPa (assuming a simplified contact area of 250mm in diameter). This value depends on inflation pressure and the coefficient of friction of the pavement surface. A low inflation pressure and a high coefficient of friction will generate a greater 'screwing' stress at the surface of the pavement (Sharp & Granger, 2003).

Overall, an alternative pavement material will need to have a compressive strength much greater than 1500kPa (to resist the formation of ruts in the wheel paths) and a shear strength of over 800kPa to ensure that it will not fail due to the screwing, cornering and braking stresses imposed by a tyre.

3.1.4. Chemical Properties

Pavements are typically expected to last at least 25 years. During this period, portions of the pavement are exposed to water, heat, air and solar radiation; all of which can cause some form of chemical degradation to certain materials.

When designing a pavement using current pavement materials, water is considered a major cause of degradation. This is due to the current materials predominantly consisting of crushed stone aggregate, where excessive water will cause erosion of the pavement and significantly reduce its mechanical properties (Duong et al., 2015). Average rainfall in New Zealand ranges from 600-1600mm (Mackintosh, 2001) by region therefore it would be expected that an alternative pavement material would need to be able to resist the effects of water such as corrosion and erosion.

Pavement materials containing bitumen (such as asphalt and chip seal) are susceptible to oxidation making the bitumen brittle and prone to fracture (Read & Whiteoak, 2003). In New Zealand, pavement temperatures can be in excess of 50°C (Jackson, Peploe, & Vercoe, 2003) with the lowest temperature as low

as -25.6°C and a maximum temperature approaching 70°C, based on an air temperature of 42.4°C and using Equation 21 (Major, 1965; NIWA, 2016).

$$T_p = 1.7905T_{air} - 80.0981$$

Equation 21

Materials located at the surface (such as bitumen) of the pavement are not only exposed to extremes in temperature but also air. These conditions allow for an environment where the bitumen can oxidise, increasing the likelihood of failure due to cracking (Fernández-Gómez, Rondón Quintana, & Reyes Lizcano, 2013). For a material to be considered as a viable alternative to the current pavement materials, it would be preferable that it does not undergo any oxidation at ambient temperatures or, if any oxidation does occur it is not to the detriment of the materials mechanical properties.

Degradation in bituminous surfaces can also occur due to solar radiation (especially UV radiation). Despite significant research into the thermal aging of bitumen (Petersen et al., 1994) there has been little investigation into the effects of UV exposure. Interestingly, one study in particular found that the contribution of UV radiation to the degradation of bitumen was more dominant than the degradation caused by thermal aging (Wu et al., 2008). In New Zealand, pavements are exposed to very high levels of solar radiation (over 325mW/m² in NZ vs global average of ~250mW/m²) therefore the resistance of a material to degradation by UV would need to be taken into consideration when evaluating alternative pavement materials (Liley & McKenzie, 2006; WHO, 2015).

3.2. Critical Material Properties for Alternative Pavement Materials

The current pavement design processes rely heavily on correlating observed performance against the design criteria. This makes it very difficult to evaluate the potential for materials other than aggregate, bitumen and cement to be used as alternatives in a pavement. The basis of a suitable asphalt/chip seal design is primarily weighted toward reducing the vertical strain in the subgrade. This results in an overwhelming focus on increasing the resilient modulus of each pavement layer to ensure that the traffic stresses are reduced at the surface of the subgrade. This approach appears to overshadow other

potential failure mechanisms which result in maintenance to the surface layers.

On the other hand, concrete pavements are able to distribute traffic loadings much more effectively than asphalt, reducing the strain placed on the subgrade. In this application, concretes main drawback is its brittle nature making it more prone to cracking than asphalt. These observations would suggest that asphalt does not possess sufficient stiffness and concrete does not provide sufficient flexibility/fracture toughness to be considered the ideal materials to be used in road construction.

Of the design methods considered, the following aspects could translate to a method for evaluating the feasibility of an alternative material for use in a pavement:

- Soil Mechanics: As the primary function of the pavement is to protect the weaker underlying layers, Mohr-Coulomb theory needs to be a primary consideration for ensuring that an alternative material can sufficiently spread a traffic load over the surface of the underlying layer and therefore avoid shear failure of this material.

- Design of Rigid (concrete) pavements: This gives an insight as to how to evaluate the load spreading ability of a material through consideration of the radius of relative stiffness (l) and its use in the Westergaard equations.

- Simply Supported Beams: Fundamental principles used in the design of both simply supported beams and beams on elastic foundations are also worth considering. The ability to determine the deflection of a beam when it is both simply supported and upon an elastic foundation, allows for the flexural strength/strain of the alternative pavement material to be considered.

- Tyre Stresses: As the surface material will need to withstand tyres stresses of up to 1500kPa, materials used at the surface of an alternative pavement material will need to possess a yield stress of greater than 1.5MPa.

- Chemical Properties: The alternative pavement material also needs to be able to withstand temperatures up to between -25^{o}C and 70 ^{o}C along with maintaining its integrity while being subjected to environmental conditions such as water from rainfall/ground water and ultraviolet radiation from the sun.

The current pavement design methods use relationships developed specifically for certain materials. Certain aspects of theses design methods can be considered for evaluating alternative pavement materials, yet to evaluate the potential use of an alternative material, it is prudent to review the stresses, strains (mechanical properties) and environmental (chemical properties) influences that a pavement will endure during its lifetime. This will ensure suitable alternative materials can be selected to resist all modes of pavement distress.

4. Economic Requirements

To evaluate alternative materials that could be used in pavement construction it is important to understand the costs associated with constructing pavements from the current materials. In New Zealand, costs associated with the pavement are considered over 40 years. These costs include the initial cost of construction along with maintenance costs and any resurfacing or reconstruction that occurs during this time (NZTA, 2016). Failure of a material used in the pavement would increase the whole of life cost of the pavement, therefore it is important to have understanding of the performance of the current materials so that the economic benefit of an alternative material, that offers a lower rate of failure, can be quantified.

This section reviews the process for considering the whole of life cost of a pavement along with the performance of the materials that could affect the costs associated with maintaining a pavement.

4.1. Whole of Life Costs

To establish if a material could be used as a viable alternative in a pavement, it needs to be more cost effective than the current options.

The New Zealand Transport Agency (NZTA) determines if something is beneficial to the travelling public by determining its benefit cost ratio (BCR). A dollar value is attributed to each benefit and if the benefits outweigh the associated costs (benefits:costs > 1) then it is considered to be economically viable (NZTA, 2016). Benefits considered are:

- Travel time cost savings (base travel time and costs due to congestion, ~$23/hr)
- Vehicle operating cost savings (running costs and any increase in running costs due the condition of the surface of the road)
- Crash cost savings
- Comfort and productivity benefits from sealing an unsealed road
- Driver frustration reduction benefits from passing options
- Carbon dioxide reduction benefits

The costs are determined as a whole of life cost using what is called Net Present Value (NPV) analysis. This analysis looks at the whole of life costs over a 40-year period. As society places greater value on short term benefits (rather than long term benefits), a discount rate is applied (of ~6%). This assumes that society would prefer to have $1 today rather than a dollar in a years' time. By applying the discount rate of 6%, a dollar available in a years' time would be equivalent to being given $0.94 today. This would be termed the present value. A basic net present value analysis looks at the cost of:

- Initial construction
- Ongoing maintenance costs to repair the defects listed in Table 1
- Periodic reapplication of the surfacing layer (resurfacing) to improve skid resistance, improve waterproofing
- Reconstructing the pavement (rehabilitation) to repair extensive defects characterised in Table 1.

Table 8 shows the basis for a Net Present Value calculation and the items that determine what is attributed to the whole of life cost of a pavement.

Table 8: Ideal scenario for Net Present Value analysis.

Year	Present Worth ($1/[1.06]^{year}$)	Activity	Activity cost ($/m2)	Present Value ($)
0	1.00	Construction	50.0	50.00
1	0.94			0.00
2	0.89			0.00
3	0.84			0.00
4	0.79			0.00
5	0.75			0.00
6	0.70			0.00
7	0.67	Re-surfacing	4.0	2.66
8	0.63			0.00
9	0.59			0.00
10	0.56			0.00
11	0.53			0.00
12	0.50			0.00
13	0.47			0.00
14	0.44	Re-surfacing	4.0	1.77
15	0.42			0.00
16	0.39			0.00
17	0.37			0.00
18	0.35			0.00
19	0.33			0.00
20	0.31			0.00
21	0.29	Re-surfacing	4.0	1.18
22	0.28			0.00
23	0.26			0.00
24	0.25			0.00
25	0.23	Rehabilitation	50.0	11.65
26	0.22			0.00
27	0.21			0.00
28	0.20			0.00
29	0.18			0.00
30	0.17			0.00
31	0.16			0.00
32	0.15	Re-surfacing	4.0	0.62
33	0.15			0.00
34	0.14			0.00
35	0.13			0.00
36	0.12			0.00
37	0.12			0.00
38	0.11			0.00
39	0.10	Re-surfacing	4.0	0.41
40	0.10			0.00
			Net Present Value ($)	**68.29**

Present Worth Factor is the cumulative annual reduction in value with a discount rate of 6% per annum

Present Worth Factor x **Cost** gives the **Present Value**

Sum of all activities undertaken during the analysis period give the whole of life cost in today's money otherwise known as the **Net Present Value (NPV)**

By undertaking this analysis, it can be determined if a new product is more cost effective over its entire life time than the current option. If it is more expensive over its life time it will need to have additional benefits (as previously listed) that will ensure that it has a more favourable (higher) benefit cost ratio than the existing option. The previous example is a typical NPV analysis for an unbound pavement with a chip seal surfacing using the design lives of the pavement and surfacing. This shows that the whole of life cost of an unbound granular pavement with a chip seal surface is ~$70/m² in today's money. The whole of life cost of this pavement option could be reduced by performing fewer reseals (reseals would need to last longer) or by having a pavement that had a design life longer than 25 years. The other option would be using a material that did not need any maintenance for 40 years and costs less than $70/m² to construct.

The weakness of this evaluation method is that it uses the design lives for the expected life time of both the pavement and surfacing which are assumed or averaged results and will therefore greatly underestimate the whole of life cost (NPV) of the existing option. It is therefore very important that the NPV analysis uses realistic life expectancies for the current techniques to ensure that potential development products are compared fairly and their true economic value can be appreciated.

4.2. Life Expectancies and Failure Modes

In order to compare the whole of life costs of a development product against an existing product, it is important to understand how and when the existing products will fail. Surfacings that have a shorter life span will require a greater investment to maintain operation over the life of a pavement. The most common failure modes are also of interest to us as this allows for identification of problematic issues and allows for our development of a product that targets this particular issue. Figure 23 adapted information from number of source to show the likelihood of failure over time for common pavement materials (Ball, 2005; Giblett, 2012; Patrick et al., 2013).

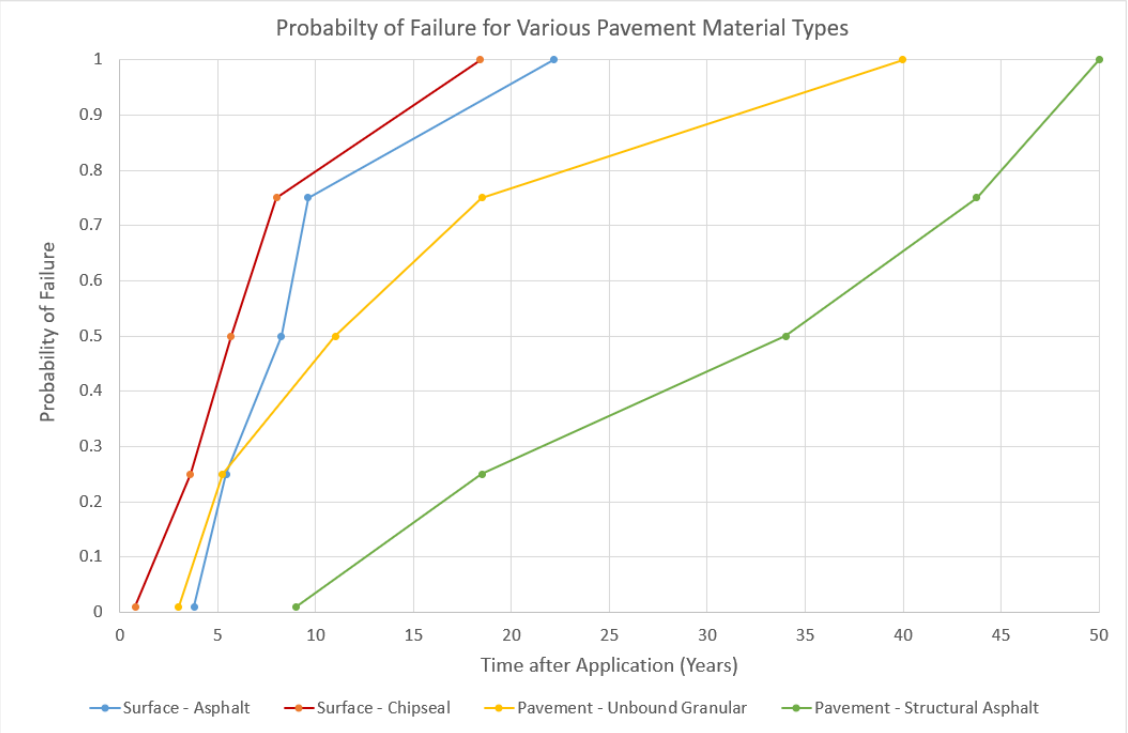

Figure 23 - The range of lives achieved by current materials and construction practices.

This graph shows that the likelihood of failure for all materials used in the pavement will increase with time. The graph considers both materials that have been used in the upper surfacing layer (Asphalt and Chip seal) and materials that have also been used to construct the lower layers of the pavement, Unbound Granular (Basecourse) and Structural Asphalt (thicker layer of asphalt of >100mm). Failure of the current pavement materials does not occur at a well-defined point in time but over a large range of time, spanning decades. This adds significant amounts of risk when making economic decisions as the point in time where the material needs to be replaced will have a large effect on the whole of life cost of the pavement (as shown in Table 8). The impact of Figure 23 will be discussed in more detail in the following sections.

4.2.1. Chip Seal

Around 60,000km of New Zealand's roads are chip sealed with about 10% of this resealed every year. Around 8% of these seals will need to be resealed within a year (Ball, 2005).

Chip seal lives are dependent on seal type and traffic volumes. Most NPV calculations would assume that a chip seal will last from 7-9 years (for a typical seal, Grade 3 chip with a single coat of bitumen trafficked by ~5000 vehicles per

day, vpd). Figure 23 shows that after 7 years, around 70% of all chip seals have failed with 25% of these failing before 4 years (Ball, 2005). This large variation in life is most likely due to a number of other factors however, it shows that there is a significant probability that the seal would need to be replaced much earlier than 9 years and that using the average life of a seal in any whole of life costing exercise will suggest that it is more cost effective than it really is. The need to resurface a pavement can add significant costs to the life cost of the pavement. In order to reduce these costs, it is important to understand the failure modes that are resulting in replacement of the surface. The graph below shows the most common reasons for all chip seals needing to be resealed as well as chip seals that have failed early in their lives after less than 2 years (Ball, 2005).

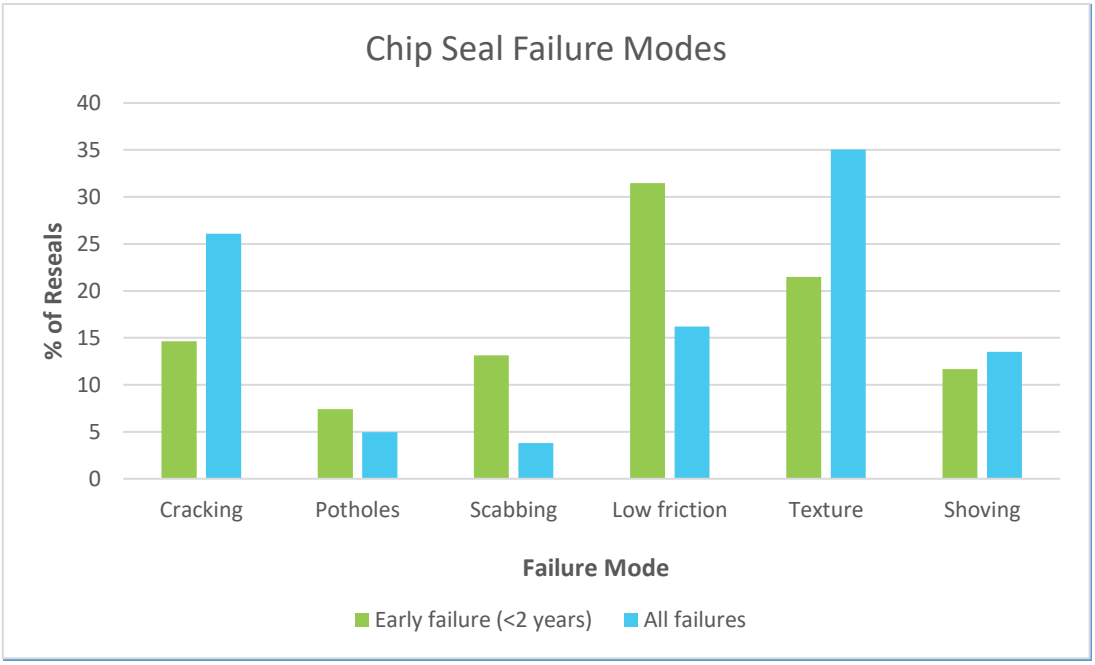

Figure 24 - Common failure modes of chip seal in New Zealand (Ball, 2005).

Figure 24 shows that chip seals that fail early (less than 2 years after sealing) are more likely to fail by scabbing (~3.5 times as likely), potholes (~1.5 times) or low friction (~2 times) than what would be expected in seals that last longer than 2 years. In the case of low friction, it is most likely due to sealing over a chip seal that is already flushed. This results in the flushing progressing into the new seal. Scabbing is more likely to be due to late season sealing (where cold temperatures in autumn would cause poor adhesion between aggregate and binder) or too low application rate of binder (not enough contact between the

bitumen and aggregate to hold it in place). Potholing early in the life of chip seal is common due to poor adhesion of the first layer of bitumen placed upon dusty compacted basecourse. These failures not only require replacement of the surface much earlier than expected, but also increase the likelihood of early failure in subsequent seals which significantly increases the whole of life cost of the pavement. Alternative materials that reduce the chance of these early failure modes would not only save the cost of rework but also reduce the future costs of maintaining a pavement.

The most common failure mechanisms for seals lasting longer than 2 years are:

- cracking (26%)
- loss of texture (35%)
- low friction (16%)
- shoving (14%).

Low friction and loss of texture could both be attributed to flushing and therefore could account for 51% of failures in a chip seal. The high rates of cracking and shoving would not be attributed to the chip seal itself but rather due to deficiencies in the underlying pavement. Considering this, cracking in a chip seal would be due to a weak pavement (high deflections/pre-existing cracking that reflects though the new seal) whereas shoving in a chip seal is caused by shear failure of the basecourse layer.

Overall the major issues for chip sealed surfaces are cracking, flushing and shear failures. Solutions to these problems require the affected pavement to be replaced therefore there is opportunity to develop more cost-effective solutions.

4.2.2. Asphalt

A significantly smaller proportion of New Zealand's 92,000km of roads are asphalt (~6000km) and around 200km of this is motorway (~0.2%) (NZTA, 2010). Application of asphalt typically cost 4 times the price of chip seal and is typically only recommended on pavements carrying >10,000 vpd (Auckland-Transport, 2014). Asphalt lives are also very dependent on traffic volumes, stresses and the condition of the pavement. The design lives used to justify asphalt expect it to last at least 10 years however Figure 23 shows that the measured lives of an asphalt can last anywhere from 4 to 22 years. A significant portion of asphalt (~25%) lasts less than 6 years (Patrick et al., 2013). In some cases, this means that the whole of life costs of asphalt could potentially be 2-3 times what was originally expected.

In order to identify how the likelihood of failure can be reduced, it is important to understand how the current materials are failing in the first place. Figure 25 shows the most common defects present in asphalts that require resurfacing.

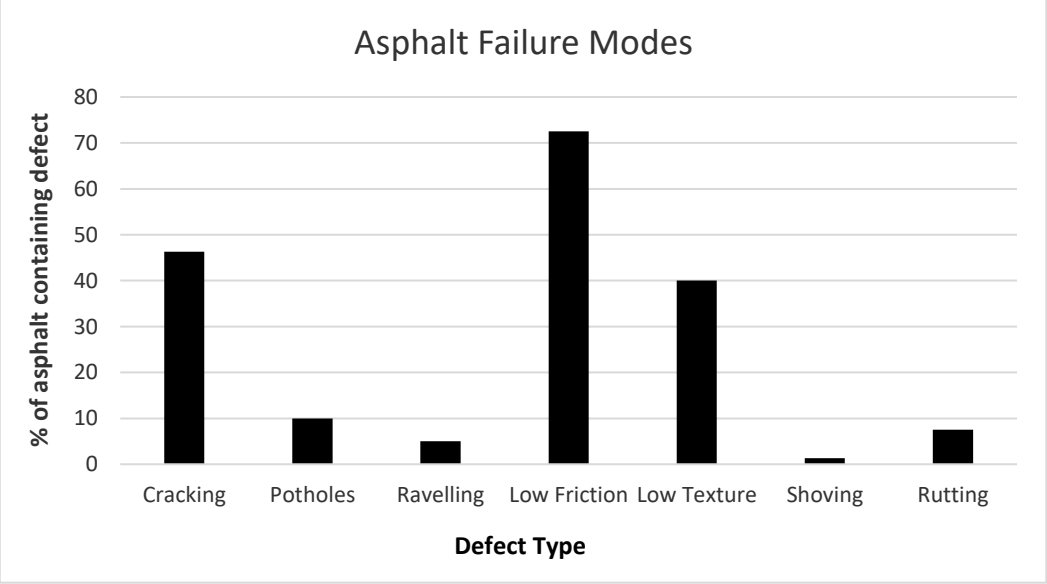

Figure 25 - Common failure of asphalt in New Zealand.

The most common failure modes in asphalt are very similar to that of chip seal where the predominant failure modes are cracking (46%) and low friction/texture (72%/40%). Potholes are typically symptomatic of a cracked surface. The cracking can also be caused by rutting even though it is only listed as the primary reason for resurfacing 7% of the time. This may suggest that specifiers are happy to live with rutting and will only act when cracking of the

surface becomes evident. The prominence of low friction and texture would be attributed to either polishing of the aggregate or migration of the bitumen to the surface due to deformation from repeated traffic loads.

Overall, the prominent failure modes such as cracking, low friction/texture, potholing and rutting are due to the stresses placed upon the pavement being greater than the strength of the materials used.

4.2.3. Pavement

In New Zealand the pavement encompasses all layers (as per Figure 3) and are designed to last for 25 years (Austroads, 2012). An extensive review of achieved pavement lives (similar to what has been undertaken with asphalt and chip seal in the previous sections) has been not been undertaken as of yet (due to the lack of reliable long-term data). There has been some consensus among pavement designers in New Zealand (through experience) as to the expected range of lives obtained by both bound (full depth asphalt) and unbound pavements in New Zealand. The probability of failure for each pavement types (as proposed by the aforementioned pavement designers) are displayed in the table below (Table 9).

Table 9 - Probability of failure for pavements constructed in NZ (Giblett, 2012).

Scenario	Unbound Granular	Structural Asphalt
Early Failure (<5 years)	0.15	0.05
Premature Failure (5-18 years)	0.4	0.1
Predicted Failure (18-33 years)	0.4	0.2
Late Failure (33-50 years)	0.04	0.25
Long Life Failure (>50 years)	0.01	0.4

The values shown in Table 9 show that unbound granular pavement is not expected to reach its design life of 25 years. In this case the group of pavement designers believe there is a 75% chance that it will fail before it reaches its

design life. As reconstructing multiple layers of the pavement (referred to as rehabilitation) is much more expensive than resurfacing it, this will have a much greater impact on the whole of life costs of the pavement. This shows that there is a large risk of early failure when using granular pavements and that there is opportunity for more robust materials to be considered.

One of these (more robust) materials could be considered to be structural asphalt (thick, multi-layered asphalt where the basecourse layer has been replaced with asphalt). Table 9 shows that it is considered to offer less risk of early failure. The group of pavement designers believed that 15% of structural asphalt pavements failed earlier than 25 years. On paper this seems like the smarter option although the upfront cost of this can be 3 times greater than the unbound granular option (Giblett, 2012). This lack of certainty around life span means that road controlling authorities are not always willing to spend extra for performance that cannot be guaranteed. For an alternative material to be considered, it would need to guarantee much greater performance but also be cost comparable to the current options.

In all cases, early failures are costing the country millions of dollars. In this regard there is certainly an opportunity to use more robust pavement materials where failure of the material could be predicted a lot more accurately. This certainty around the life span of the pavement would afford the road controlling authorities better oversight over their budgets and allow targeted funding for pavements that are nearing the end of their life. This would remove a lot of risk associated with pavement construction resulting in huge economic benefits.

The following section focus on highlighting the key properties required of an alternative pavement material which will allow potential materials to be compared to the current options.

The best opportunity to introduce new materials is when the existing pavement comes to the end of its life and needs to be rehabilitated. The majority of pavement rehabilitations involve reconstruction using unbound granular material. Typically this costs anywhere from \$30-\$40/m^2 (Patrick & Aramoorthy, 2012). Approximately 75% of this cost (or \$22-\$30/m^2) is

associated with materials whereas the rest is associated with labour, traffic control and machinery. As the use of unbound granular material requires significant amount of time to construct, there are further savings that could be made through efficiency which could reduce the traffic management, labour and machinery costs.

The use of unbound granular material also carries the risk of early failure. If a pavement fails earlier than expected and needs to be replaced, there is a significant increase in the whole of life cost associated with using that material. Pavements using unbound granular material are designed to last for 25 years (Austroads, 2012) however, due to the inhomogeneous nature of the material it is very difficult to guarantee this in the design phase.

The likelihood of a pavement constructed from unbound granular material failing before its 25 years design life is listed below.

Table 10: Probability of failure for pavements constructed of unbound granular materials in NZ (Giblett, 2012).

Scenario	Probability of Failure
Early Failure (<5 years)	0.15
Premature Failure (5-18 years)	0.4
Predicted Failure (18-33 years)	0.4
Late Failure (33-50 years)	0.04
Long Life Failure (>50 years)	0.01

Table 10 reveals that it is extremely unlikely that a pavement constructed from this material will reach its design life as it is expected that over 50% of pavement will fail before this point, therefore its whole of life cost is actually much greater than the initial cost incurred at completion of construction. The NPV analysis below (Table 11) uses the NVP analysis values from Table 10 to show the effects of early failure on the whole of life cost of the pavement.

Table 11: The failure on the whole of life cost at various stages in the life cycle in a pavement.

Scenario	*Year*	*Discount*	*Type*	*Cost ($/m²)*	*NPV (Cost x Discount)*	*Probability of occurring*	*Adjusted NPV (NPV x probability of occurring)*
Early Failure	2	0.89	Rehabilitation	30.0	26.7	0.15	4.00
Premature Failure	12	0.50	Rehabilitation	30.0	14.9	0.4	5.96
Predicted Failure	25	0.23	Rehabilitation	30.0	7.0	0.4	2.80
Late Failure	42	0.09	Rehabilitation	30.0	2.6	0.04	0.10
Long Life Failure	50	0.05	Rehabilitation	30.0	1.6	0.01	0.02
						Total ($/m²)	**12.88**

If the material was robust enough to ensure that it would achieve the design life of 25 years there would be an almost $13/m^2$ saving over using unbound granular material. Considering all of these factors it is assumed that a $35/m^2$ material cost would be viable for consideration as an alternative pavement material. This analysis does not take into account any reduced maintenance required. Typically, ~1% of the initial cost of the pavement is spent on maintenance of the pavement every year (Patrick & Aramoorthy, 2012). If this cost is also added to an NPV calculation it would add another $4/m^2$ to the whole of life cost/m^2. If these costs are considered properly and an alternative material was able to perform for 25 years without requiring maintenance, it is feasible that another $17/m^2$ could be added to the initial cost of the pavement.

5. Geometric Requirements

5.1. Current State

Rehabilitation of a pavement in New Zealand is normally performed on the full width which can be anywhere from 7.5m to 12m wide with typical lane widths of 3.5m (Cottingham, 2017), defined by the distance from the edge line to the centre line of the road. This can be seen in Figure 26 below.

Vehicles per day	Lane characteristics			
	Lane width	Shoulder width	Gravel strip	Total width
>4000*	>3.5m	>1.5m	>0.5m	<12m
2000-4000	3.5m	1.5m	0.5m	10m
500-2000	3.5m	0.75m	0.5m	8.5m
<500	3.3m	0.2m	0.5m	7m

*If funding allows, the road width can be up to 12m.

Figure 26 - Typical road/lane widths in New Zealand (reprinted from (Cottingham, 2017).

In any pavement the majority of the distress will occur in the wheel paths of a lane. The wheel paths vary from vehicle to vehicle, however an average truck in New Zealand would be 2.5m wide (NZTA, 2014) with dual tyres each approximately 355mm wide (Dunlop, 2017). An average car is 2m wide (automobiledimension.com, 2017) with tyre widths of around 300mm (Dunlop, 2017). Traffic will also not follow exactly the same line as the vehicle before it (referred to as traffic wander) and therefore certain areas are trafficked more frequently than others. Research has found that, on average, vehicles will travel 1m away from the edge line and wander up to 580mm (95th percentile of all readings) either side of centre of the vehicle, which can be seen in Figure 27 (Buiter, Cortenraad, Van Eck, & Van Rij, 1989; Stempihar, Williams, & Drummer, 2009; D. H. Timm & Priest, 2005).

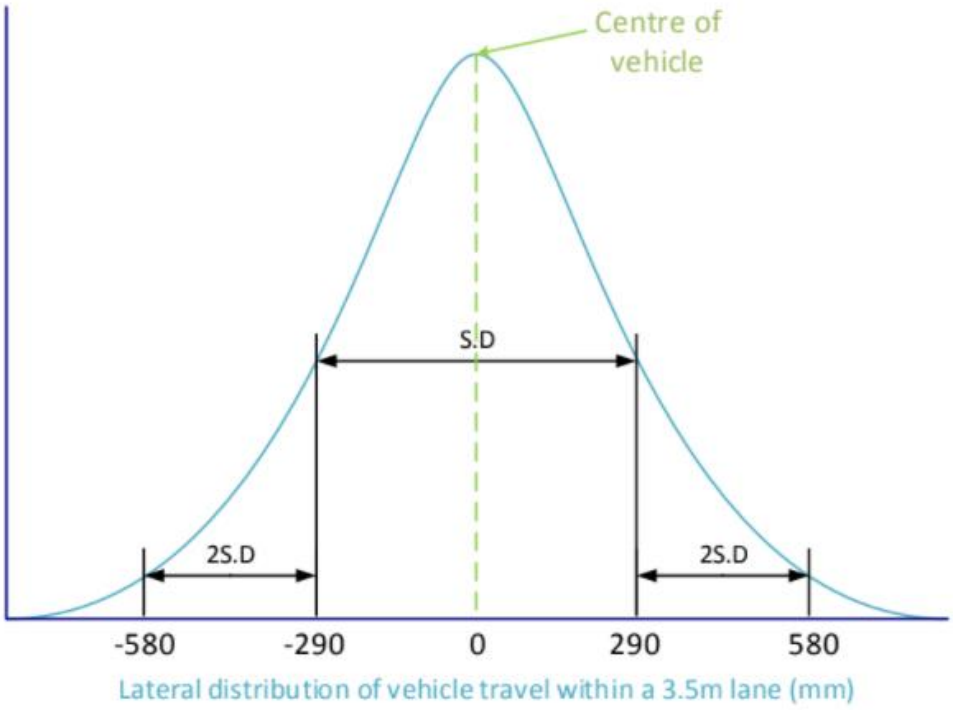

Figure 27 - Typical lateral distribution of wheel passes within a 3.5m lane (Buiter et al., 1989).

Considering Figure 27, it can be seen that 68% (S.D) of wheel passes from truck traffic will vary by 290mm either side of the centre line of the vehicle. 95% of passes would occur within 580mm either side of the vehicle centre line. Considering this alongside the typical width of a truck it would be expected that over two thirds of truck traffic would travel over 3m (vehicle width + 2xS.D = 3.08m) of the lane width. Using the same approach, 95% of wheel passes could also be considered to travel up to 3.66m over a 3.5m lane. The greater lateral wander than the width of the lane is not surprising considering traffic does not always drive within the designated road markings.

Considering this information, it is feasible that only the lane widths could be rehabilitated if the road width is sufficient (greater than 7.3m due to the 3.66m of truck wander). If only the lane widths were to be rehabilitated, anywhere from 1.1-4.6m of the width of the road could be left undisturbed. This could save anywhere from 13-40% of the cost of a rehabilitation.

Rehabilitation of only the lane width is currently difficult when using unbound granular materials as the discontinuous nature of the material makes it very difficult to ensure quality of construction when any other configurations are

attempted. There is potential that using alternative materials that are more continuous may allow for smaller and more targeted reinforcing of the pavement.

5.2. Future State

It is predicted that sometime between 2040-2050 the majority of cars will be driverless (Davidson & Spinoulas, 2015; Litman, 2017). Autonomous Vehicles (A.V's) will use an array of sensors to help with guidance on the road. The majority of the current sensors use mapping to determine their position on the road and therefore will standardise the travel of a vehicle. This will remove the vehicle wander experienced with human drivers which could allow for lane widths to be reduced by 25% (Bowman, 2016).

Currently, traffic moving at free-flowing speeds will only use around 11% of the lane length. The rest of the lane is taken up by gaps between vehicles to ensure the driver has enough reaction to brake unexpectedly. An autonomous fleet could reduce the distance between cars with some theoretical models suggesting the capacity of roads could be doubled by using shorter following distances allowed for by advanced sensors on autonomous vehicles (Pinjari, Augustin, & Menon, 2013).

Congestion is mainly caused by unexpected braking, or changes in speed from driving errors due to inattentiveness by a human driver. In the U.S, 25% of traffic congestion can be attributed to accidents. A fully autonomous fleet is expected to remove human error and therefore the technology is expected to reduce accidents and relieve congestion (Pinjari et al., 2013).

The reduction in pavement width and the increase in capacity it is expected that demand for the current construction materials could decline by a third or more (Bowman, 2016). This is speculation at the moment and could very well be the antithesis of this scenario where the increased traffic density and channelising of traffic (due to reduced wander) from autonomous vehicles could actually put even greater demands on the current materials. Any repairs will need to be undertaken quickly while being able to withstand far greater loading than current pavement materials.

Due to current congestion that can be caused by road construction, a number of regions in America are currently requiring precast concrete to be used to repair high demand pavements, due to its faster construction time (PCA, 2010). The current bituminous and granular materials do not lend themselves to this type of construction due to either their discontinuous nature, in the case of unbound granular materials, or low strength of bituminous materials making the logistics of prefabrication impossible. Use of alternative materials would allow for greater flexibility in materials selection which would permit materials more conducive to prefabrication to be investigated.

Overall, an alternative material would need to be investigated to meet the future demands of higher traffic density and opportunities for prefabrication to ensure that the pavement remains in service or, in the event of failure, can be returned to normal service as quickly as possible.

6. Materials Selection

The previous section shows how pavement design is typically developed based on the materials currently used in practice. As these design principles are very specific to these materials it makes it difficult to use the same design methods to evaluate alternative materials. Of these design principles the Westergaard equations at least show some consideration for basic material properties where there is potential for an alternative material to be considered under this design regime. Bitumen alternatives should also be considered as materials that can be easily blended with aggregate could also be handled, manufactured and applied in a similar manner to a conventional asphalt and could therefore be easily adopted.

The previously mentioned design methods of pavements favour construction of pavements using materials with high elastic modulus to ensure that the underlying substructure is protected from the stress due to traffic. This also assumes that the substructure is homogenous possessing the same mechanical properties throughout. The reality is that areas of the pavement will have regions of inhomogeneity resulting in “soft spots” where the mechanical properties are lower than the bulk of the material and can potentially offer very

little support to the upper layers. This lack of support can cause the upper layers to behave more like a simply supported beam rather than a beam supported by an elastic foundation. As the upper layers have not been designed as a simply supported beam capable of bridging these soft spots, the stress applied to these areas will result in regions of the pavement that will deform much faster than the surrounding pavement. This results in deformation, cracking and subsequent patching of the area. To allow for this in a materials selection analysis it is recommended that the material be capable of supporting traffic loads as a simply supported beam at a span on 200mm (tyre width). Considering this, Figure 28 outlines the key failure mechanisms that an alternative pavement would need to resist.

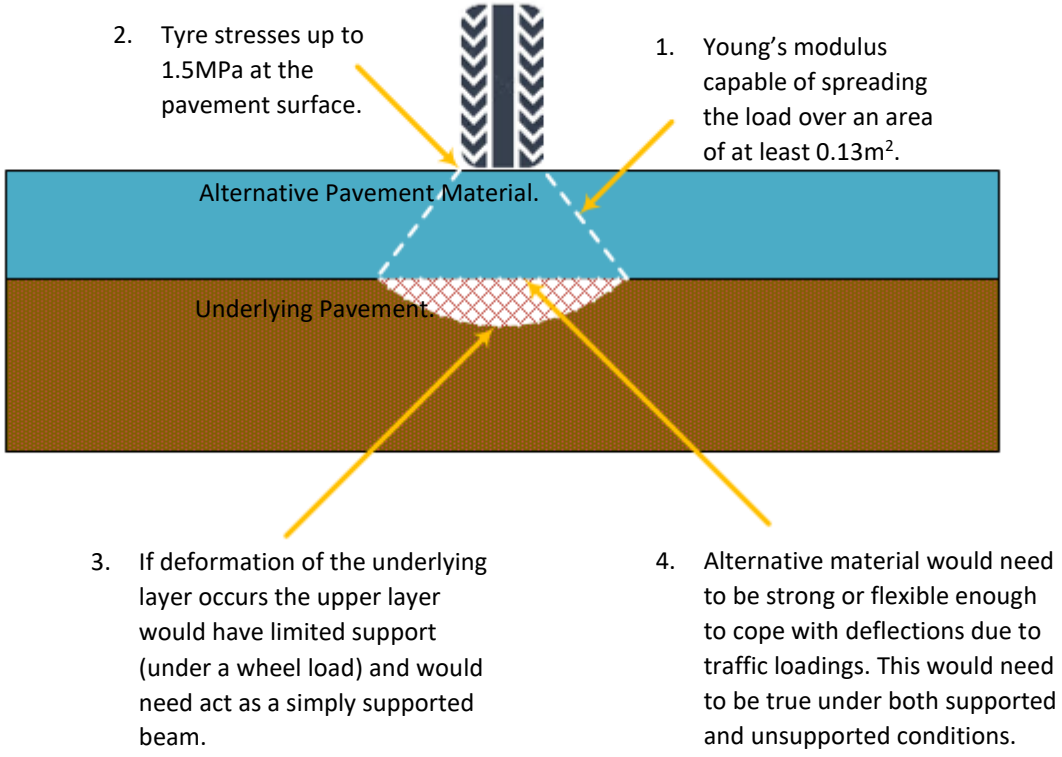

Figure 28 - Key considerations for an alternative pavement material.

1. Alternative material will need to possess a yield strength greater than 1.5MPa to resist failure from tyre stresses at the surface of the pavement.
2. The young's modulus of the alternative pavement material will need to be sufficiently high to ensure that the load is distributed across the surface of the underlying layer. As determined in Section 2.1.1, to avoid shear failure

of an underlying basecourse layer, the area required to sufficiently distribute a truck wheel load is at least 0.13m^2.

3. If the load on the underlying layer were to exceed the shear strength, localised deformation would occur. The maximum allowable depth for deformation in New Zealand is 20mm (where the width of this deformation is approximately 400mm).

4. In the scenario outlined in the previous point (3), a material would need to either bridge this deformation (minimise tensile stress) or be flexible enough to move with the deformed underlying layer (maximum flexural strain).

5. Materials used at the surface would also need to be durable against exposure to water and ultraviolet radiation however in some cases other treatments could be considered at a later date to mitigate this exposure.

6.1. Materials Selection Method

To identify alternative materials for use in pavements the Ashby method was employed (Ashby & Cebon, 2004). This process considers the functional and geometric constraints along with the critical material properties. Using this information, material indices can be used to determine the performance of a material for a given application and aid in the selection of an appropriate material.

$$p = f(F, G, M)$$

Equation 22

Where:

p = Performance

F = Functional requirements

G = Geometric parameters

M = Material properties

Equation 22 is referred to as the performance index. In this case the optimum design uses material properties and geometry to maximise the performance against the functional requirements. As the groups are separable, the

optimum material can be identified that will maximise the performance of the design i.e. the performance of F and G is maximised by maximising M.

The following procedure is normally used to derive performance indices:

- Identify the attribute to be maximised or minimised i.e. weight, cost, stiffness, strength, etc. This is referred to as the objective
- Identity the constraints and rank them in order of importance
- Identify the free (unspecified) variables
- Develop an equation for this attribute in terms of the functional requirements, the geometry and the material properties (the objective function)

The following strategy can then be employed for selection of an appropriate material.

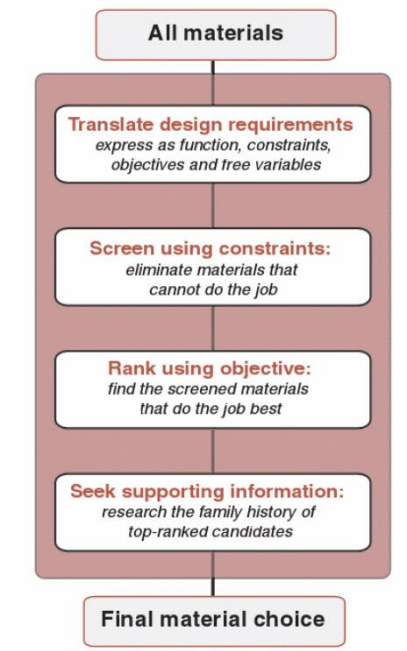

Using the equation derived in the objective function allows appropriate materials to be ranked by comparing the performance (e.g. stiffness) against the objective (weight) as per Figure 29 below.

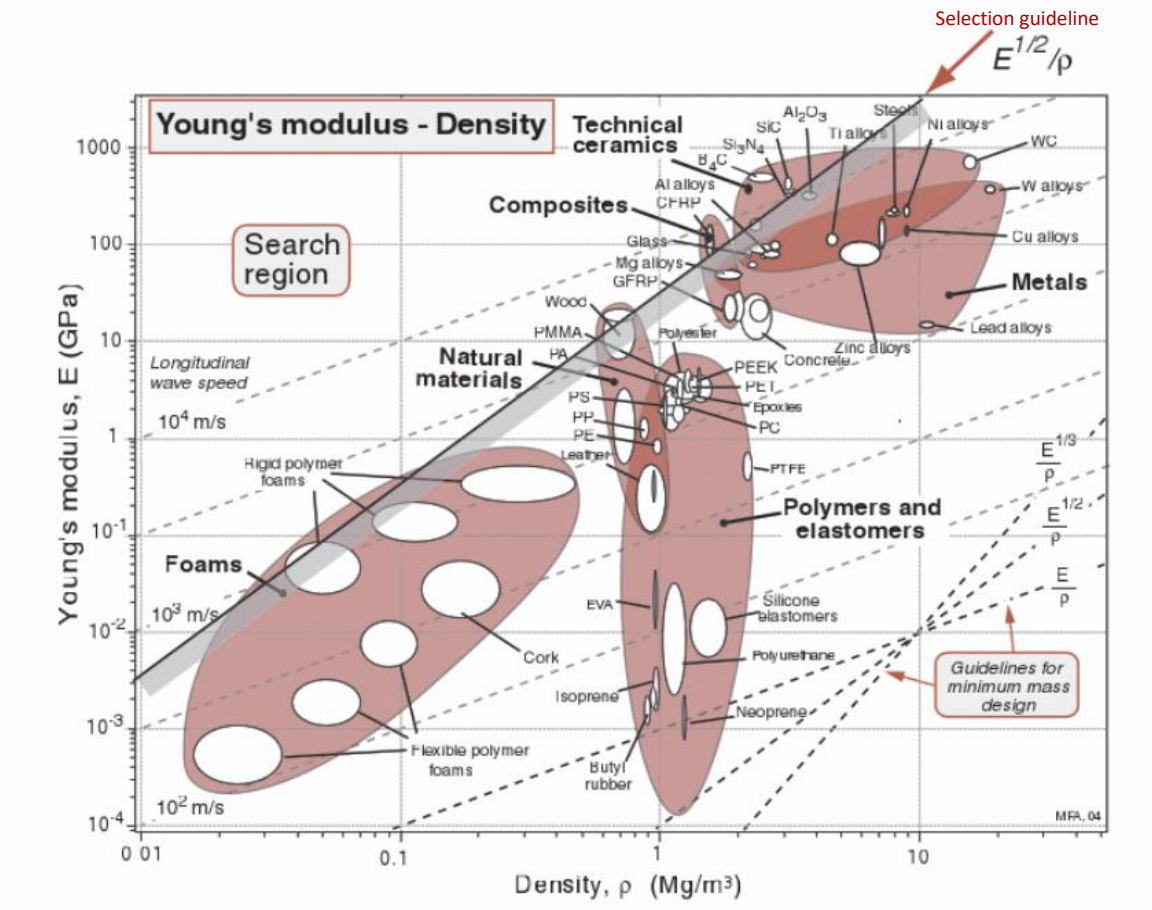

Figure 29 - Typical material selection chart with selection guide lines (Ashby & Cebon, 2004).

Figure 29 shows a typical selection graph comparing the stiffness of a material against density. By applying a selection guideline, materials that lie on this line give equivalent performance against the objective (in this case, stiffness for a given weight). The further above the selection guideline a material lies, the greater the performance of the material, whereas materials below the line will give lesser performance. This allows a subset of appropriate materials to be identified against a defined range.

This process was used to identify appropriate alternative pavement materials under the following scenarios:

1. Material supported by an elastic foundation
2. Material bridging a weak spot in the pavement

Using the scenarios presented above, the following material configurations where considered

a. Substitution of upper pavement layer with bulk alternative material

b. Substitution of bitumen matrix in asphalt with an alternative material
c. Substitution of upper pavement layer with a sandwich panel

The following section uses the materials selection procedure described above to identify materials that offer the greatest performance under Scenarios 1&2 using Configurations a-c.

6.2. Material Supported by an Elastic Foundation (Scenario 1)

This scenario assumes that the upper pavement layer will be continuously supported by an elastic foundation. The material sitting upon this foundation needs to spread the load over a large enough area in order to reduce the stress placed on the foundation and therefore avoid shear failure.

Function: A panel with a defined width (b) and length (L)

Objective: Pavements are typically of a fixed width and length where weight has little bearing on cost other than for transport of the materials to site. The objective is therefore to minimise cost per cubic metre, C:

$$C = hbLC_m\rho$$

Equation 23

Where:

C = cost/m^3

h = panel height

b = panel width

L = panel length

C_m = material cost/kg

ρ = material density (kg/m^3)

Constraint: For an alternative material to be successful under this scenario it needs to sufficiently spread the wheel load across the surface of the underlying pavement (basecourse in this case). To achieve this, the load would need to be distributed over an area of at least 0.13m^2. The design formulae used in the design of concrete pavements (Section 2.1.3) considers the load spreading ability of the material through calculation of the radius of relative stiffness (l). The minimum area of 0.13m^2 can be converted into the critical radius of relative stiffness (l^*) of 0.203m via Equation 24.

$$l^* = \sqrt{A/\pi}$$

Equation 24

To achieve sufficient distribution of the traffic load, the material needs to satisfy Equation 25:

$$l^* \leq \sqrt[4]{\frac{Eh^3}{12(1-\upsilon^2)k}}$$

Equation 25

The material would also need to have acceptable resistance to both UV and water to withstand environmental conditions.

Free Variables: Material choice and panel height, h:

$$h = \sqrt[3]{\frac{l^{*4}12(1-\nu^2)k}{E}}$$

Equation 26

Performance Index: By substituting Equation 26 into Equation 23 the performance index can be determined (Equation 27):

$$C = \left(\sqrt[3]{l^{*4}12k}\right)(bL)\left(C_m\rho\left[\frac{(1-\nu^2)}{E}\right]^{\frac{1}{3}}\right)$$

Equation 27

Equation 28 displays the material index for this scenario where materials with a small M_1 (low cost/kg and density with high Poisson ratio and Young's modulus) being more favourable.

$$M_1 = \left(C_m\rho\left[\frac{(1-\nu^2)}{E}\right]^{\frac{1}{3}}\right)$$

Equation 28

6.3. Material Bridging a Weak Spot in the Pavement (Scenario 2)

This scenario assumes that the upper pavement layer will be bridging a weakness in the pavement and therefore support from the underlying layer

will be limited. In this case the upper layer would be acting as a simply supported beam.

Function: A Panel with a defined width (b) and length (L). The length and width would be considered to be bridging over a span of approximately 400mm.

Objective: To minimise cost per cubic metre (C), as per Equation 23.

Constraint: For an alternative material to be successful under this scenario it needs to:

a. Have sufficient yield stress (σ_y) to be able to bridge the load of a truck (20kN, F) over a weak area in the pavement. Width (b) and length (L) = 400mm, Equation 29.

b. Be flexible enough to accommodate deflections of up to 20mm. % elongation >0.6% strain, Figure 20.

$$\sigma_y > \frac{3FL}{bh^2}$$

Equation 29

Free Variables: Material choice and panel height, h:

$$h = \sqrt{\frac{3FL}{\sigma_y b}}$$

Equation 30

Performance Index: By substituting Equation 30 into Equation 23 the performance index can be determined (Equation 31):

$$C = (3Fb)^{\frac{1}{2}}(L)^{\frac{3}{2}}\left(\frac{C_m\rho}{\sigma_y{}^{\frac{1}{2}}}\right)$$

Equation 31

Equation 32 displays the material index for this scenario where materials with a small value for M_2 (low cost/kg and high yield strength) being more favourable.

$$M_2 = \left(\frac{C_m \rho}{\sigma_y^{\frac{1}{2}}} \right)$$

Equation 32

6.4. Substitution with Bulk Alternative Pavement Material (Configuration a)

By applying Equation 26 and Equation 30 directly to homogenous materials, the most appropriate bulk materials can be determined under Scenarios 1 and 2. Unless otherwise stated, all alternative materials with yield stresses below 1.5MPa and poor durability to water, UV or temperatures below -25^{o}C and above 70 ^{o}C were not considered in this analysis (as identified in Section 3.2).

6.4.1. Scenario 1, Configuration a

To determine homogenous materials that could be used as an alternative pavement material upon an elastic foundation (Scenario 1), materials selection charts where generated using CES Selector (EduPack, 2016) and the material index, M_1 in Equation 28. Figure 30 shows homogenous materials (and their respective material groups) characterised by M_1.

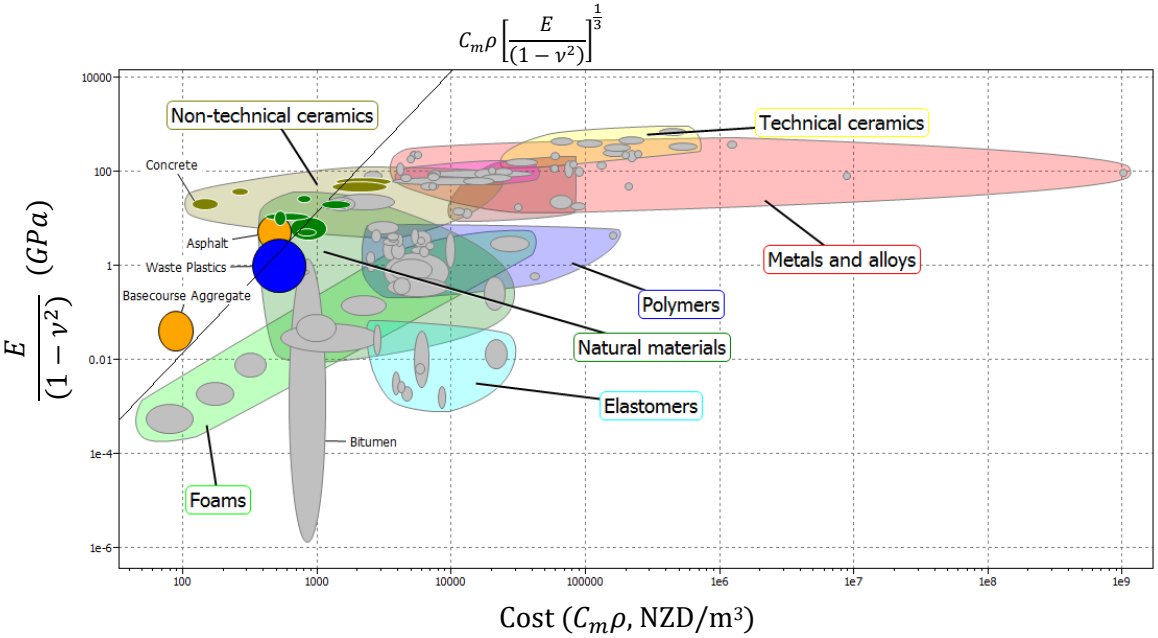

Figure 30 - Potential homogenous, alternative pavement materials for use under Scenario 1 / Configuration a.

By applying a selection guideline with a gradient of 3 (considering the material index, M_1) to the selection chart, materials with equivalent (or greater)

performance than basecourse (used in conventional pavement design) can be identified. Only a limited number of materials met or exceeded the performance of M_1 (materials either on or above the selection guideline). Conventional pavement materials such as asphalt and concrete meet these requirements. Under this scenario the only viable alternative materials are:

- Natural materials such as wood (plywood, hardwood, pine & bamboo)
- Non-technical ceramics such as marble and limestone
- Waste plastics (plastics that are collected and can be recycled)

6.4.2. Scenario 2, Configuration a

To consider homogenous materials that could be used to bridge weak areas in the pavement (as per the requirements of Scenario 2), the materials index M_2 was used to generate a materials selection chart in Figure 31.

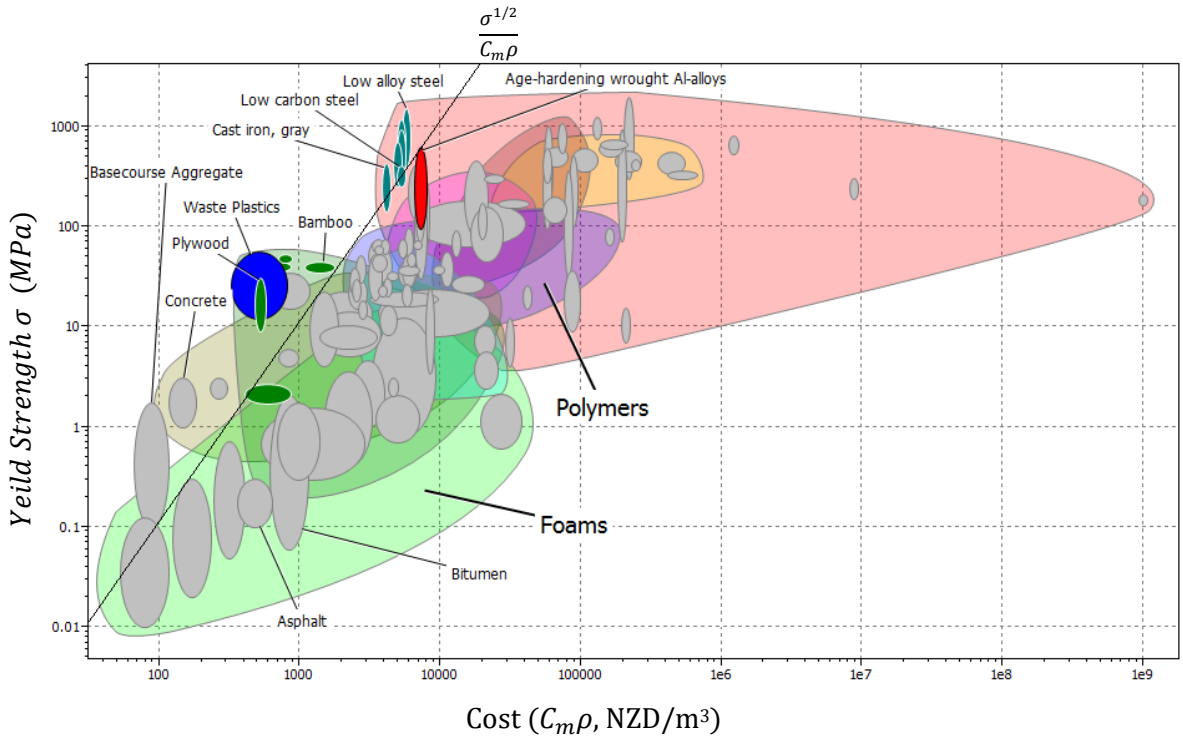

Figure 31 - Potential homogenous, alternative pavement materials for use under Scenario 2/Configuration a.

A selection guideline with a gradient of 2 (considering the material index, M_2) was applied to the selection chart to identify materials with performance equivalent to, or greater than, basecourse used in conventional pavement design. Alternative materials that met or exceeded the performance of M_2

(materials either on or above the selection guideline) were similar to the homogenous materials identified under Scenario 1 with the exception of the non-technical ceramic group. This group was excluded due to the poor flexibility of these materials as they did not meet the constraint of 0.6% strain elongation (Section 6.3). Interestingly conventional pavement materials such as basecourse, concrete and asphalt did not meet the requirements of this scenario due to low flexibility (<0.6% strain elongation) in the case of concrete and basecourse or low strength in the case of asphalt. This may go some way to explain the prominence of cracking and rutting in New Zealand's pavements.

Considering homogenous materials under this scenario the only viable alternative materials are:

- Natural materials such as wood (plywood, hardwood, pine & bamboo)
- Steel alloys (low-high carbon)
- Waste plastics (plastics that are collected and can be recycled)
- Age-hardened wrought Aluminium alloys were also identified as potential alternatives in Figure 31. As it barely meets the criteria (only the strongest grade in this group), it was not considered to be a viable alternative.

6.4.3. Favourable Materials for Configuration a

Homogenous materials that pass both Scenarios (1&2) are shown in the selection chart below (Figure 32).

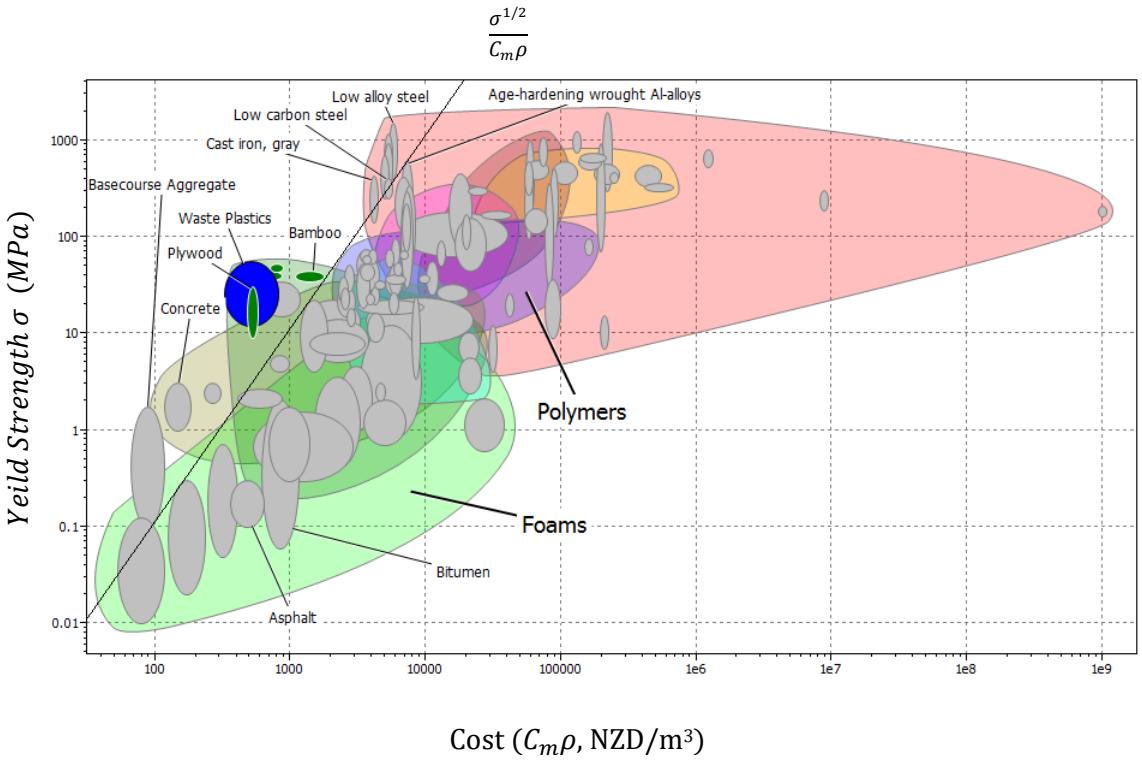

Figure 32 - Potential homogenous, alternative pavement materials that pass both Scenario 1 & 2 using Configuration a.

Considering both of these scenarios, only waste plastics and wood would be considered viable alternative materials under this configuration.

6.5. Substitution of Bitumen Matrix in Asphalt (Configuration b)

The industry has already invested in infrastructure for asphalt production therefore it makes sense to utilise this equipment if possible. The easiest way to achieve this is to substitute the bitumen matrix of the asphalt with a more robust material. For the purposes of investigating possible alternative matrix materials the formulae for estimating the Young's modulus of an asphalt mix (Ossa, 2005) can be applied, as per Equation 33 to Equation 35.

$$E_{mix} = E_{bit}\left\{1 + \frac{2.5c}{k(1-c)}\right\}^{k}$$

Equation 33

$$k = 0.83 \log\left\{\frac{4x10^4}{E_{bit}}\right\}$$

Equation 34

Where:

E_{mix} = Young's modulus of asphalt mix (MPa)

E_{bit} = Young's modulus of bitumen matrix (or alternative material, MPa)

c = volume fraction of aggregate

Most asphalt mixes contain around 95% aggregate and 5% bitumen by mass. The average densities of these materials are 2400kg/m3 and 1030kg/m3, respectively. Considering these values, the aggregate volume fraction would be 0.89. Substituting c with 0.89 produces Equation 35.

$$E_{mix} = E_{bit}\left\{1 + \frac{2.225}{0.0913log\left(\frac{4x10^4}{E_{bit}}\right)}\right\}^{0.83log\left(\frac{4x10^4}{E_{bit}}\right)}$$

Equation 35

By substituting Equation 35 into Equation 28, the material index for an asphalt with an alternative matrix show that high E_{bit} and high Poisson ratio will yield a low value for M_3.

$$M_3 = \left(C_m \rho \left[\frac{(1-\nu^2)}{E_{mix}} \right]^{\frac{1}{3}} \right)$$

Equation 36

Equation 36 would give the best indication of performance for Configuration b under Scenario 1. As there is currently no formula for predicting asphalt strength from the material properties of the matrix, it would need to be assumed that the yield strength and elongation properties of the matrix would be the best indication of success under Scenario 2.

6.5.1. Scenario 1, Configuration b

The performance of an asphalt upon an elastic foundation requires a sufficiently high Young's modulus of the mix (as per the material index M_3 Equation 36). The performance of an asphalt mix when considering the index M_3 will vary greatly due to bitumen being very sensitive to temperature. A change in temperature from 20°C to 50°C can reduce the Young's modulus of the bitumen from 3MPa down to 0.03MPa. Interestingly, standard design of asphalt only considers the modulus at the average temperature it will be exposed to (typically ~20°C). This means that when considering alternative matrices in asphalt the performance needs to be considered at both the typical design temperature (20°C) and at higher operating temperatures where the material is more likely to fail (due to rutting/deformation).

Alternative matrix materials for asphalt were considered by substituting E_{bit} (from Equation 35) with the Young's modulus of an alternative material. The predicted Young's modulus for an asphalt mix using an alternative material in Equation 35 (E_{mix}) can then be applied to Equation 36 to produce the material index for evaluating alternatives to bitumen in an asphalt, M_3. As there is no strength calculation to consider under this scenario, the flexibility constraint from Scenario 2 (>0.6% strain elongation) was used. A constrain around processability was also added requiring the materials considered had excellent

moldability rating of at least 5 under CES Selector (EduPack, 2016). This ensure that materials considered can mix with and coat the aggregate particles used in an asphalt mix.

The following materials selection charts consider the performance of alternative matrices in an asphalt mix using the materials index, M_3. As asphalt would give varying performance under normal service temperatures, selection guide lines were placed at locations that identify matrix materials which give equivalent (or better) performance to a bitumen at 20°C and 50°C.

6.5.2. Alternative Matrices to Bitumen at 20°C

Figure 33 shows the materials selection chart for the performance of materials when used as an alternative matrix in an asphalt mix.

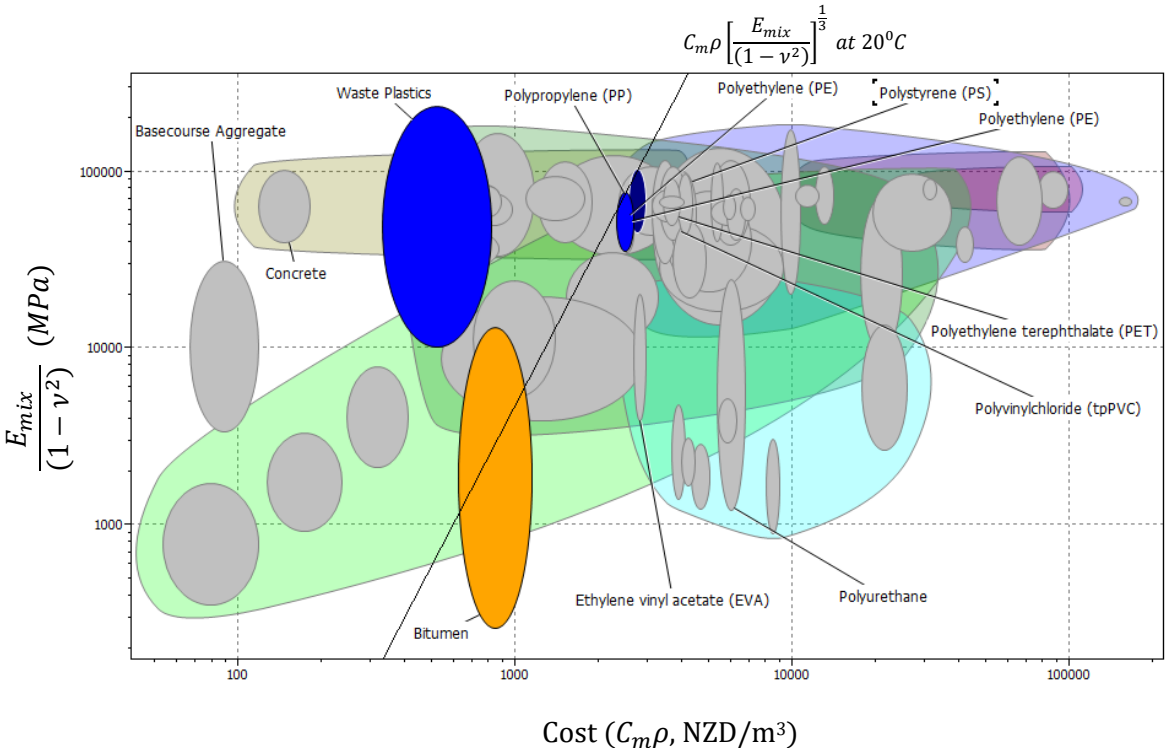

Figure 33 - Potential bitumen substitutes for asphalt for use under Scenario 1 / Configuration b at 20°C.

The selection guide line in Figure 33 is aligned with the performance of bitumen in an asphalt mix at 20°C. The only materials that give equivalent or greater performance at this temperature are plastics. Waste plastic was very favourable under this scenario whereas virgin plastics, such as Polypropylene, only just offered performance that was equivalent to bitumen at 20°C. As

failure of asphalt rarely occurs at 20°C it is also important to consider its performance under M_3 at the higher service temperature of 50°C as well.

6.5.3. Alternative Matrices to Bitumen at 50°C

Figure 34 shows the materials selection chart for the performance of materials when used as an alternative matrix in an asphalt mix.

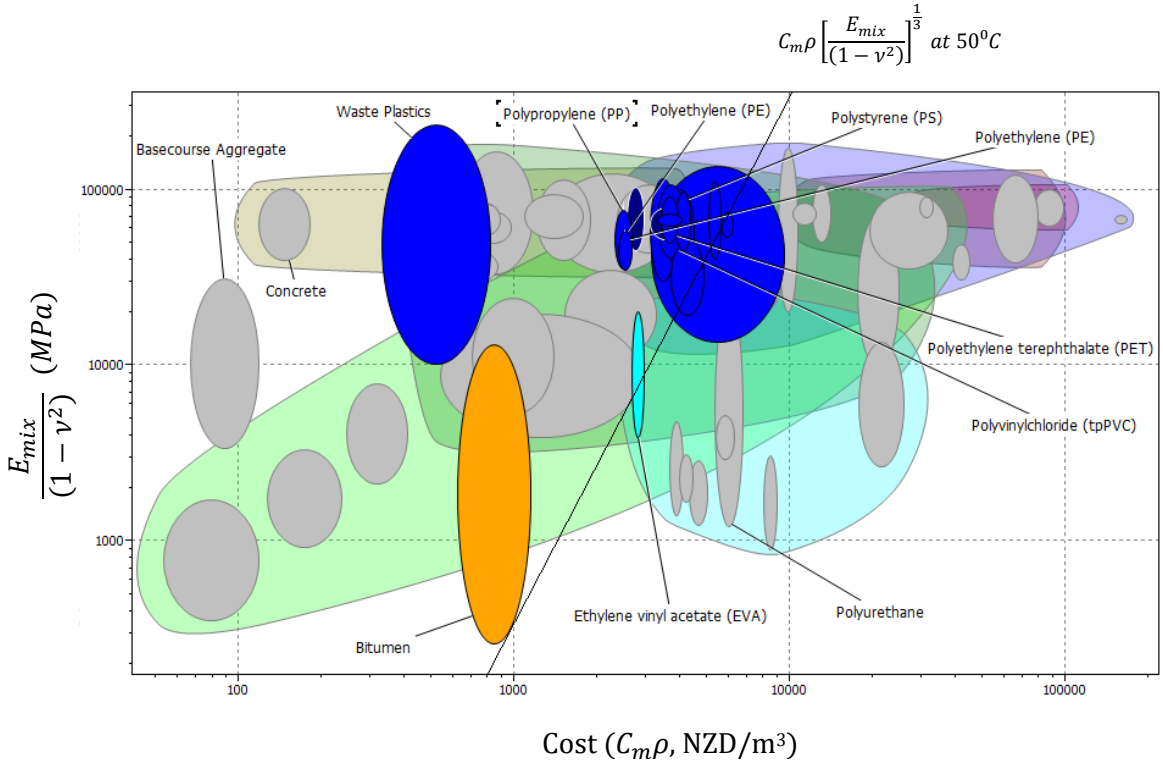

Figure 34 - Potential bitumen substitutes for asphalt for use under Scenario 1 / Configuration b at 50°C.

The selection guide line in Figure 34 is aligned with the performance of bitumen in an asphalt mix at 50°C. In this case plastics are also the only viable alternative with the increased temperature allowing for a greater variety of virgin plastics to be considered. This also includes one elastomer in the form of Ethylene Vinyl Acetate (EVA).

6.5.4. Favourable Materials for Configuration b

Overall, waste plastic is the most favourable option under this scenario with a number of virgin plastics becoming quite favourable at higher service temperatures. This should be considered for further analysis as a potential alternative pavement material.

6.6. Substitution with a Sandwich Panel (Configuration c)

As the success of Scenarios 1 and 2 rely on both high strength and stiffness at low cost and density, sandwich panels are an ideal candidate. Sandwich panels achieve these properties by use of a light weight core sandwiched between two stiff and strong face materials. The separation of the faces by the core, increases its moment of inertia (I), allowing it to resist bending under load.

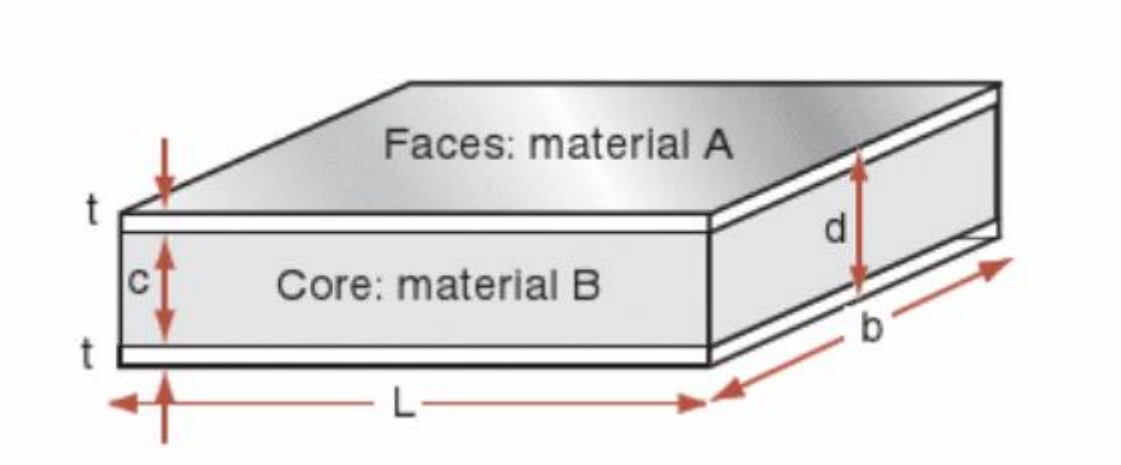

Figure 35 - Dimensions of a sandwich panel (Ashby & Cebon, 2004).

Where:

t = Face thickness (m)

c = Core thickness (m)

d = Overall panel thickness (m)

L = Panel length

b = Panel width

The strength and stiffness of a sandwich panel can be estimated by the following calculations and will allow it to be considered under Scenarios 1 and 2.

As sandwich panels are composite materials, their properties need to be determined by the contribution that each material provides to the end material. Material properties of a sandwich panel can be compared to that of homogenous materials by calculating “equivalent” properties. As previously

identified, the important material properties that need to be identified are strength, stiffness and cost/m^3.

Equivalent cost/m^3 ($C_m\rho$) can be determined by the following equation.

$$\tilde{C}_m\tilde{\rho} = fC_{mf}\rho_f + (1-f)C_{mc}\rho_c$$

Equation 37

Where:

f = Volume fraction occupied by the face material (2t/d)

C_{mf} & C_{mc} = Cost/kg of face and core material respectively

ρf & ρc = Material density (kg/m3) of face and core material respectively

Equivalent flexural modulus can be considered by as:

$$\frac{1}{\widetilde{E}_{flex}} = \frac{1}{E_f\left\{(1-(1-f)^3)+\frac{E_c}{E_f}(1-f)^3\right\}} + \frac{48}{4}\left(\frac{d}{L}\right)^2\frac{(1-f)}{G_c}$$

Equation 38

Where:

E_f = Young's modulus of face material (GPa)

E_c = Young's modulus of core material (GPa)

G_c = Shear modulus of core material (GPa)

Considering the constituents of Equation 38, to achieve greater panel stiffness higher Young's modulus is favourable for both the face and the core along with a high shear modulus for the core and a greater volume fraction of the face.

$$M_4 = \left(C_m\rho\left[\frac{(1-\nu^2)}{\tilde{E}_{flex}}\right]^{\frac{1}{3}}\right)$$

Equation 39

A sandwich panel can fail in a number of different manners as both the core and the face materials need to be able to withstand the loads applied. Equivalent flexural strength is considered to be the least of the following failure mechanisms (Figure 36).

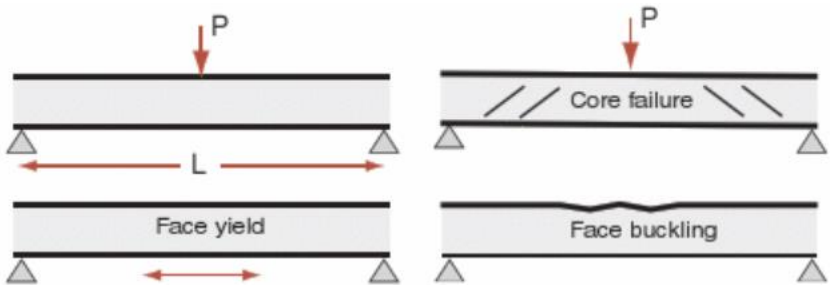

Figure 36 - Failure modes of sandwich panel in flexure (Ashby & Cebon, 2004).

Face yield (σflex 1)

$$\tilde{\sigma}_{flex\,1} = (1-(1-f)^2)\sigma_f + (1-f)^2\sigma_c$$

Equation 40

Where:

σ_f = Yield strength of face material (MPa)

σ_c = Yield strength of core material (MPa)

Face buckling (σflex 2)

$$\tilde{\sigma}_{flex\,2} = 1.14f\left(E_f {E_c}^2\right)^{\frac{1}{3}}$$

Equation 41

Core failure/shear (σflex 3)

$$\tilde{\sigma}_{flex\,3} = \frac{2}{4}\left\{4\frac{L}{d}(1-f)\tau_c + f^2\sigma_f\right\}$$

Equation 42

Where:

τ_c = Shear strength of core material (MPa)

In a sandwich panel the minimum yield strength of $\sigma_{flex\ 1\text{-}3}$ (from the equations above) is determined as the yield strength of the sandwich panel and is denoted as $\sigma_{flex\text{-}min}$. By substituting this value with the yield strength in Equation 32 the materials index, M_5 (Equation 43) can be produced. This equation considers the performance of a sandwich panel bridging a weak spot in the pavement as per Scenario 2.

$$M_5 = \left(\frac{C_m \rho}{\tilde{\sigma}_{flex-min}^{\frac{1}{2}}} \right)$$

Equation 43

In order to maximise the strength of a sandwich panel and therefore the materials index M_5, both the face and core materials need to possess high Young's modulus and yield strength. In addition to these requirements, the core material also benefits from possessing a high shear strength.

6.6.1. Scenario 1, Configuration c

Maximising the Young's modulus of a sandwich panel is important to maximise performance upon an elastic foundation as per Scenario 1.

In this scenario, the Young's modulus of a sandwich panel is calculated using Equation 38. This equation shows that higher panel stiffness is achieved through high Young's modulus in both the face and the core along with a high shear modulus for the core and a greater volume fraction of the face. The best combination of these materials will maximise the modulus of the sandwich panel and therefore offer the greatest performance under the materials index M_4.

As the young modulus of the face and the core material have the greatest effect on Equation 38 (and therefore M_4), only the Young's modulus of the face and core will be used to identify potential face and core materials for further analysis, as per the materials index in Equation 44.

$$M_6 = \left(\frac{C_m \rho}{E^{\frac{1}{3}}}\right)$$

Equation 44

Using the material index M_6, a materials selection chart was generated to identify appropriate face materials (Figure 37, below).

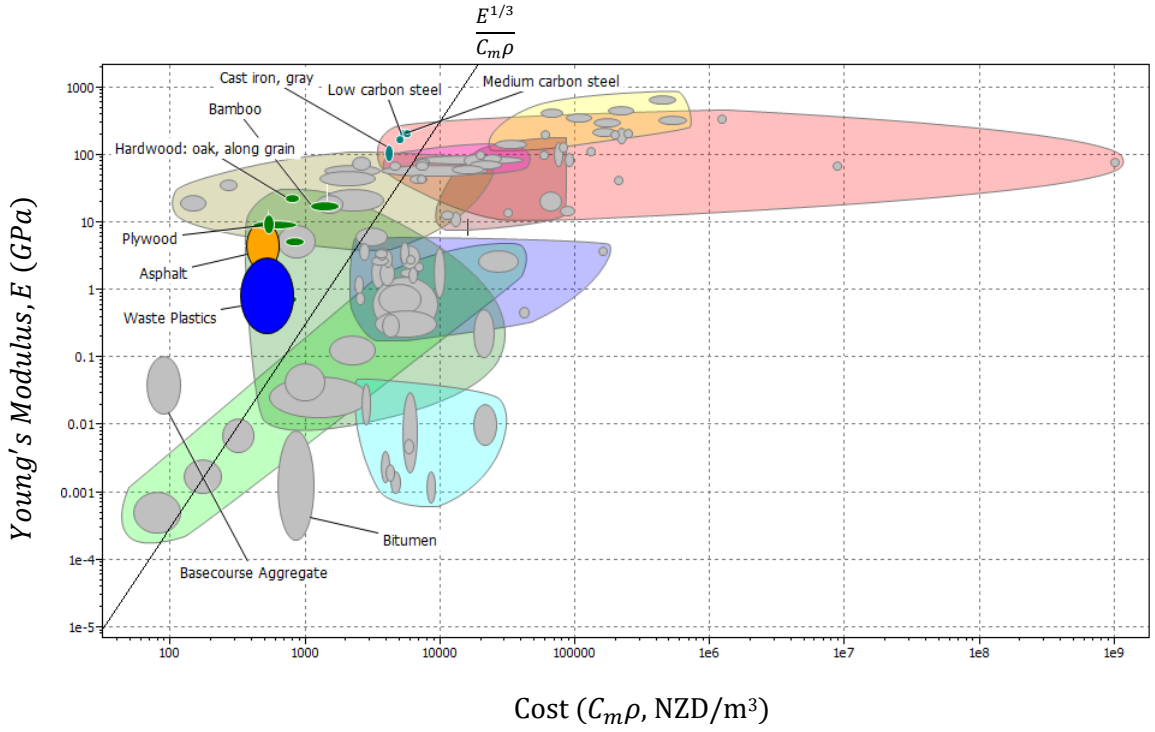

Figure 37 - Potential face materials to be used in a sandwich panel as an alternative pavement material under Scenario 1 / Configuration c.

As the material will be used as a face containing a thicker core, materials that lacked flexibility were not considered (i.e. ceramics). To keep this consistent with previous materials selection a minimum elongation of 0.6% strain was applied to the selection chart. As the face material only makes up part of the sandwich panel it is possible that a more expensive material can be considered under M_6 ($/m³/GPa) than the previous material indices considered in Scenario 1 (M_1). To account for this, the selection guide line was set at half the Young's modulus achieved by basecourse aggregate under M_6. This allows for a greater range of materials to be considered than what M_1 allows. Based on this, the most favourable face materials under the material index M_6 are:

- Waste plastics

- Wood (plywood, bamboo, hard oak etc.)
- Steel alloys (Low carbon, medium carbon etc.)

Asphalt was also considered to be viable in Figure 37, however due to the particulate nature of this material, it may be difficult to use as a face material in practice.

Core materials were also considered using the material index M_6. Only materials labelled as core materials under the CES Selector's material tree were considered for this analysis. This constraint and the material index M_6 are displayed in Figure 38 below.

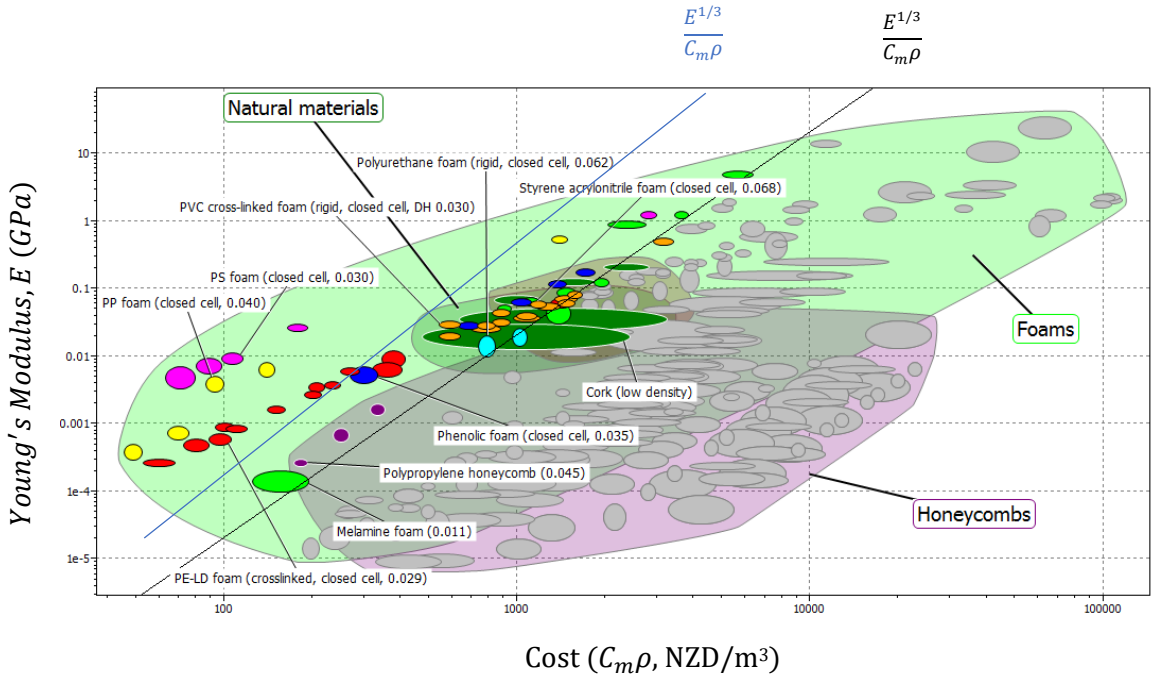

Figure 38 - Potential core materials to be used in a sandwich panel as an alternative pavement material under Scenario 1 / Configuration c.

The materials of varying density displayed in Figure 38 are colour coded based on their base material. Materials of the same colour with higher or lower cost represent materials of the same type but with lower of higher densities relative to the cost. This figure contains two selection guidelines at a gradient of 3. The blue selection guideline considers core materials that offer equivalent performance using M_6 to that of basecourse aggregate. In this case no core materials offer equivalent (or greater) performance to that of basecourse, however the closest material is Polystyrene foam at densities of 10-30 kg/m^3.

The second selection guideline compares the commonly available, rigid polyurethane foam at a density of 62kg/m^3. This allows for a greater number of core materials to be considered. In this case Polystyrene, Polypropylene, Polyethylene and Polyvinylchloride foams offer greater performance than Polyurethane foam under M_6.

6.6.2. Scenario 2, Configuration c

The success of a sandwich panel in bridging a weak spot in the pavement (Scenario 2) is dependent on the failure mode of the panel. This is governed by the yield strength of the face and the core, if yielding of the faces is predicted to be the failure mode. If failure is due to core shear, then it's performance is governed by the yield strength of the face and the shear strength of the core. From this it is clear that face materials considered under Scenario 2 will favour higher values for yield strength whereas the most favourable core materials will possess high values for yield strength and shear strength.

To identify face materials that would give the greatest performance under Scenario 2 the yield strength of the face material was considered as per the previously identified materials index $M_{2,}$ in Section 6.4. In this case, Figure 31 - Potential homogenous, alternative pavement materials for use under Scenario 2/Configuration a.Figure 31 (Section 6.4) can be used to identify face materials that would give the greatest performance under M_2 and would therefore improve the performance of a sandwich panel using the materials index $M_{5.}$ The most favourable face materials in this case are as follows:

- Natural materials such as wood (plywood, hardwood, pine & bamboo)
- Steel alloys (low-high carbon)
- Waste plastics (plastics that are collected and can be recycled)

When considering the contribution that the core material makes to resisting failure of a sandwich panel, Equation 42 (failure by core shear) is the most relevant. In this equation the shear strength of the core offers the greatest contribution to the strength of the sandwich panel. For the purposes of identifying core materials with high shear strength, at an appropriate cost, the material index M_7 was generated (Equation 45).

$$M_7 = \left(\frac{C_m \rho}{\tau^{\frac{1}{2}}}\right)$$

Equation 45

The materials selection chart below

Figure 39) uses the materials index M7 to identify favourable core materials under Scenario 2.

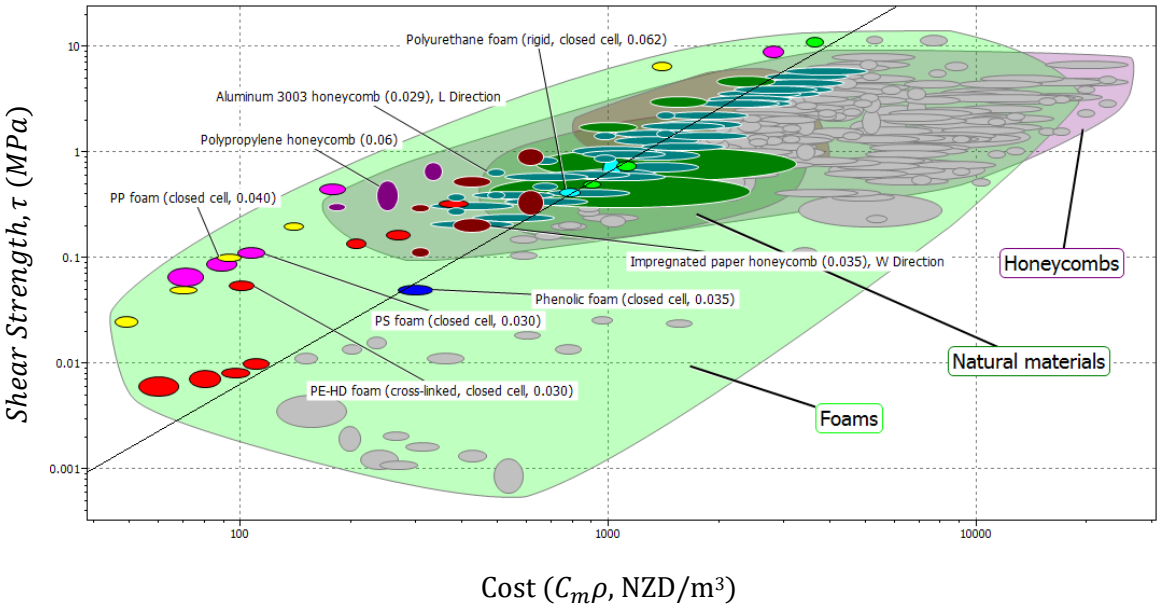

Figure 39 - Potential core materials to be used in a sandwich panel as an alternative pavement material under Scenario 2 / Configuration c.

A selection guideline (with a gradient of 2) was applied to Figure 39 in order to identify materials with equivalent (or greater) performance to rigid polyurethane foam (62 kg/m^3) under M_7. This figure reveals that the core materials offering the greatest performance under M_7 are:

- Polystyrene foam
- Polypropylene foam
- Polyethylene foam (high density)
- Polypropylene honeycomb

Materials that offer equivalent (or similar) performance to the selection guideline are:

- Rigid polyurethane foam
- Phenolic foam
- Aluminium honeycomb
- Impregnated paper honeycomb
- Cork (high density)

6.6.3. Favourable Materials for Configuration c

The most favourable face and core materials that would give the performance under both Scenario 1 and 2 are identified below.

By combining the materials that meet or exceed the selection guidelines in Figure 31 and Figure 37, the most favourable face material for use under both scenarios can be identified as per Figure 40.

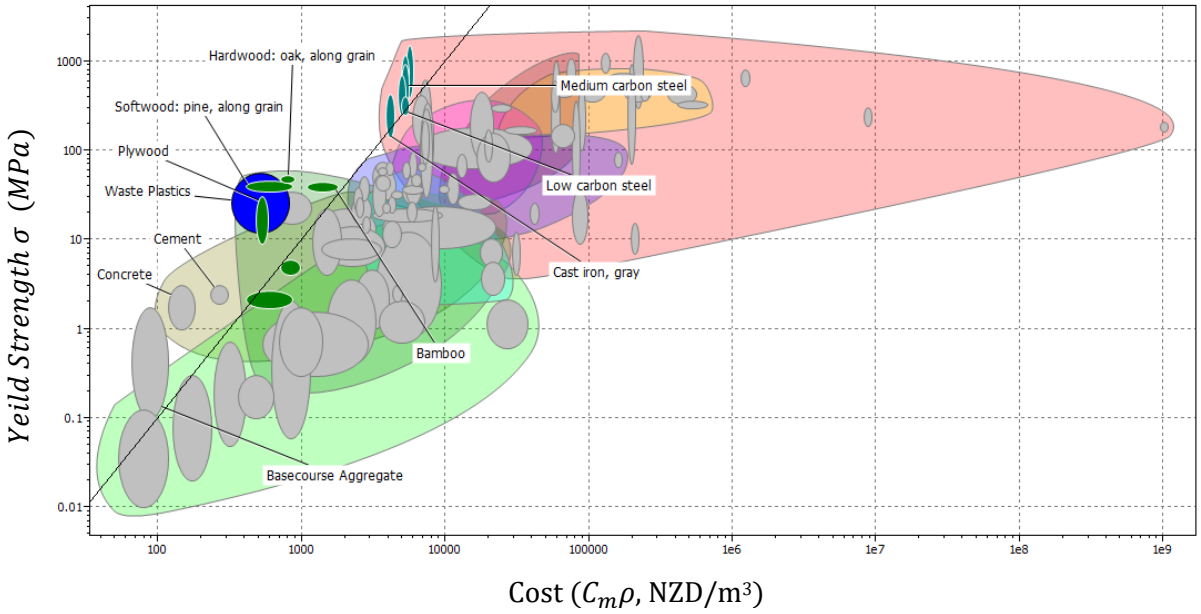

Figure 40 - Potential face materials to be used in a sandwich panel that passes the requirements of Scenario 1&2 for Configuration c

Considering Figure 40, the most favourable face materials for use in a sandwich panel that could cope with the requirements of Scenarios 1&2 are:

- Natural materials such as wood (plywood, hardwood, pine & bamboo)
- Steel alloys (low-high carbon)
- Waste plastics (plastics that are collected and can be recycled)

Core materials that meet both the requirements of Scenarios 1&2 were determined by combining the selection guidelines in Figure 38 and Figure 39. Figure 41 shows the result of this analysis below.

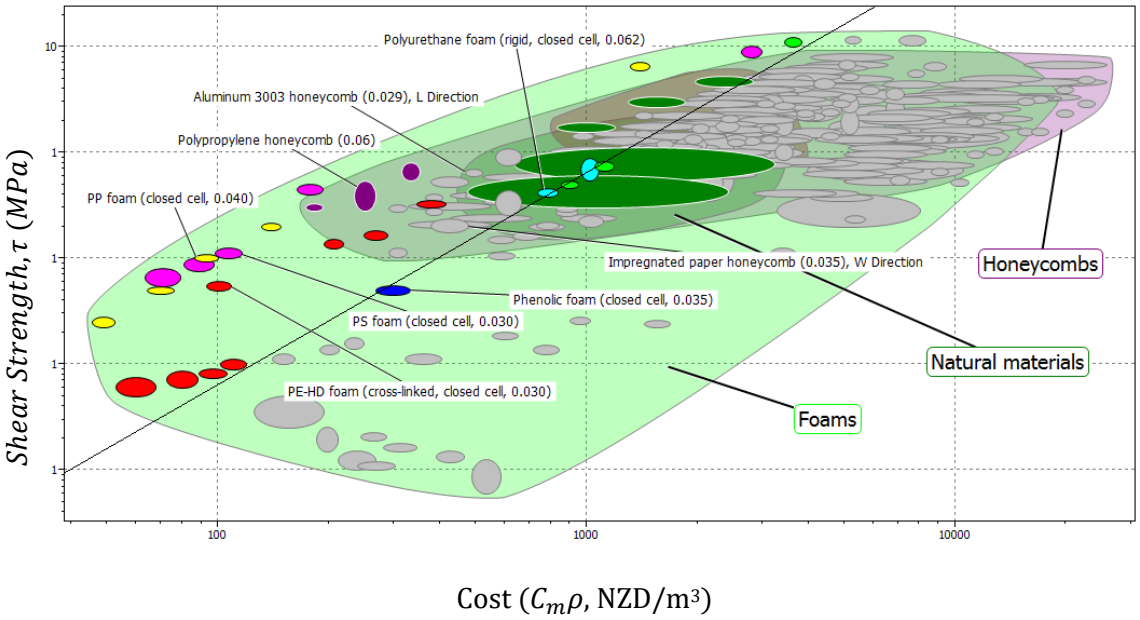

Figure 41 - Potential core materials to be used in a sandwich panel that passes the requirements of Scenario 1&2 for Configuration c.

Figure 41 reveals that the most favourable core materials for use in a sandwich panel that could cope with the requirements of Scenarios 1&2 are:

- Polystyrene foam
- Polypropylene foam
- Polyethylene foam (high density)
- Polypropylene honeycomb
- Materials that offer equivalent (or similar) performance to the selection guideline are
- Rigid polyurethane foam
- Phenolic foam
- Cork (high density)

The figures above show potential materials that could be used to construct sandwich panels that would achieve sufficient performance under Scenarios 1&2. This analysis only considers the core and face materials as individual components and not its performance when used in a sandwich panel. The following section focuses on the ideal sandwich panel configuration, using an

assortment of the materials identified above, that will offer sufficient performance under Scenarios 1&2.

7. Sandwich Panel Design

The scope of this report focuses on the viability of the use of alternative materials in pavements. Testing of every single face and core combination (identified in the previous section) is considered to be outside the scope of the report. In order to confirm the feasibility of the approach, a selection of face and core materials were evaluated instead. As the face materials could be represented by certain material groups, the face materials considered for design are as follows:

- Steel alloy - Low Carbon Steel
- Natural material - Plywood
- Waste plastics - virgin PET and PVC

PET and PVC were selected to represent waste plastics as they both offer the highest Young's modulus and yield strength of recyclable plastics. Virgin polymers were selected instead of material collected for recycling in order to reduce the preparation time required for any subsequent testing of these materials.

Only two core materials were selected, one to represent the cores with very favourable performance and another to represent the group of cores with similar performance to the selection guideline (in Figure 41). The core materials considered for design are as follows:

- Favourable performance - PS foam (30kg/m^3)
- Similar performance - PU foam (62kg/m^3)

These core materials were selected to represent each group based on commercial availability, as this would help reduce preparation time for any subsequent testing required.

Based on the materials identified above, the following combinations were considered for design of a sandwich panel:

- Low Carbon Steel (face) & Polyurethane foam (core)
- Low Carbon Steel (face) & Polystyrene foam (core)
- Plywood (face) & Polystyrene foam (core)
- PET (face) & Polystyrene foam (core)
- PVC (face) & Polystyrene foam (core)

Only one combination using polyurethane foam as the core was considered. This was used to provide a comparison with the performance of a sandwich panel using polystyrene foam under the materials indices M_4 and M_5.

Using the core and face materials identified above, the panel design can be optimised (for each combination). To identify the optimum design, the volume fractions of the face (f) and core material (1-f) where adjusted and the resultant performance under the materials indices M_4 and M_5 were plotted.

In the absence of actual test data, it was assumed that the Poisson's ratio of the sandwich panels in question would be dominated by the contribution of the core material. As the Poisson's ratio of the core materials analysed were very similar (both ~0.3), the contribution of the Poisson's ratio in the material index M_4 was ignored.

As the equivalent mechanical properties of a sandwich panel are dependent on d/L (see Equation 38). The d/L value accounts for the fact that the flexural properties have two factors that contribute to bending of the beam and shear of the core. The flexural properties of a beam will be greater if deformation only occurs through bending of the beam (low d/L). A greater contribution due to shear (higher d/L) in the core will reduce the flexural properties of a beam.

To account for this, the following materials selection charts use a consistent d/L which was set at 0.1232 to reflect the likely loading scenario the material would experience in the pavement (L of 406mm i.e. 2 times l^*, Section 6.2 and d of 50mm). The following charts show the cost/m^3 of the various sandwich panel combinations/fractions, plotted against the equivalent Young's modulus (Equation 38) and equivalent yield strength (Equation 40 to Equation 42), as per Figure 42 and Figure 43 respectively.

For each of these graphs, each point represents the following face volume fractions, 0.0 (core only), 0.003, 0.005, 0.01, 0.02, 0.03, 0.05, 0.1, 0.2, 0.3, 0.5, 0.7, 0.9, 1.0 (face only).

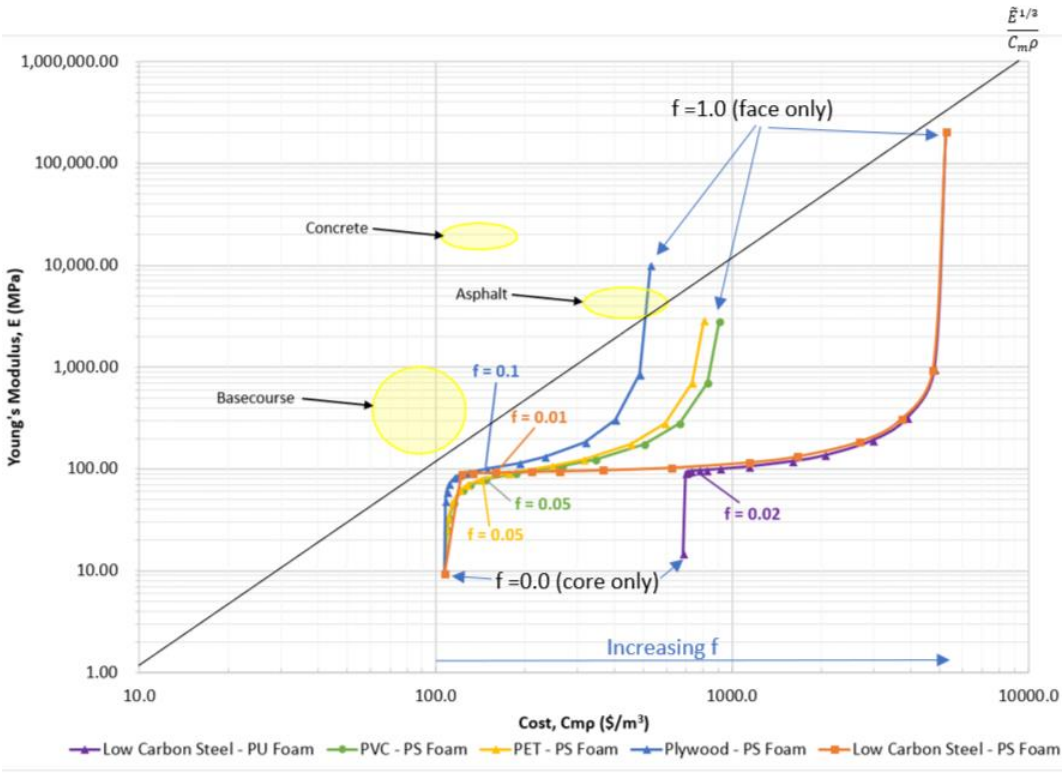

Figure 42 - Comparison of cost/m3 vs equivalent young's modulus at various face volume fractions of a sandwich panel combination

Figure 42 shows that at low volume fractions (of the face material, f) the performance of the sandwich panel under M_4 is dominated by the properties of the core. As f increases, the face material becomes the dominant contributor to the equivalent Young's modulus of the panel.

Comparison of the Low Carbon Steel-PU foam and the Low Carbon Steel - PS foam panels show very similar relationships between face volume fraction and equivalent Young's modulus. The major difference is the cost/m^3 ($C_m\rho$), which is much higher for the PU foam option.

All panels using PS foam as the core material show very similar performance at low f with very little differences in equivalent Young's modulus until f reaches ~0.2.

The optimum panel design under M_4 /Figure 42 is the volume fraction which offer the greatest stiffness at the lowest cost/m^3. In Figure 42 this is defined by the contour which is tangent to the trajectory. These points are labelled for each combination in Figure 42 and also in Table 12 below.

Table 12: Volume fraction of optimum panel designs for each sandwich panel combination under M_4.

Sandwich Panel Combination	Optimum volume fraction (f) in terms of Stiffness per $/$m^3$ (MPa/$/$m^3$)
Low Carbon Steel - PS Foam	0.01
Low Carbon Steel - PU Foam	0.02
Plywood - PS Foam	0.1
PET - PS Foam	0.05
PVC - PS Foam	0.05

The selection guideline in Figure 42 shows that none of the sandwich panel combinations give equivalent performance to that of basecourse aggregate in terms of stiffness and may not be the most appropriate materials for use under Scenario 1. Despite this, the sandwich panels containing PS foam with low face volume fractions are close to the selection guideline and would be worth considering more closely if they offer sufficient strength under Scenario 2.

PVC and PET at f=1.0 also no longer compare favourably in Figure 42, despite being identified as options as a waste plastic in Figure 37. This is due to Figure 37 considering the range of prices and densities (both min and max) that these materials would achieve. In Figure 42 only the average properties were considered, therefore these materials may appear less feasible than previously presented.

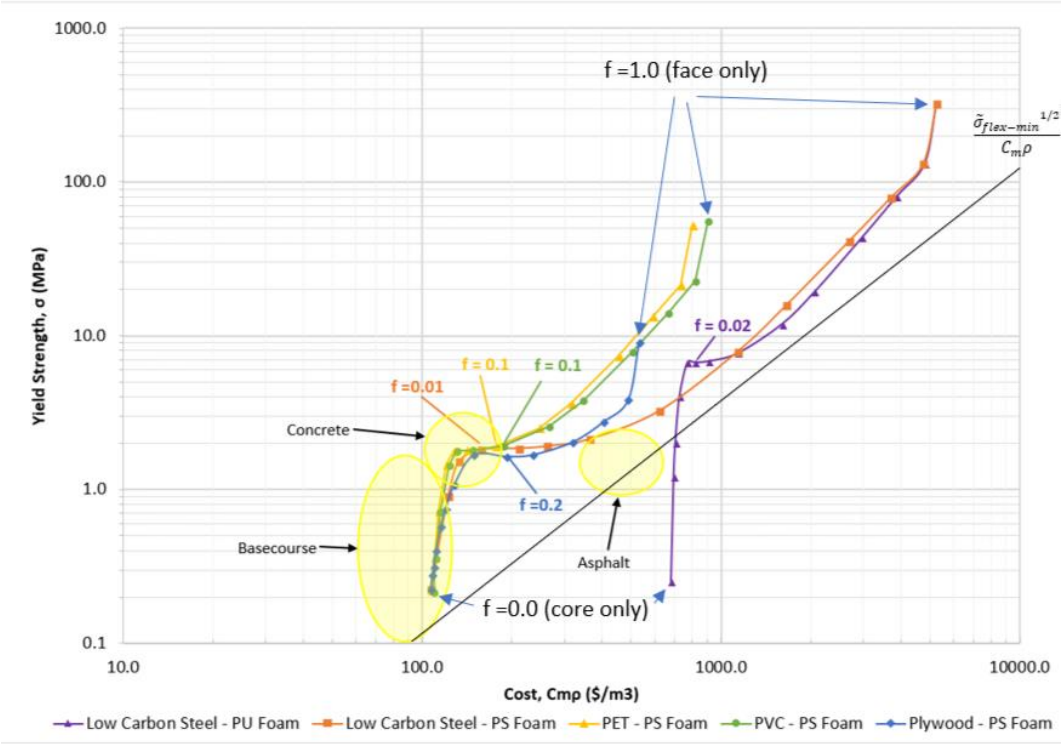

Figure 43 - Comparison of cost/m3 vs equivalent yield strength at various face volume fractions of a sandwich panel combination.

Figure 43 shows the effect of the face volume fraction on the equivalent yield strength and cost of the sandwich panel combinations. At low volume fractions (of the face material, f) the performance of the sandwich panel under M_5 is also dominated by the properties of the core. As f increases, the face material becomes the dominant contributor to the equivalent yield strength of the panel.

Comparison of the Low Carbon Steel-PU foam and the Low Carbon Steel-PS foam panels show that the PU foam sample produces much higher yield strength for the equivalent volume fraction, although this also comes at a much higher cost/m^3. This is similar to the relationship between face volume fraction and equivalent Young's modulus. The major difference is the cost/m^3 ($C_m\rho$), which is much higher for the PU foam option.

All panels using PS foam as the core material show very similar performance at low f with very little differences in equivalent yield strength until f reaches ~0.2-0.3.

The optimum panel design under M_5/Figure 43 is the volume fraction which offer the greatest strength at the lowest cost/m^3. This is defined by the contour which is tangent to the trajectory. These points are labelled for each combination in Figure 43 and also in Table 13, below.

Table 13: Volume fraction of optimum panel designs for each sandwich panel combination under M_5.

Sandwich Panel Combination	Optimum volume fraction (f)	Failure due face yield, σ_{flex1} (volume fraction, f)	Failure due face buckling, σ_{flex2} (volume fraction, f)	Failure due core shear, σ_{flex3} (volume fraction, f)
Low Carbon Steel - PS Foam	0.02	0.0 & 1.0	0.003-0.005	0.01-0.9
Low Carbon Steel - PU Foam	0.02	0.0 & 1.0	0.003-0.01	0.02-0.9
Plywood - PS Foam	0.2	0.0-0.05 & 1.0	None	0.1-0.9
PET - PS Foam	0.1	0.0 & 1.0	0.003-0.02	0.03-0.9
PVC - PS Foam	0.1	0.0 & 1.0	0.003-0.02	0.03-0.9

The failure mode at each volume fraction is also highlighted in Table 13. All panel combinations (except for the Plywood/PS foam) are predicted to exhibit face buckling (σ_{flex2}, Equation 41) at low f and core shear (σ_{flex3}, Equation 42) at high f. The Plywood-PS foam combination is predicted to fail by face yielding (σ_{flex1}, Equation 40) at low f and core shear at high f. It is not expected to undergo face buckling as per the other combinations.

Using the optimum volume fractions identified for stiffness and strength in Table 12 and Table 13, the optimum design for each sandwich panel can be identified. The optimum volume fraction for a panel that account for both stiffness and strength uses the maximum optimum volume fraction from Table 12 and Table 13, for each combination. For a constant core height (set at 50mm for this analysis) the optimum face thickness for each combination can be calculated using Equation 46 with results displayed in Table 14.

$$t = \frac{df}{2}$$

Equation 46

Table 14: Optimum sandwich panel design

Sandwich Panel Combination	Volume fraction for optimum stiffness, f	Volume fraction for optimum strength, f	Maximum optimum volume fraction, f	Design height, d (mm)	minimum face thickness, t =(df)/2 (mm)
Low Carbon Steel - PS Foam	0.01	0.02	0.02	50	0.5
Low Carbon Steel - PU Foam	0.02	0.02	0.02	50	0.5
Plywood - PS Foam	0.1	0.2	0.2	50	5.0
PET - PS Foam	0.05	0.1	0.1	50	2.5
PVC - PS Foam	0.05	0.1	0.1	50	2.5

Overall, the sandwich panel combinations identified in this section show promise under Scenario 2 but may offer borderline performance under Scenario 1. As the majority of pavement failures in New Zealand are due to lack of strength, there is still a lot of potential for sandwich panels to be a viable replacement for conventional pavement materials.

8. Confirmation of Material Properties

The homogenous materials considered under Configuration a have very well-defined material properties and therefore the values contained within CES Selector would be sufficient to determine whether the materials would be considered a viable alternative to the current pavement materials. As Configurations b (substitution of bitumen) and c (sandwich panels) only consider theoretical material properties, it is prudent to perform some testing on a selection of materials to confirm viability.

8.1. Alternatives to Bitumen in an Asphalt Mix (Configuration b)

Under Configuration b, the most viable alternative to bitumen in an asphalt mix is waste plastics. As the incorporation of waste plastic into an asphalt mix would require further research into appropriate temperatures, mixing times and compaction methodology it was deemed outside the scope of this report. Despite this, there is a product on the market called Ultra Mender (roadscience.co.nz, 2018) which uses Polyurethane resin as an alternative to bitumen in an asphalt mix. In this case the appropriate mixing and compaction

temperature/methodology has already been established therefore it can easily be evaluated within the scope of this report. As Ultra Mender uses polyurethane as the binder, it is not commercially viable to use it as a large scale alternative pavement material due to its high cost/m^3 (as highlighted in Figure 34). It is however, appropriate for use as a localised treatment of pavement defects as the economies of scale associated with repairing small areas mean that materials cost is of less importance.

Table 15 (below) shows the typical properties that could be expected of waste plastics (EduPack, 2016) compared to the Polyurethane binder used in Ultra Mender.

Table 15: Typical properties of recyclable plastic vs Ultra Mender.

Number	Name	Youngs Modulus, E (MPa)	yield strength, σ (MPa)	Elongation (% strain)	E_{mix}, Equation 33 (GPa)
1	PET	2900	52.5	300	29.4
2	HDPE	1000	28.6	1,205	17.3
3	PVC	2800	55.5	60	28.9
4	LDPE	230	11.73	375	7.2
5	PP	1700	28.95	142	22.8
6	PS	1900	42.45	52.5	24.1
N/A	Ultra Mender	1500	50	20	21.4

Ultra Mender offers very similar mechanical properties to waste plastics and therefore could be used as a substitute to determine whether a bitumen alternative in an asphalt mix would produce comparable results to what was predicted in Section 6.5. Applying the formula for determining the effect that the Young's modulus of a binder has on the Young's modulus of an asphalt mix (E_{mix}, Equation 33), shows that Ultra Mender binder is also predicted to produce very similar performance in an asphalt to one using waste plastic as the binder.

The Ultra Mender mix has also already been used in service, therefore confirmation of its material properties can be related to the observed in-field performance.

Considering this, it was decided that the Ultra Mender would be used as the benchmark for evaluating whether other binders could be used as an alternative binder in an asphalt mix.

8.2. Sandwich Panel Options (Configuration c)

The Sandwich panel combinations outlined in Section 7 offer an ideal cross section of potential core and face materials that could be used in a sandwich panel as an alternative pavement material. To confirm the properties predicted in Section 7, each combination was designed to have dimensions as close as possible to the optimum identified in Table 14. Some concessions were made around both core height and face thickness due to the availability of certain material geometries. Core materials are readily available at a height of 50mm, therefore the standard height for all panels constructed was 50mm. Face materials were then sourced at thicknesses equal to or greater than the optimum volume fraction at a core height of 50mm.

Table 16: Design of samples tested

Sandwich Panel Combination	Maximum optimum volume fraction, f	Design core height, c_{design}(mm)	minimum face thickness, t where c=50mm, $t = \frac{c}{(1-f)} \frac{f}{2}$ (mm)	Design face thickness, t_{design} (mm)	Design volume fraction, f_{design} using c_{design} and t_{design}
Low Carbon Steel - PS Foam	0.02	50	0.51	1.4	0.05
Low Carbon Steel - PU Foam	0.02	50	0.51	1.4	0.05
Plywood - PS Foam	0.2	50	6.25	7.0	0.25
PET - PS Foam	0.1	50	2.78	5.0	0.18
PVC - PS Foam	0.1	50	2.78	5.0	0.18

8.3. Sample Preparation

Beams of Ultra Mender were prepared according to the manufacturers procedure outlined in Appendix A. The Ultra Mender beams where moulded to the dimensions outlined in ASTM C393 - Core Shear Properties of Sandwich Construction by Beam Flexure (75mmx200mm) with a core height of 50mm. The author recognises this is a test method for evaluating the flexural properties of a sandwich panel however the test conditions are also applicable to this material. This allows for additional flexural properties of specimens with a standardised geometry to be compared against the sandwich panel samples.

Sandwich panel samples were also constructed to the width (75mm) and length (200mm) dimensions outlined in ASTM C393. The panel heights were determined by the core and face thicknesses outlined in Table 16. West Systems 105 epoxy resin and 206 hardener (West-Systems, 2018) was used (as per the manufacturer instructions) to bond the face and core materials together. The epoxy was applied to the face at an application rate of 0.33kg/m^2. The face and core materials were compressed under a 100N load for 24 hours to allow the epoxy to cure.

8.4. Testing

Review of the standard test method for the flexural properties of sandwich panels revealed that ASTM C393 - Core Shear Properties of Sandwich Construction by Beam Flexure, was the most commonly used. The author accepts that the test method is used to evaluate the shear properties of the core, however in this case it is more beneficial to use a standard set of test conditions to evaluate the flexural properties of a sandwich beam and confirm the theoretical properties determined in Section 7. If these theoretical properties are confirmed, then the sandwich panel would be a viable option as an alternative pavement material. To ensure consistency across all samples, the Ultra Mender samples were also tested under the same conditions.

A 3-point loading configuration (meeting the requirements of ASTM C393) was used for all samples tested. The key dimension listed in this specification are as follows:

- Support span, L = 150mm
- Specimen width, b = 75mm
- Specimen height, d = as per design in Table 16
- Specimen length = 200mm
- Loading speed = 6mm/min
- Temperature = room temperature ~20-24^{o}C

The material properties calculated from ASTM C393 were not appropriate for comparison to the theoretical properties determined in Section 7, therefore the

flexural properties of all samples were calculated using the formula outlined in ASTM D7264 - Flexural Properties of Polymer Matrix Composites, as follows:

$$E_{flex} = \frac{L^3 m}{4bd^3}$$

Equation 47

$$\sigma_{flex} = \frac{3FL}{2bd^2}$$

Equation 48

$$\epsilon_{flex} = \frac{6Dd}{L^2}$$

Equation 49

Where:

F = Load (N)

D = Deflection (mm)

m = Initial gradient of load vs deflection plot (N/mm)

ε_{flex} = Flexural strain

Five specimens of each sandwich panel and Ultra Mender were manufactured, measured and tested as described above. The following section shows a summary of the results and the raw data can be found in Appendix C.

9. Results

Failure mode of the panels containing Low Carbon steel as the face failed due to core-face debonding. The PVC, PET and Plywood-PS foam sandwich panels failed due to core shear. Both of these failure modes are acceptable under ASTM C393. The Ultra Mender sample failed due to cracking at the base of the beam directly under the loading point. Recording of deflection and load information was stopped once one of these failure modes occurred.

The graph below shows the average load vs deflection for each material tested.

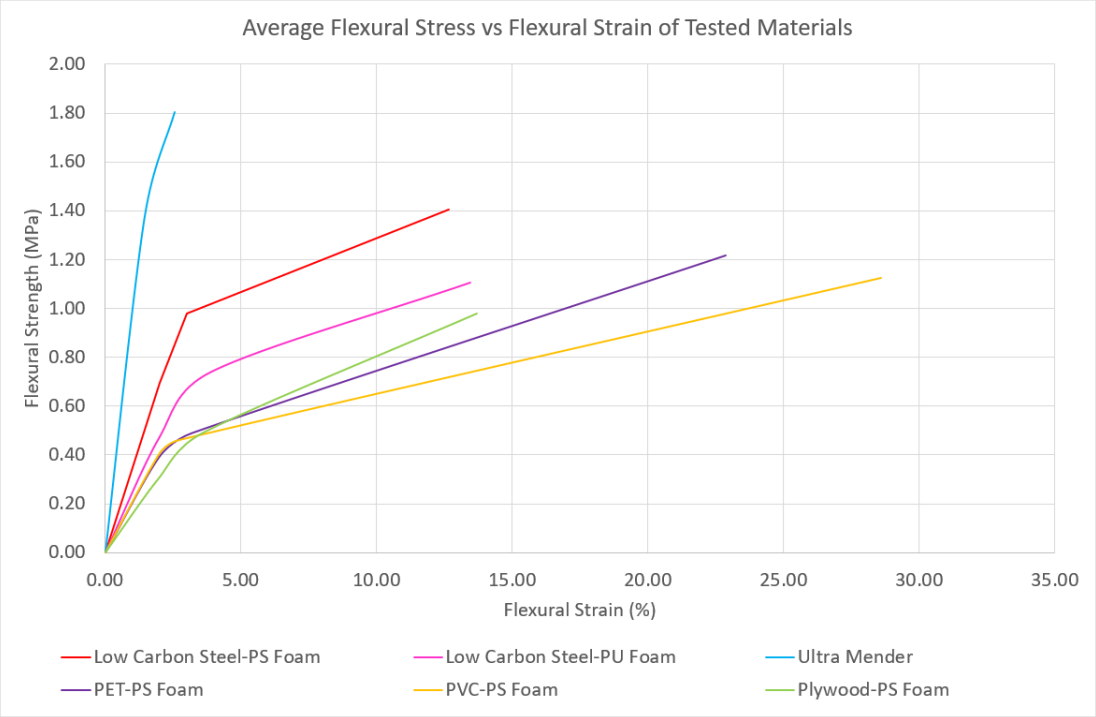

Figure 44 - Average load (strength) vs deflection (strain) for all samples tested

Figure 44 shows that the Ultra Mender specimen possesses the greatest stiffness and strength (high strength at low strain) whereas the specimen with the plastic face material PET & PVC offer the greatest flexibility (high maximum flexural strain). The Low Carbon Steel specimen containing PS foam offers much greater load bearing capacity (higher maximum load) than its PU foam counterpart. Of all sandwich panels tested, the Low Carbon Steel-PS foam specimen had the greatest load bearing capacity (highest maximum strength) but lower flexibility than the other sandwich panel specimens. The Plywood-PS foam sample offer similar flexibility to the sample containing Low Carbon Steel,

the lowest ultimate strength and similar yield strength to the panels with plastic as the face material.

Some of these differences will certainly be due to the different geometries of the panel so the load and deflection data was converted to material properties using Equation 47 (flexural modulus) and Equation 48 (flexural strength). Equation 49 (flexural strain) was used to determine the deflection relating to flexural strain at 2% which was used a reference point for all the sandwich panels as per the requirements of both ASTM C393 and ASTM D7264. Table 17 shows the summary of the results from all samples tested and compares the material properties determined from testing to that of the theoretical properties using the equations outlined in Section 6.6.

Table 17: Comparison of predicted material properties to tested material properties

Sandwich Panel Combination	target f	measured d/L	predicted $\tilde{E}$ (MPa)	tested $\tilde{E}$ (MPa)	predicted σ_{flex} (MPa)	tested σ_{flex} at 2% strain (MPa)	tested ultimate σ_{flex} (MPa)
Low Carbon Steel - PS Foam	0.05	0.34	12.1	33.9	1.1	0.7	1.4
Low Carbon Steel - PU Foam	0.05	0.32	12.3	17.5	2.7	0.5	1.1
Plywood - PS Foam	0.25	0.44	9.9	16.6	0.6	0.3	1.0
PET - PS Foam	0.18	0.40	10.5	15.0	1.2	0.4	1.2
PVC - PS Foam	0.18	0.39	10.5	15.8	1.2	0.4	1.1
Ultra Mender	N/A	N/A	21400*	153.3	N/A	N/A	1.8

* = predicted E_{mix} from Table 15

Table 17 shows that the tested flexural modulus was slightly higher than what was predicted for the sandwich panel specimens with the majority being ~5MPa higher than the theoretical values. The Low Carbon Steel-PS foam specimen was the only one that produced significantly higher than predicted (at over 20MPa higher). This may be because the prediction uses nominal material properties extracted from CES Selector. Actual testing of the material properties of the core would yield more accurate results however the difference presented was deemed sufficient for the purposes of this report. This relationship shows that the theoretical values (for the flexural modulus)

could be used to determine the feasibility of a given sandwich panel combination, for use as an alternative pavement material.

The difference between the theoretical and tested flexural strength of the sandwich panel combinations were also reasonably small. Both the flexural stress (at 2% strain) and ultimate flexural strength where compared to the theoretical values. In all combinations, the ultimate flexural strength was much closer to the theoretical value. The Low Carbon Steel-PU foam sample was the only one that possessed a significant difference to the tested and theoretical flexural strengths. This is again likely due to differences in the actual material properties to that which was extracted from CES Selector.

The Ultra Mender sample was also compared to the theoretical E_{mix} value predicted by Equation 33. In this case the theoretical modulus was significantly different to what was tested. This may be due to the formula only being applicable to bitumen-based asphalt mixes tested under a method that is designed for measuring asphalt modulus. If plastics were to be evaluated using theoretical value only, another equation would need to be developed to determine the asphalt mix modulus from matrix properties. Despite this, it is likely that the tested properties of this mix would be representative of an asphalt with a plastic matrix.

Currently there is no equation to predict the flexural strength of the Ultra Mender specimen however the tested results show that it is significantly higher than that of a standard asphalt mix (1.8MPa vs 0.9MPa).

As the flexural properties of the sandwich panels are dependent on the bending-to-shear balance (d/L), the tested values for the sandwich panels are much lower than what would be achieved in practice. Table 18 shows the d/L that would be achieved by the sandwich panels in practice when bridging an area that is 406mm in diameter (L = 2 times l^* from Section 6.2). Increasing the loading span (L) means that the flexural properties of the sandwich panels will be dominated by bending rather than core shear and will therefore offer much higher flexural properties than offered by the tested results. As the theoretical values predicted by the calculations in Section 7 are very similar to the tested

values, there is confidence that the theoretical material properties of the sandwich panels would still be applicable when operating at full scale. This allows these materials to be evaluated for use as an alternative pavement material.

Table 18 compares the performance in terms of the strength, stiffness and cost of each alternative material to that of the current pavement materials using the material indices M_6 and M_2. In this case a lower value of $\$/m^3/MPa$ would mean that a material is more favourable.

The table includes the theoretical performance of the sandwich panel combinations using a bending-to-shear ratio comparable to what would be experienced in a full-scale pavement (d= design height from Table 16 and L = 406mm). This table also compares the tested properties from the Ultra Mender as it does not need to be scaled as it is not a sandwich panel configuration and does not need to account for shear in the core. The Ultra Mender values are assumed to be very similar to an equivalent material using plastic as the matrix and are used for comparative purposes in combination with the expected $cost/m^3$ of an asphalt containing waste plastic as the matrix.

Table 18: Comparison of alternative material performance to current materials

Material	d/L where L=406mm	$C_m\rho$ ($/m^3)	Young's / Flexural Modulus E (MPa)	σ_{flex} (MPa)	$\left(\frac{C_m\rho}{E^{\frac{1}{3}}}\right)$, M_6	$\left(\frac{C_m\rho}{\sigma_y^{\frac{1}{2}}}\right)$, M_2
Basecourse	N/A	60.0	150.0	0.1	11.3	189.7
Asphalt	N/A	330.0	4000.0	0.9	20.8	347.9
Concrete	N/A	660.0	25000.0	3.5	22.6	352.8
Low Carbon Steel - PS Foam	0.13	388.1	88.2	2.2	87.2	261.7
Low Carbon Steel - PU Foam	0.13	932.0	90.2	6.5	207.8	365.6
Plywood - PS Foam	0.16	211.0	72.0	1.3	50.7	185.1
PET - PS Foam	0.15	233.6	73.2	2.0	55.8	165.2
PVC - PS Foam	0.15	251.6	73.0	2.0	60.2	177.9
Asphalt with Ultra Mender matrix	N/A	1690.5	153.3	1.8	315.9	1226.4
Asphalt with Waste Plastic matrix	N/A	130.5	153.3	1.8	24.4	97.3

The analysis shows that the current materials (Basecourse, Asphalt and Concrete) are more favourable if stiffness at a low cost is desired (~$10-$20/m^3/MPa). The closest sandwich panel materials would cost almost three times more to achieve equivalent performance (Plywood, PET, PVC-PS foam, ~$50-$60/m^3/MPa). As expected, the Ultra Mender sample does not compare favourably to the current materials in terms of stiffness ($315/m^3/MPa) however substituting the price of the Ultra Mender binder with that of waste plastic would make this option a lot more viable ($22/m^3/MPa).

The alternative materials become a lot more viable if strength at low cost is desired. In this case the current materials are all low strength and cost ~$180-$350/m^3/MPa. All sandwich panel materials compare favourably to the current materials if strength is the main performance indicator with costs ~$160-$370/m^3/MPa. Again, the Ultra Mender is not favourable if it is to be used on large areas (at ~$1200/m^3/MPa), however substation with a waste plastic matrix would make it considerably more favourable than the current pavement materials at a cost of ~$100/m^3/MPa.

These costs only take into account the base material cost, however the whole of life cost analysis in Section 5 has shown that higher initial costs can be offset by materials that offer lower failure rates and therefore less expenditure over its life time. If the materials cost/m^3 in Table 18 were to be considered as a whole of life cost, the alternative materials could be considerably more favourable. In the absence of research into the potential whole of life cost of the alternative materials, only the initial materials cost has been considered in this analysis. Despite this, the alternative materials are very favourable if strength is the primary performance requirement.

Overall, alternative materials become favourable if the pavement material requires high strength over stiffness. All current pavement design methodologies focus almost completely on increasing the stiffness of the material whereas review of failure modes show the majority are due to lack of strength in the material. For an alternative material to be considered there needs to be greater consideration for the strength of the pavement material and the effect it could have on lessening pavement defects.

10. Field Trial

Ultra Mender has been used on New Zealand pavements for the past 2 years in various locations. Due to the cost of the material, it is typically used on areas of weak pavement where multiple failures have occurred (using the current pavement materials).

Ultra Mender has been used on sites with an area of approximately $1m^2$, where deformation due to rutting and shoving has been the primary failure mode. In these cases, the underlying pavement is weak and repairs using conventional pavement materials (despite their high stiffness) have failed very quickly due to their lack of strength. Ultra Mender does not offer any benefits in terms of stiffness when compared to conventional pavement materials, however it does offer much greater strength. In this regards it can be used as a benchmark for evaluating whether materials with higher strength can offer advantages when used in a pavement.

The following sites are examples of where Ultra Mender has been used and its performance to date.

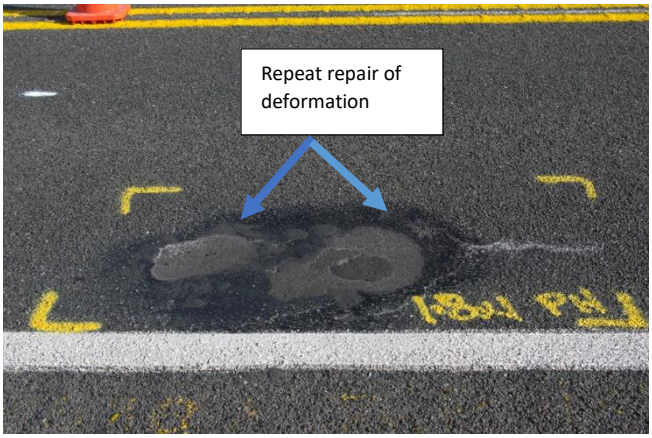

Figure 45 - Site A prior to repair with Ultra Mender.

Site A shows an area that has deformed due to a weak pavement. Asphalt was the material used for repair. The success of this repair was limited with further deformations occurring, requiring repeated repairs on a monthly basis. To alleviate this, Ultra Mender was applied at 30mm deep (Figure 46, left).

Figure 46 - Repair of site using Ultra Mender (left), and Ultra Mender repair after 4 months (right).

After treating the defect with Ultra Mender, the site did not need to be repaired after 10 months of service (Figure 46, right). This highlights how the lack of strength in the current materials (despite sufficient stiffness) can lead to failure.

The second example is from an airfield where a patch had repeatedly deformed (repaired every 2 months) due to traffic loadings from heavy aricraft and a weak underlying layer.

Figure 47 - Deformed area of runway requiring repeated repair

Ultra Mender was applied at a depth of 40mm. Grooving of the airfield took place not long after. The grooving process cuts a series of parallel lines in the surface of the aspahlt to allow for surface water to drain off, reducing the risk of aquaplaning.

Two months after completion of the grooving process it was observed that the previously straight grooves had bowed. This was due to the asphalt surface shifting under the weight of the aircraft loadings. Figure 48 (below) depicts the movement of grooves in the asphalt (that were previously straight) which have shifted by ~200mm, forming curved groove lines at the surface. The surrounding asphalt could not cope with this large amount of deformation, resulting in cracks forming at either end of the deformed area. The groove lines in the Ultra Mender patch (in the centre of the image) have remained straight due to the superior strength of the mix.

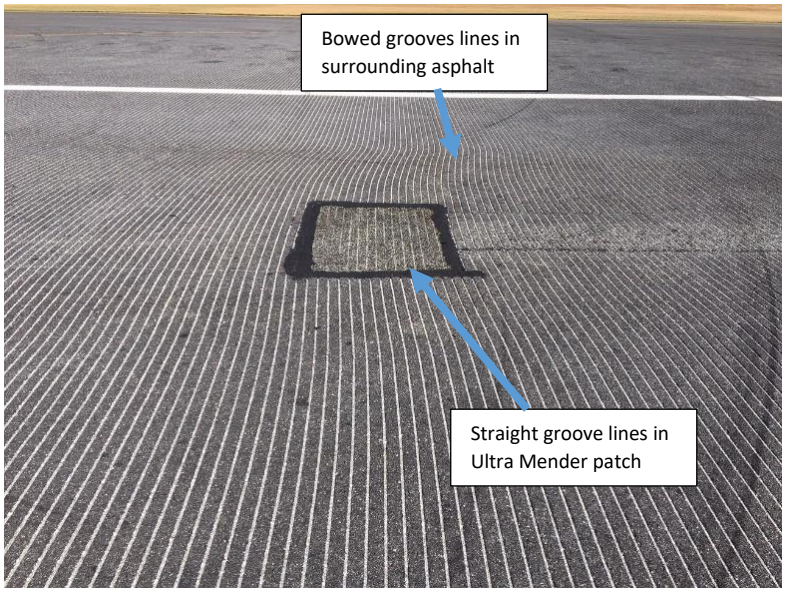

Figure 48 - Deformation in surrounding asphalt with none in the Ultra Mender patch

Both of these cases show that materials with higher strength than the current pavement materials reduce the risk of common failures, reducing the amount of maintenance required. This confirms that greater consideration for material strength is required when designing pavement materials to resist failure. This also confirms that replacing the matrix, of an asphalt mix, with a more robust material can offer greater performance in practice.

11. Discussion

Current pavement design methodologies have been developed over decades of research, using empirical relationships and a small set of material types. Being able to draw on decades worth of experience with these materials gives pavement designers a lot of confidence, however it makes it very difficult for alternative materials to be evaluated under the same design procedures.

The early empirical relationships, that form the basis of many pavement design methodologies, consider the stiffness of the material as the only material property of importance in regards to pavement performance. This has led to only a small subset of materials being used. The relationship between strength and stiffness for these materials is fairly consistent which has led to some designers treating strength and stiffness as one in the same. The focus on stiffness due to the empirical relationships formed over these years has led to common design methods not valuing the benefits of high strength materials to the degree that they should. The current pavement materials possess relatively low strength and the effect of this is evident in the current defects found in New Zealand pavements, which has resulted in the majority of maintenance spend going towards repair of these faults.

The alternative materials identified in this report don't offer as much performance in terms of stiffness, when compared to the current materials, however they do possess much higher strength. This higher strength would help reduce the number of pavement defects and in turn, improve the whole of life cost of the pavement due to less frequent replacement and a lower maintenance spend.

Field trials using Ultra Mender have confirmed that higher strength materials (than conventional pavement materials) can reduce failures occurring in the pavement. The success of Ultra Mender in these scenarios would suggest that materials with sufficient strength would offer better performance in the weak pavement than materials that only offer high stiffness.

Considering this, there does appear to be an opportunity to use materials that may not have sufficient stiffness (under conventional pavement design

methods) but possess sufficient strength and/or flexibility to cope with pavement weaknesses.

If material strength is considered as the key material property for material success, alternative materials are much more favourable than the current materials. This opens up opportunity for homogenous materials, sandwich panels and alternate asphalt matrices. Wood, steels and waste plastic materials in these configurations were found to be viable options and deserve further consideration. The use of the materials could offer much lower whole of life costs but also be future proofed against the inevitable rise of autonomous vehicles, where more channelised traffic will require high strength materials to be used in the wheel paths of the pavement. The disruption due to road works will only become more of an issue with higher traffic density due to an ever-increasing population. Alternative materials lend themselves to easier prefabrication with sandwich panels, with their low density and could allow for materials to be transported in greater volumes along with faster repair/replacement of a pavement.

Overall, alternate pavement materials deserve further consideration. This report has shown that there is potential for alternatives to be considered under standard materials selection processes employed in other industries. The report has outlined the process in order to identify potential materials which can be further developed into a material that is fit for use in a pavement. For this to happen the author believes that the following areas need to be considered more closely for a given material:

- Design procedure for alternative high strength materials
- Incorporation of a skid resistant surface
- Ongoing maintenance strategies/replacement/recycling
- Manufacturing at commercial volumes
- Long term environmental performance
- Rolling resistance of vehicle driving upon it

The author also believes that there are other opportunities that should also be considered once an alternative material has been developed, such as:

- Easier instrumentation of the pavement
- Strategies for more localised treatment (i.e. only the wheel paths)
- Opportunities for down-cycling of waste materials from other industries

12. Conclusion

This report set out to review the potential use of alternative materials that could offer greater performance in a pavement and meet the current and future transport demands.

Review of the performance of the current materials showed that they have extremely variable performance, ranging from 1 year to over 20 years. Often the whole of life cost analysis will use average lives for evaluating the economic benefits of these materials however, the large range in life spans for these materials means that this cost is underestimated. This makes it difficult for a higher performing, but more expensive material to be considered on equal grounds. To allow an alternative to be fairly compared with the current pavement materials, a review of common failure modes was undertaken. This allows opportunities for more robust materials to be employed to stop common pavement failures from occurring which reduces the whole of life cost of the pavement. The review of these failure modes revealed that the majority of pavement failures (that require maintenance) are due to deformation of the pavement, which appears as cracking, rutting/shoving and potholing of the pavement surface.

A review of the functional requirements of the pavement revealed that the current pavement materials are high in stiffness but lacking in strength. This is because the current pavement design methods favour high stiffness materials as empirical relationships have found these materials to offer greater protection to the sub grade layer. This means that the focus of common pavement design methods is on reducing strain in the subgrade layer, as deformation in this is thought to be the primary cause of pavement failure.

Other design methods have recognised that deformation can occur in the layers above the subgrade and incorporate test methods that can predict this behaviour however, they are only appropriate for use with a very specific set of materials (i.e. unbound granular). Review of the current pavement materials revealed that despite all materials possessing high stiffness, a number of materials did not have sufficient strength to cope with the stresses place upon them.

To identify other alternative materials that could be used, two failure scenarios were considered. The first being the more conventional model, used in current pavement design, where a material is sitting upon a homogenous and elastic foundation. In this case the upper layer spreads traffic loads over a large area to reduce the stress placed on the lower layers. The formulae used for the design of concrete pavements was found to be a good starting point for considering alternative materials under this scenario. A second scenario was also considered as the review of common pavement failures would suggest that sections of the pavement are not homogenous or elastic. In this scenario it was assumed that there would be very little support and that the material sitting upon the pavement would act as a simply supported beam, bridging the weak spot in the pavement.

Three potential material configurations were considered under each of these scenarios: homogenous materials, alternative asphalt matrices and sandwich panels. The Ashby materials selection process was employed to evaluate alternative materials under each of the configurations and scenarios. This analysis found that waste plastics were favourable under all configurations and scenarios with wood and steel also featuring heavily in most scenarios and configurations. In the case of homogenous materials, waste plastic and wood were most favourable. Wood along with waste plastic and steel were also favourable as a face material in a sandwich panel configuration. Due to the requirement of a material to coat aggregate particle in an asphalt, only waste or virgin plastics were favourable as an alternative matrix to bitumen.

Testing of a selection of sandwich panel configurations and one alternative asphalt matrix showed that the alternative materials outperformed the current

pavement materials in terms of strength. Comparisons with the stiffness of the conventional pavement materials showed that the alternative materials were not as favourable under that scenario.

To confirm whether material with lower stiffness but much higher strength would offer greater performance, trials sites using an asphalt mix with an alternative matrix (Ultra Mender) were undertaken. The Ultra Mender trials sites showed that higher strength materials will bring greater performance over the current materials even if it does not bring any benefits in term of stiffness.

In conclusion, there has been little investigation into use of alternative pavement materials. By reviewing the failure modes that limit the performance of a pavement there is an opportunity to reduce the whole of life costs associated with constructing and maintaining a pavement. Based on the analysis of current failure modes there appears to be an opportunity for higher strength materials to assist with this. This report has shown that alternative materials have the potential to improve the performance of weak pavements if strength is the primary consideration for design.

13. References

A.A.A Molenaar, L. J. M. H. (2004). *Geometric and Structural Design of Roads and Railways*. Retrieved from http://www.citg.tudelft.nl: http://www.citg.tudelft.nl/fileadmin/Faculteit/CiTG/Over_de_faculteit/Afdelingen/Afdeling_Bouw/-_Secties/Sectie_Weg_en_Railbouwkunde/-_Leerstoelen/Leerstoel_Wegbouwkunde/-_Onderwijs/-_College_Dictaten/doc/CT3041_UK_Hoofdstuk_5.pdf

Abdel-Fattah, H., & Hamoush, S. A. (1997). Variation of the fracture toughness of concrete with temperature. *Construction and Building Materials, 11*(2), 105-108. doi:http://dx.doi.org/10.1016/S0950-0618(97)00005-6

Adlinge, S. S., & Gupta, A. (2013). Pavement Deterioration and its Causes. *International Journal of Innovative Research and Development, 2*(4), 437-450.

AIA. (2017). *Annual Local Authority Road Maintenance Survey*. Retrieved from http://www.asphaltuk.org/wp-content/uploads/ALARM-2017.pdf

Arnold, G., & Gaddum, G. (1995). Corduroy for forest roads.

Arnold, G., Morkel, C., & van der Weshuizen, G. (2012). *Development of tensile fatigue criteria for bound materials*.

Arnold, G., Werkmeister, S., & Alabaster, D. (2008). *Performance tests for road aggregates and alternative materials*.

Arnold, G. K. (2004). *Rutting of granular pavements.* University of Nottingham.

Ashby, M. F., & Cebon, D. (2004). Materials selection in mechanical design. *Le Journal de Physique IV, 3*(C7), C7-1-C7-9.

Auckland-Transport. (2014). Reseal Guidelines. https://at.govt.nz/media/339774/Reseal-Guidelines-Feb2014.pdf: Auckland Transport.

Austroads. (2008). *Guide to pavement technology. Part 2, Pavement structural design / [project manager David Hubner ; prepared by Geoff Jameson]*. Sydney: Austroads.

Austroads. (2012). *Guide to pavement technology. Part 2, Pavement structural design / [project manager David Hubner ; prepared by Geoff Jameson]*. Sydney: Austroads.

automobiledimension.com. (2017). Automobile dimensions and sizes Retrieved from http://www.automobiledimension.com/car-search-engine.php

Ball, G. P., J. (2005). *Failure Modes and Lifetimes of Chipseals on New Zealand State Highways*. Retrieved from Opus Central Laboratories:

Beer, M. D. (1996). Measurement of tyre/pavement interface stresses under moving wheel loads. *International Journal of Heavy Vehicle Systems, 3*(1-4), 97-115.

Berthelot, C., Crockford, B., & Lytton, R. (1999). Comparison of alternative test methods for predicting asphalt concrete rut performance. *Proceedings of the 44th Annual Canadian Technical Asphalt Association, Québec City, Quebec*, 14-17.

BoeingConsulting.com. (1999). Bearing capacity, plastic falure, slip circle & retaining structures. Retrieved from http://www.boeingconsult.com/tafe/bcg5005/bearing.htm

Bowman, J. (2016). How Autonomous Vehicles Will Change the Future of Road Design and Construction. Retrieved from FMI Quarterly website:

Buiter, R., Cortenraad, W., Van Eck, A., & Van Rij, H. (1989). Effects of transverse distribution of heavy vehicles on thickness design of full-depth asphalt pavements. *Transportation Research Record*(1227).

Cenek, P., Herrington, P., Henderson, R., Holland, B., McIver, I., & Walton, D. (2011). *High-stress corners*.

Christopher, B. R., Schwartz, C., Boudreau, R., & Berg, R. R. (2006). *Geotechnical Aspects of Pavements: Reference Manual*: US Department of Transportation, Federal Highway Administration.
Colas. (2017). Vegecol. Retrieved from https://www.colas.com/en/press-media/media/vegecol
Cottingham, D. (2017). Are wider roads safer, and how are road widths decided? Retrieved from https://www.drivingtests.co.nz/resources/are-wider-roads-safer-and-how-are-road-widths-decided/
D'Angelo, J. A. (2009). The relationship of the MSCR test to rutting. *Road materials and pavement design, 10*(sup1), 61-80.
Davidson, P., & Spinoulas, A. (2015). *Autonomous vehicles: what could this mean for the future of transport.* Paper presented at the Australian Institute of Traffic Planning and Management (AITPM) National Conference, Brisbane, Queensland.
De Beer, M., & Fisher, C. (1997). Contact stresses of pneumatic tires measured with the Vehicle-Road Surface Pressure Transducer Array (VRSPTA) system for the University of California at Berkeley (UCB) and the Nevada Automotive Test Center (NATC). *University of California at Berkeley (UCB) and the Nevada Automotive Test Center (NATAC)*.
De Beer, M., Fisher, C., & Jooste, F. (2002). *Evaluation of non-uniform tyre contact stresses on thin asphalt pavements.* Paper presented at the Ninth international conference on asphalt pavements.
De Beer, M., Fisher, C., & Jooste, F. J. (1997). *Determination of pneumatic tyre/pavement interface contact stresses under moving loads and some effects on pavements with thin asphalt surfacing layers.* Paper presented at the Proc., 8th International Conference on Asphalt Pavements.
Douglas, R. A., Werkmeister, S., & Gribble, M. (2009). *Tyre/road contact stresses measured and modelled in three coordinate directions*: New Zealand Transport Agency.
Dunlop. (2017). Dunlop Tyre Selector. Retrieved from http://www.dunlop.co.nz/tyreselector.aspx
Duong, T. V., Cui, Y.-J., Tang, A. M., Dupla, J.-C., Canou, J., Calon, N., & Robinet, A. (2015). Effects of water and fines contents on the resilient modulus of the interlayer soil of railway substructure. *Acta Geotechnica*, 1-9.
EAPA.org. (2015). Asphalt. Retrieved from http://www.eapa.org/asphalt.php
Ecoserve, E., & Network, S. (2004). Baseline Report for the Aggregate and Concrete Industries in Europe. *ECO-SERVE Network, Cluster, 3*.
EduPack, C. (2016). Granta Design Limited: Cambridge: UK.
Fernández-Gómez, W. D., Rondón Quintana, H., & Reyes Lizcano, F. (2013). A review of asphalt and asphalt mixture aging: Una revisión. *Ingeniería e Investigación, 33*, 5-12.
FHWA. (2017). Tech Brief - Bases and Subabses for Concrete Pavements. Retrieved from https://www.fhwa.dot.gov/pavement/concrete/pubs/hif16005.pdf
Giblett, C. (2012). *Risk-based economic evaluation of pavement construction options.* Paper presented at the ARRB Conference, 25th, 2012, Perth, Western Australia, Australia.
Greaves, A. (2017). *Maintaining State-Controlled Roadways*. Retrieved from https://www.audit.vic.gov.au/sites/default/files/20170622-Maintaining-Roadways.pdf
Gribble, M., Patrick, J., & Land Transport, N. (2008). *Adaptation of the AUSTROADS pavement design guide for New Zealand conditions*: Land Transport New Zealand.
Gundersen, B. (2008). *Chipsealing Practice in New Zealand*. Paper presented at the 1st Sprayed Sealing Confenrence, Adelaide, Australia.

Gupta, A., Kumar, P., & Rastogi, R. (2014). Critical review of flexible pavement performance models. *KSCE Journal of Civil Engineering, 18*(1), 142-148.
Haranki, B. (2009). *Strength, modulus of elasticity, creep and shrinkage of concrete used in florida.* University of Florida.
Herrington, P., & Alabaster, D. (2008). Epoxy modified open-graded porous asphalt. *Road materials and pavement design, 9*(3), 481-498.
Huang, Y., Bird, R. N., & Heidrich, O. (2007). A review of the use of recycled solid waste materials in asphalt pavements. *Resources, Conservation and Recycling, 52*(1), 58-73. doi:http://dx.doi.org/10.1016/j.resconrec.2007.02.002
Im, S., Zhou, F., Lee, R., & Scullion, T. (2014). Impacts of rejuvenators on performance and engineering properties of asphalt mixtures containing recycled materials. *Construction and Building Materials, 53*(0), 596-603. doi:http://dx.doi.org/10.1016/j.conbuildmat.2013.12.025
Jackson, J., Peploe, R., & Vercoe, J. (2003). The influence of pavement temperatures on predicted pavement performance. *Publication of: ARRB Transport Research, Limited*.
Jameson, G. (2008). *Guide to pavement technology: part 2: pavement structural design*.
Jameson, G. (2013). *Technical basis of Austroads Guide to Pavement Technology: part 2: pavement structural design*.
Jooste, F. v. d. W., P. (2017). *Analysis of Pavement Treatment Performance.* Paper presented at the NZIHT 18th Annual Conference, Tauranga, NZ.
Kim, K. W., & El Hussein, M. (1997). Variation of fracture toughness of asphalt concrete under low temperatures. *Construction and Building Materials, 11*(7–8), 403-411. doi:http://dx.doi.org/10.1016/S0950-0618(97)00030-5
Knappett, J. (2012). *Craig's soil mechanics* (Vol. 8): Spon Press London, UK.
KWS. (2017). Plastic Roads. Retrieved from https://www.plasticroad.eu/en/
Lay, M. G. (1992). *Ways of the World: A History of the World's Roads and of the Vehicles that Used Them*: Rutgers university press.
Lay, M. G. (2009). *Handbook of road technology*: CRC Press.
Lesueur, D. (2009). The colloidal structure of bitumen: Consequences on the rheology and on the mechanisms of bitumen modification. *Advances in colloid and Interface Science, 145*(1), 42-82.
Liley, J. B., & McKenzie, R. L. (2006). Where on Earth has the highest UV. *This issue*.
Litman, T. (2017). *Autonomous vehicle implementation predictions*: Victoria Transport Policy Institute.
Mackintosh, L. (2001). Overview of New Zealand climate. Retrieved from https://www.niwa.co.nz/education-and-training/schools/resources/climate/overview
Major, N. (1965). Basis for the selection of binders for chip sealing. *New Zealand Engineering, 20*(12), 521.
Meyer, C. (2009). The greening of the concrete industry. *Cement and concrete composites, 31*(8), 601-605.
Meyer, K. G. (2002). *Managing degraded off-highway vehicle trails in wet, unstable, and sensitive environments*. Retrieved from
NAPA. (1999). History of Asphalt. Retrieved from http://www.asphaltpavement.org/index.php?option=com_content&task=view&id=21
NIWA. (2016). Climate Extremes. Retrieved from https://www.niwa.co.nz/education-and-training/schools/resources/climate/extreme
NZTA. (1986). Notes on Sub-base Aggregate Specification TNZ M/3. http://www.nzta.govt.nz: New Zealand Transport Agency.
NZTA. (2006). Base Course Aggregate Specification TNZ M/4. http://www.nzta.govt.nz: New Zealand Transport Agency.

NZTA. (2010). *Guide to State Highway Noise*. Retrieved from nzta.govt.nz: http://www.nzta.govt.nz/assets/resources/road-surface-noise/docs/nzta-surfaces-noise-guide-v1.0.pdf
NZTA. (2013). Vehicle dimensions and mass – guide to factsheet 13 series. NZTA.govt.nz.
NZTA. (2014). Heavy rigid motor vehicle definitions and specifications. Retrieved from https://www.nzta.govt.nz/resources/roadcode/heavy-vehicle-road-code/information-for-heavy-vehicle-drivers/heavy-rigid-vehicle-definitions-and-specifications/
NZTA. (2015). Visual Audit Guideline. nzta.govt.nz.
NZTA. (2016). *Economic Evaluation Manual*. Retrieved from nzta.govt.nz: https://www.nzta.govt.nz/assets/resources/economic-evaluation-manual/economic-evaluation-manual/docs/eem-manual-2016.pdf
Olanike, A. O. (2014). http://www.ajer.org/papers/v3(2)/T032141147.pdf. *American Journal of Engineering Research (AJER), 3*(2), 141-147.
Ossa, E. A. (2005). *Deformation behaviour of bitumen and bituminous mixes.* University of Cambridge.
Patrick, J., & Aramoorthy, H. (2012). *Factors influencing the decision to rehabilitate a pavement*.
Patrick, J., Arampamoorthy, H., Kathirgamanathan, P., & Towler, J. (2013). *Improvement of the performance of hotmix asphalt surfacings in New Zealand*.
PavementInteractive.org. (2008a). Pavement History. Retrieved from http://www.pavementinteractive.org/article/pavement-history/
PavementInteractive.org. (2008b). Pavement Structure. Retrieved from http://www.pavementinteractive.org/article/structural-designpavement-structure/
PCA. (2010). Precast Concrete Pavement Systems Save Time, Cut Congestion on Highway Repair. Retrieved from https://www.roadsbridges.com/precast-concrete-pavement-systems-save-time-cut-congestion-highway-repair
Peploe, R. (2008). *Flexural modulus of typical New Zealand structural asphalt mixes*.
Petersen, J. C., Robertson, R., Branthaver, J., Harnsberger, P., Duvall, J., Kim, S., . . . Bahia, H. (1994). *BINDER CHARACTERIZATION AND EVALUATION. VOLUME 1* (Vol. 1).
Pinjari, A. R., Augustin, B., & Menon, N. (2013). Highway capacity impacts of autonomous vehicles: An assessment. *Centre for Urban Transportation Research. Florida, USA*.
Porter, O. (1939). *The preparation of subgrades.* Paper presented at the Highway Research Board Proceedings.
Prowell, B. D. (2010). *Validating the fatigue endurance limit for hot mix asphalt* (Vol. 646): National Academies.
Read, J., & Whiteoak, D. (2003). *The shell bitumen handbook*: Thomas Telford.
Reynolds, C. E., Steedman, J. C., & Threlfall, A. J. (2007). *Reinforced concrete designer's handbook*: CRC Press.
Richardson, D. N., & Lusher, S. M. (2008). Determination of creep compliance and tensile strength of hot-mix asphalt for wearing courses in missouri.
roadscience.co.nz. (2018). Products - Ultra Mender.
Ruiz, J. M., Rasmussen, R. O., Chang, G. K., Dick, J. C., & Nelson, P. K. (2005). *Computer-Based Guidelines for Concrete Pavements. Volume II--Design and Construction Guidelines and HIPERPAV II User's Manual*. Retrieved from
Selig, E. (1987). Tensile zone effects on performance of layered systems. *Geotechnique, 37*(3), 247-254.
Seyhan, U., Tutumluer, E., & Yesilyurt, H. (2005). Anisotropic aggregate base inputs for mechanistic pavement analysis considering effects of moving wheel loads. *Journal of Materials in Civil Engineering, 17*(5), 505-512.

Sharp, R., & Granger, R. (2003). On car steering torques at parking speeds. *Proceedings of the Institution of Mechanical Engineers, Part D: Journal of Automobile Engineering, 217*(2), 87-96.
Sitharam, T. (2015). Advanced Foundation Engineering.
Sorrell, S., Speirs, J., Bentley, R., Brandt, A., & Miller, R. (2010). Global oil depletion: A review of the evidence. *Energy Policy, 38*(9), 5290-5295.
Southern-Testing. (2015). Plate Bearing Test. Retrieved from http://www.southerntesting.co.uk/services/ground-investigation/plate-bearing-test
Stempihar, J., Williams, R., & Drummer, T. (2009). *Quantifying Lateral Displacement of Trucks for Use in Flexible Pavement Design.* Paper presented at the 88th Annual Meeting of the Transportation Research Board, January.
Swaddiwudhipong, S., Lu, H.-R., & Wee, T.-H. (2003). Direct tension test and tensile strain capacity of concrete at early age. *Cement and Concrete Research, 33*(12), 2077-2084. doi:http://dx.doi.org/10.1016/S0008-8846(03)00231-X
Texas-Department-of-Transport. (2001). Pavement Design Guide. http://onlinemanuals.txdot.gov/txdotmanuals/pdm/index.htm: Texas Department of Transport.
Timm, D., Birgisson, B., & Newcomb, D. (1998). Development of mechanistic-empirical pavement design in Minnesota. *Transportation Research Record: Journal of the Transportation Research Board*(1629), 181-188.
Timm, D. H., & Priest, A. L. (2005). *Wheel wander at the NCAT test track*. Retrieved from
Tomasi, D. (2011). Fitting of a tyre's experimental data. Retrieved from http://www.multibody.net/teaching/dissertaions/2011-tomasi/
Transit-New-Zealand. (2005). *Chipsealing in New Zealand*: Transit New Zealand, Road Controlling Authorities, Roading New Zealand.
Vorobieff, G. (2004). *Modification versus bound pavements.* Paper presented at the Proceedings from stabilisation of road pavements seminar, NZ Highway Institute of Technology, Auckland, NZ.
Werkmeister, S., Dawson, A., & Wellner, F. (2004). Pavement design model for unbound granular materials. *Journal of Transportation Engineering, 130*(5), 665-674.
West-Systems. (2018). Epoxy Products. Retrieved from https://www.westsystem.com/
Westergaard, H. (1926). Stresses in concrete pavements computed by theoretical analysis. *Public roads*.
Westergaard, H. M. (1948). New Formulas for Stress in Concrete Pavements of Airfields. *American Society of Civil Engineers Transactions*.
WHO. (2015). Ultraviolet radiation and the INTERSUN Programme. Retrieved from http://www.who.int/uv/intersunprogramme/activities/uv_index/en/index3.html
Withington, N. (2005). *Sustainable End-of-Life Options for Plastics in New Zealand*. Retrieved from
Wu, S., Pang, L., Mo, L., Qiu, J., Zhu, G., & Xiao, Y. (2008). UV and thermal aging of pure bitumen-comparison between laboratory simulation and natural exposure aging. *Road materials and pavement design, 9*(sup1), 103-113.
Yamashita, H., Matsutani, Y., & Sugiyama, H. (2015). Longitudinal Tire Dynamics Model for Transient Braking Analysis: ANCF-LuGre Tire Model. *Journal of Computational and Nonlinear Dynamics, 10*(3), 031003.
Yoder, E. J., & Witczak, M. W. (1975). *Principles of pavement design*: John Wiley & Sons.
Young, W. C., & Budynas, R. G. (2002). *Roark's formulas for stress and strain* (Vol. 7): McGraw-Hill New York.

14. Appendices

14.1. Appendix A – Availability and cost of waste plastics in New Zealand

Table 19 - Summary of availability and costs of recycled plastics in New Zealand (Withington, 2005).

Number	Name	Plastic used in Manufacturing (T/year)	Proportion of Total Plastic Consumed (%)	Plastic Recovered for Recycling (T/year)	Proportion of Total Recovered Plastics (%)	Recovery Success Rate by Plastic Type (%)	Price ($/T)	Comment
1	PET	22,433	9%	8,016	23%	36%	$550-$660/T flaked	99.8% of product recovered are bottles
2	HDPE	52,587	20%	8,932	25%	17%	$600/T pelletised	89% of product recovered are bottles
3	PVC	39,202	15%	2,412	7%	6%	$300/T	mostly cable/wiring coatings
4	LDPE	79,513	30%	12,444	35%	16%	$300/T	all film or bags
5	PP	32,402	12%	1,415	4%	4%		80% film the rest containers
6	PS	12,942	5%	417	1%	3%		
7	EPS	8,123	3%	218	1%	3%		
8	Other	15,702	6%	1,588	4%	10%	$300/T	
	Total	262,904	100%	35,442	100%	100%	Average = $450/T	

14.2. Appendix B – Ultra Mender Mixing Instructions (previously called TLP).

How to use

ROAD SCIENCE
LEADING PAVEMENTS TECHNOLOGY

TLP
THE LAST PATCH
VERSATILE PAVEMENT REPAIR SOLUTION

EASY TO USE!

PERFECT FOR

POTHOLES | PATCHES | CRACK SEALING

- READY TO GO
- FLEXIBLE
- LONG-LASTING

0800 180 200 | www.roadscience.co.nz

STEP 1
Prepare

- Mark out and measure area to be treated.

- Remove loose material.
- Sweep the surface.
- Ideally the surface should be dry.

STEP 2
Preparation of surface

- Tear the foil sachet containing TLP binder.

- Apply and spread a thin coat of TLP binder as a tack coat.
- Apply this coat over the full width of the marked area.
- Use a squegee or disposable paint brush to spread the product.

STEP 3
Mixing TLP

- Using a 10 litre bucket fill the plastic concrete mixer with 20 litres of grade 6 chip.
- Start the concrete mixer and steadily squeeze the binder from the 2.5 litre bag (one packet of TLP) into the concrete mixer.
- Mix until the chip is well coated.

- For smaller areas TLP can be easily mixed in a bag and/or a plastic bucket.
- Make sure the chip is well coated before applying to area to be treated.
- Refer over page for mixing table.

STEP 4
Applying TLP mix to surface

- Pour TLP mix onto the area.
- Screed immediately.
- If needed - sand or grit can be spread to prevent pick up on compactor.

Compact

- Compact with a plate compactor immediately.

STEP 5
Finish

- If needed more sand or grit can be spread.

Mixing Quick Tips

- Mix ratio is 20 litres of grade 6 aggregate to 2.5 litres (one packet) of TLP.
- 1 shovel full of aggregate is approximately 2L.
- TLP will not stick to plastic.
- Make sure you use latex gloves.
- If TLP makes contact with your skin it will flake off over time.

Diameter of repair (mm)	Coverage (m²)	Mix Ratio	
		Aggregate (L)	Binder
300	0.1	2	1/10 bag
450	0.2	5	1/4 bag
650	0.3	10	1/2 bag
800	0.5	15	3/4 bag
900	0.7	20	1 bag

For a 'how to' video go to iDowner

0800 180 200 | www.roadscience.co.nz

14.3. Appendix C – Test Results

Low Carbon Steel – PS Foam

Sample	A	B	C	D	E	Average	S.D	C.V
t face thickness (mm)	1.3	1.3	1.3	1.3	1.3	1.3	0.00	0.00
d1 (mm)	50.95	51.44	49.66	51.75	51.47	51.05	0.74	1.45
d2 (mm)	50.67	51.72	49.34	50.95	50.08	50.55	0.80	1.59
d3 (mm)	51.45	51.45	50.97	51.92	51.79	51.51	0.33	0.64
d sandwich thickness (mm)	51.02	51.54	49.99	51.54	51.11	51.04	0.57	1.11
c core thickness	48.42	48.94	47.39	48.94	48.51	48.44	0.57	1.17
b1 (mm)	74.35	73.43	73.4	76.22	73.68	74.22	1.06	1.43
b2 (mm)	74.80	74.46	73.78	76.17	74.39	74.72	0.80	1.07
b3 (mm)	75.22	75.54	73.98	76.15	74.45	75.07	0.77	1.03
b width (mm)	74.79	74.48	73.72	76.18	74.17603	74.67	0.83	1.12
S Span length (mm)	150	150	150	150	150	150	0.00	0.00
d/L	0.34	0.34	0.33	0.34	0.34	0.34	0.00	1.11
Failure type,area and location	COC	COC	COC	COC	COC			
$P^{2\%}$ (N)	588.7	507.7	551.9	706.4	658.3	602.6	71.6	11.9
P_{max} (max force N)	1199.4	1236.2	1280.4	1081.7	1259.7	1211.5	70.3	5.8
Displacement at P_{max} (mm)	9.39	11.57	9.25	7.34	8.95	9.30	1.35	14.50
Strain at P_{max} (%)	12.77	15.89	12.33	10.09	12.20	12.66	1.86	14.73
m N/mm	415.8	301.0	359.0	587.4	341.69	400.98	100.25	25.00
σ facing stress (MPa)	4.21	3.79	4.31	3.84	4.23	4.08	0.21	5.25
equivalent E_{flex} (MPa)	35.32	24.91	32.89	47.52	29.11	33.95	7.64	22.52
equivalent σ_{flex} (MPa)	1.39	1.41	1.56	1.20	1.46	1.40	0.12	8.42
equivalent σ_{flex} (MPa) at 2% strain	0.68	0.58	0.67	0.79	0.76	0.70	0.07	10.64

Low Carbon Steel – PU Foam

Sample	A	B	C	D	E	Average	S.D	C.V
t face thickness (mm)	1.30	1.30	1.30	1.30	1.30	1.3	0.00	0.00
d1 (mm)	48.09	48.22	49.00	47.29	48.80	48.28	0.60	1.24
d2 (mm)	47.94	47.93	49.27	47.29	47.94	48.07	0.65	1.35
d3 (mm)	48.19	49.03	48.63	47.93	48.31	48.42	0.38	0.78
d sandwich thickness (mm)	48.07	48.39	48.97	47.50	48.35	48.26	0.48	0.99
c core thickness	45.47	45.79	46.37	44.90	45.75	45.66	0.48	1.04
b1 (mm)	75.91	75.80	75.84	76.03	75.84	75.88	0.08	0.11
b2 (mm)	75.45	75.55	74.51	76.98	75.89	75.68	0.80	1.05
b3 (mm)	75.32	75.52	75.89	76.91	75.35	75.80	0.59	0.78
b width (mm)	75.56	75.62	75.41	76.64	75.69	75.79	0.44	0.58
S Span length (mm)	150	150	150	150	150	150	0.00	0.00
d/L	0.32	0.32	0.33	0.32	0.32	0.32	0.00	0.99
Failure type,area and location	COC	COC	COC	COC	COC			
$P^{2\%}$ (N)	301.7	390.0	478.3	323.8	368.43	372.44	61.48	16.51
P_{max} (max force N)	875.6	860.9	897.7	831.5	870.50	867.24	21.57	2.49
Displacement at P_{max} (mm)	14.95	10.28	7.48	11.77	7.84	10.46	2.74	26.21
Strain at P_{max} (%)	19.16	13.27	9.77	14.90	10.11	13.44	3.45	25.66
m N/mm	143.4	147.4	225.8	181.3	187.7	177.1	30.1	16.9
σ facing stress (MPa)	4.43	3.98	4.30	4.15	4.38	4.25	0.16	3.83
equivalent E_{flex} (MPa)	14.41	14.51	21.52	18.62	18.51	17.51	2.72	15.51
equivalent σ_{flex} (MPa)	1.13	1.09	1.12	1.08	1.11	1.11	0.02	1.49
equivalent σ_{flex} (MPa) at 2% strain	0.39	0.50	0.60	0.42	0.47	0.47	0.07	14.99

Plywood – PS Foam

Sample	A	B	C	D	E	Average	S.D	C.V
t face thickness (mm)	6.5	6.5	6.5	6.5	6.5	6.5	0.00	0.00
d1 (mm)	65.38	65.43	65.53	66.54	66.00	65.78	0.44	0.67
d2 (mm)	65.73	65.11	65.71	66.13	65.83	65.70	0.33	0.51
d3 (mm)	65.53	65.03	65.44	66.96	65.20	65.63	0.69	1.05
d sandwich thickness (mm)	65.55	65.19	65.56	66.54	65.67	65.70	0.45	0.69
c core thickness	52.55	52.19	52.56	53.54	52.67	52.70	0.45	0.85
b1 (mm)	75.84	75.50	73.99	75.08	75.56	75.19	0.65	0.86
b2 (mm)	76.12	74.81	74.80	75.54	75.83	75.42	0.53	0.71
b3 (mm)	76.61	74.97	74.78	75.42	75.07	75.37	0.65	0.87
b width (mm)	76.19	75.09	74.52	75.35	75.49	75.33	0.54	0.72
S Span length (mm)	150	150	150	150	150	150	0.00	0.00
d/L	0.44	0.43	0.44	0.44	0.44	0.44	0.00	0.69
Failure type,area and location	COC	COC	COC	COC	COC			
$P^{2\%}$ (N)	419.40	331.10	404.70	544.50	534.43	446.83	81.41	18.22
P_{max} (max force N)	963.90	1074.30	1832.20	2148.60	1064.98	1416.80	480.48	33.91
Displacement at P_{max} (mm)	7.19	10.61	6.92	7.22	7.82	7.95	1.36	17.12
Strain at P_{max} (%)	12.56	18.44	12.09	12.82	13.70	13.92	2.32	16.66
m N/mm	442.40	387.30	359.00	493.40	428.93	422.21	46.34	10.97
σ facing stress (MPa)	0.70	0.64	0.70	0.65	0.70	0.68	0.03	3.79
equivalent E_{flex} (MPa)	17.40	15.71	14.42	18.75	16.93	16.64	1.48	8.87
equivalent σ_{flex} (MPa)	0.66	0.76	1.29	1.45	0.74	0.98	0.32	33.09
equivalent σ_{flex} (MPa) at 2% strain	0.29	0.23	0.28	0.37	0.37	0.31	0.05	17.01

PET – PS Foam

Sample	A	B	C	D	E	Average	S.D	C.V
t face thickness (mm)	5.20	5.20	5.20	5.20	5.20	5.2	0.00	0.00
d1 (mm)	60.35	61.46	58.40	58.59	59.06	59.57	1.16	1.95
d2 (mm)	59.70	60.13	58.72	58.64	58.68	59.17	0.62	1.05
d3 (mm)	59.24	59.26	59.74	59.81	59.26	59.46	0.26	0.43
d sandwich thickness (mm)	59.76	60.28	58.95	59.01	59.00	59.40	0.53	0.90
c core thickness	49.34	49.88	48.55	48.61	48.60	49.00	0.53	1.08
b1 (mm)	75.80	75.25	74.95	75.47	75.68	75.43	0.30	0.40
b2 (mm)	75.28	75.06	74.91	75.49	74.99	75.15	0.21	0.28
b3 (mm)	75.31	75.13	75.02	75.50	75.40	75.27	0.18	0.23
b width (mm)	75.46	75.15	74.96	75.49	75.36	75.28	0.20	0.27
S Span length (mm)	150	150	150	150	150	150	0.00	0.00
d/L	0.40	0.40	0.39	0.39	0.39	0.40	0.00	0.90
Failure type,area and location	COC	COC	COC	COC	COC			
$P^{2\%}$ (N)	500.37	441.50	485.65	404.71	494.48	465.34	36.70	7.89
P_{max} (max force N)	1412.80	1427.50	1515.80	1420.20	1413.73	1438.01	39.25	2.73
Displacement at P_{max} (mm)	13.82	14.40	15.52	14.27	14.18	14.44	0.57	3.97
Strain at P_{max} (%)	22.02	23.15	24.39	22.45	22.31	22.87	0.85	3.71
m N/mm	295.06	277.34	310.16	209.70	309.60	280.37	37.31	13.31
σ facing stress (MPa)	2.47	2.49	2.71	2.52	2.51	2.54	0.09	3.43
equivalent E_{flex} (MPa)	15.46	14.21	17.04	11.41	16.88	15.00	2.07	13.80
equivalent σ_{flex} (MPa)	1.18	1.18	1.31	1.22	1.21	1.22	0.05	3.95
equivalent σ_{flex} (MPa) at 2% strain	0.42	0.36	0.42	0.35	0.42	0.39	0.03	8.26

PVC – PS Foam

Sample	A	B	C	D	E	Average	S.D	C.V
t face thickness (mm)	5.10	5.10	5.10	5.10	5.10	5.1	0.00	0.00
d1 (mm)	59.86	59.81	60.16	60.32	60.25	60.08	0.21	0.34
d2 (mm)	57.51	57.69	59.38	59.26	58.01	58.37	0.79	1.36
d3 (mm)	56.27	57.65	58.90	58.38	56.44	57.53	1.04	1.80
d sandwich thickness (mm)	57.88	58.38	59.48	59.32	58.23	58.66	0.63	1.07
c core thickness	47.68	48.18	49.28	49.12	48.03	48.46	0.63	1.30
b1 (mm)	75.38	75.41	75.65	75.35	75.37	75.43	0.11	0.15
b2 (mm)	75.35	75.40	75.45	75.33	75.34	75.37	0.05	0.06
b3 (mm)	75.23	75.40	75.45	75.28	75.45	75.36	0.09	0.12
b width (mm)	75.32	75.40	75.52	75.32	75.39	75.39	0.07	0.10
S Span length (mm)	150	150	150	150	150	150	0.00	0.00
d/L	0.39	0.39	0.40	0.40	0.39	0.39	0.00	1.07
Failure type,area and location	COC	COC	COC	COC	COC			
$P^{2\%}$ (N)	507.73	397.4	507.7	493.0	440.46	469.26	43.65	9.30
P_{max} (max force N)	1405.4	1376	1265.6	1214.1	1215.33	1295.29	80.63	6.22
Displacement at P_{max} (mm)	22.943	19.007	14.517	12.923	22.21	18.32	4.01	21.91
Strain at P_{max} (%)	35.41	29.59	23.03	20.44	34.48	28.59	5.99	20.96
m N/mm	245.4934	263.0	343.1	328.3	249.88	285.95	41.29	14.44
σ facing stress (MPa)	2.60	2.52	2.27	2.19	2.23	2.36	0.17	7.04
equivalent E_{flex} (MPa)	14.18	14.79	18.22	17.62	14.16	15.79	1.76	11.14
equivalent σ_{flex} (MPa)	1.25	1.20	1.07	1.03	1.07	1.12	0.09	7.77
equivalent σ_{flex} (MPa) at 2% strain	0.45	0.35	0.43	0.42	0.39	0.41	0.04	8.88